National Aeronautics and Space Administration

A stunning image of NGC 2174, known as the Monkey Head Nebula, was unveiled in Rome by John Grunsfeld, NASA Associate Administrator for the Science Mission Directorate, and Fabio Favata, Head of ESA's Science Planning and Community Coordination Office.

⌈ 2014 ⌋ VOL ⌈ 31 ⌋ ISSUE ⌈ 01 ⌋

NEWSLETTER

Space Telescope Science Institute

HST IV & Looking to the Future

Neill Reid, *inr@stsci.edu*, **Antonella Nota,** *nota@stsci.edu*, **& Pam Jeffries,** *jeffries@stsci.edu*

April 24, 2014, marked the 24th anniversary of the launch of the *Hubble Space Telescope*. This year also marks the 37th anniversary of the completion of the formal, cooperative memorandum of understanding regarding *Hubble*'s construction and operation—signed in October 1977 between NASA and the European Space Agency (ESA). Throughout those years ESA has played a crucial role in promoting *Hubble*'s mission, providing technical expertise, instrumentation, and support scientists. Just as significantly, the ESA research community has made extensive use of *Hubble*'s extraordinary capabilities, winning more than 22% of the observing time allocated over the past 24 years and accounting for 27% of the investigators on *Hubble* proposals in Cycle 21. Representatives from ESA nations serve on all Institute committees, including the Space Telescope Users Committee, the Space Telescope Institute Committee, the Institute Visiting Committee, and the *JWST* Advisory Committee.

ESA has hosted a series of meetings to celebrate *Hubble* science: Sardinia in 1992; Paris in 1995, immediately following the first servicing mission; Venice in 2011, after Servicing Mission 4; and now, celebrating *Hubble*'s continued longevity, in the Eternal City—Rome.

"*HST* IV" was designed not only to take stock of *Hubble*'s more recent scientific contributions, but also to look forward to future research by *Hubble* and its immediate successor, the *James Webb Space Telescope*, and to explore the path towards further transatlantic space-astronomy collaborations. It is therefore appropriate that the conference was hosted by the *Accademia dei Lincei* (named after the far-sighted lynx), which counts the visionary Galileo Galilei as its sixth member. The meeting also honored the Italian physicist Piero Amaldi, who played pivotal roles in establishing both ESA and the European Organization for Nuclear Research (CERN), the premier multi-national scientific enterprises in post-war Europe. Roger Davies (Oxford) co-chaired the Science Organizing Committee, composed of astronomers from Europe and the U.S. For additional information on the conference and final electronic records, see: **http://www.stsci.edu/institute/conference/hst4**.

Hubble observations span almost every discipline within astronomy, and that versatility was reflected in the widely varied science program at the conference. The diverse topics were drawn together by a common theme: the ground-breaking research made possible by *Hubble*'s essential technical capabilities: high spatial resolution, exquisite instrumental stability, and multi-wavelength access, particularly at near- and far-ultraviolet wavelengths.

The science enabled by those technical characteristics is amplified and enhanced by *Hubble*'s longevity. A longer baseline for observations has had direct impact on the ability to measure the motions of individual stars within a crowded stellar cluster; to track features in an expanding galactic or extragalactic jet; and to monitor long-term variations in planetary atmospheres, stellar light echoes, and active nuclei. Furthermore, longevity has changed the kind of science tackled by *Hubble*, the types of observing programs, and the impact of those programs. Today, researchers can develop in-depth investigations by building on data from past Treasury programs.

As a well-established facility, *Hubble* has made ambitious, larger-scale programs credible, notably in the PHAT, CLASH and CANDELS Multi-Cycle Treasury

Figure 1: From the past to the future: The *James Webb Space Telescope* meets Athena, the goddess of wisdom and knowledge, at the *Accademia dei Lincei* in Rome.

(MCT) programs, which were barely underway at the time of *HST* III. These programs are now complete, archived, and generating high-impact results.

Hubble has also proven that a mature, well-understood telescope system can be adapted to new purposes. For example, spatial scanning with Wide Field Camera 3 has not only revolutionized exoplanet spectroscopy, but also offers the potential for *Gaia*-like accuracy in targeted, relative astrometry.

Hubble's growing archive provides a rich trove for novel research, extending to fundamental physics: analyses of archived ultraviolet spectra of standard stars are setting stringent constraints on variations in the fine-structure constant in high gravitational fields.

Finally, *Hubble* is often referenced as a cultural icon, but achieving iconic status takes time: *Hubble* would not have penetrated so deeply within the popular psyche were it not for its active scientific presence over the past 24 years.

The *HST* IV conference featured an array of research presentations of the highest quality. While we can touch on only a few highlights here, the individual presentations are all available from the *HST* IV website (**http://www.stsci.edu/institute/conference/hst4/presentations**).

Within the Solar System, *Hubble*'s ultraviolet observations of auroral activity on Jupiter, Saturn, and even Uranus evidence interactions of solar plasma with the planetary magnetic fields. Optical and ultraviolet spectroscopy of comets trace the diversity of chemical composition, particularly carbon monoxide and water in objects arriving from the Oort cloud. Closer to Earth, *Hubble* imaging is yielding insight into the enigmatic nature of main-belt comets, testing whether the newly seen ejecta are more consistent with icy sublimation or dust generated by more disruptive processes.

The first detection of exoplanets postdates *Hubble*'s launch, but the veritable avalanche of discoveries over the last 15 years, particularly by *Kepler*, has established a new realm of comparative planetology.

In transiting planets, *Hubble* and *Spitzer* are playing key roles in mapping the surface temperature structure, constraining atmospheric circulation, and searching for spectral diagnostics—in short, laying the groundwork for *Webb*. Spanning the ultraviolet, optical, and near-infrared regions, *Hubble* can detect water and methane in hot Jupiters and probe the properties of atmospheric scattering at shorter wavelengths. It can map ultraviolet signatures of accreted material in white dwarfs and map the chemical composition of terrestrial bodies in exosolar systems. *Hubble* can probe hot Neptunes and, with a significant investment of time, reach super-Earths. The flat, haze-dominated spectrum it found for GJ 1214b emphasizes that *Webb*'s access to thermal wavelengths will be vital to elucidating the nature of such systems.

Massive stars are an important source of ionizing flux for the interstellar medium and make significant contributions to the evolution of metallicity in galaxies. *Hubble* has conducted a thorough census of young clusters, notably the Orion Nebula and the 30 Doradus region in the LMC. Spectroscopic observations of the latter system indicate that six stars are responsible for half the ionizing flux. At the same time, the PHAT MCT program is compiling a census of star clusters and star-forming environments within the Andromeda galaxy. Indeed, analyses of *Hubble* data put the stellar populations of all Local Group galaxies in sharp relief, mapping the distributions of age and metallicity, and tracking their star-forming history. Such detailed observations are crucial in defining templates for investigations of field stars and clusters in moderately distant galaxies—for example, in the Legacy ExtraGalactic UV Survey (LEGUS) program—and in unresolved star-forming galaxies at higher redshift, establishing clear synergies with *Webb*'s space-based infrared observations and with ALMA's millimeter and sub-millimeter observations from the ground.

Hubble's unparalleled angular resolution has been vital in probing the central regions of globular clusters. The Faint Object Camera's detection of blue stragglers in the cores of 47 Tucanae and M15 featured among its early science results. Subsequent imaging of these stellar mergers with wider-field detectors has investigated the relative dynamical evolution of different clusters. A major paradigm change in recent years is the realization that globular clusters are not simple stellar populations and mono-metallicity products of a single star-forming event. Abundance anomalies have long been known for cluster red giants, but *Hubble*'s exquisite photometric accuracy from ultraviolet to near-infrared wavelengths has been fundamental to extending coverage to the main sequence and cementing this conceptual change. Recent investigations suggest that almost all globular clusters harbor multiple stellar populations, with corresponding implications for the role played by such systems in the early evolution of galaxies like the Milky Way.

Art inspired by science—specifically by *Hubble*'s results—is a signature of the conference series, "Science with the *Hubble Space Telescope*." Following the success of Tim Otto Roth's *From the Distant Past* (**https://blogs.stsci.edu/newsletter/2012/07/30/the-art-of-hubble-spectra/**)—which was displayed in Venice, Baltimore, and New York—the artist premiered *Heaven's Carousel*, in Rome. This artwork was inspired by the research by Adam Riess and colleagues on the accelerating expansion of the universe, which was awarded the Nobel Prize.

The new piece takes the form of a rotating carousel, with 36 illuminated, spherical loudspeakers mounted on long strings. In the words of artist, "When you look up at the night sky you see it in black and white, but in reality it is full of colors, colors which are too faint to be perceived by the eye's color receptors. It is the most dominant of these colors that I have translated into sound as part of the *Heaven's Carousel*."

In representing the universe in this way, *Heaven's Carousel* allows the audience to experience phenomena such as the Doppler effect: at the center of the installation there is no significant effect, but as the visitor moves outwards, the frequencies start to oscillate dramatically and weave into a mesmerizing tapestry of sound.

During the 25-minute sound performance, other phenomena that inspired the piece become evident. For example, one can experience the progress from the high-pitched, bright-blue tones, which represent the beginning of the universe, to the deep tones of red, low-frequency sounds, which illustrate what we observe in the distant universe with *Hubble* today.

Tim Otto Roth's website is **http://www.imachination.net/**.

HST IV
from page 3

Galaxy evolution itself has been a signature feature for *Hubble* science. Prompted by observations of high-redshift ($z \sim 1.2$) radio galaxies, the original *Hubble* Deep Field (HDF) revealed a dynamic, evolving universe, far beyond the predictions of contemporary theoretical models. Subsequent campaigns (GOODS, the Ultra Deep Field, COSMOS, GEMS, UDF09, CANDELS, UDF12) have expanded coverage in solid angle and depth, complemented by extensive multi-wavelength observations from space missions (*Chandra*, *Spitzer*, *Herschel*) and ground-based facilities (Keck, Gemini, KPNO, CTIO, VLT, Magellan). Those surveys extend well beyond the HDF, currently encompassing more than 11,000 galaxies at redshifts $4 < z < 8$. The observations provide a firm description of galaxy properties and have produced general agreement on the evolution of the galaxy luminosity function throughout this redshift range. The overall star formation rate per unit volume peaks at ~10 times the current value at $z \sim 2$ (lookback time, $\tau \sim 10$ Gyrs), matching the current level at $z \sim 8$ ($\tau \sim 13$ Gyrs).

At lower redshifts, deep ultraviolet spectroscopy probes the metal content of galactic halos, mapping gaseous recycling between star-forming galaxies and the circumgalactic medium. Wide-field grism observations track the evolution of star formation at moderate redshifts. Recent years have seen the development of computationally-intense theoretical models based on sophisticated physical recipes. Those models show a growing concordance with observations, notably matching the evolution, with size and mass, of gas-rich and gas-poor systems, and tracking the role played by mergers and active nuclei in quenching star formation.

The new frontier for galaxy evolution lies beyond redshift $z \sim 8$. Theory predicts that galaxies form in the redshift range $\sim 15 < z < 30$, with the onset of reionization at $z \sim 11$. This is *Webb*'s universe, but *Hubble* observations have started to lift the curtain. Field surveys reveal a handful of high-luminosity galaxies at $9 < z < 11$, while the CLASH survey highlighted the utility of galaxy clusters as cosmic telescopes, amplifying the light from background galaxies and probing the high-redshift universe. The Frontier Fields program capitalizes on both techniques, compiling multiband observations of 4–6 strong-lensing galaxy clusters and offset blank field with Wide Field Camera 3 and Advanced Camera for Surveys. These observations will set the scene and offer guidance on how best to employ *Webb*'s unparalleled capabilities to survey the first galaxies.

Galaxy formation is an essential component that drives the evolving universe, and *Hubble* has played a significant role in constraining cosmological parameters. The CLASH survey has constrained the distribution of dark matter in clusters. Probing the cosmic flow itself, *Hubble* remains the only means of detecting Type Ia supernovae beyond $z \sim 1.2$; its observations indicate a low frequency of occurrence, consistent with the double-degenerate formation model. *Hubble* is also fundamental to calibrating supernovae as standard candles, constraining the range of their intrinsic properties through detailed spectroscopic observations of local supernovae, and establishing accurate, Cepheid-based measurements of the distances to host galaxies. At the same time, spatial scanning is being used to refine the zeropoint defined by Galactic Cepheids. The ultimate goal is to define H_0 to 1% accuracy and to set correspondingly tight constraints on the dark-energy equation of state parameter w.

What's next? Looking to the immediate future, *Hubble* remains the pre-eminent facility for observations at visual, blue and ultraviolet wavelengths. The ultraviolet properties of galaxies in what is now the low-redshift universe ($0.5 < z < 2$) and the gas content in galactic halos over the same redshift regime remain open questions in galaxy evolution. The new technique of spatial scanning is proving effective not only for exoplanet spectroscopy, but also for relative astrometry at the ~30–50 microarcsec level. Programmatically, past MCT programs have proven highly productive, and it may be time to contemplate new ventures on that scale in other science areas.

Areas of synergy with *Webb* and *WFIRST*/AFTA are being defined by recent *Hubble* and *Spitzer* results. Thus, *Webb* will be most effective at investigating atmospheric signatures at near- and mid-infrared wavelengths in transiting exoplanets, but blue/visual *Hubble* observations remain crucial to probing atmospheric scattering. *Gaia*, *TESS* and *PLATO* will all play roles in identifying future exoplanet targets. Similarly, Cepheids in nearby galaxies are detected most easily at blue/visual wavelengths. Nevertheless, their lower intrinsic amplitudes and insensitivity to foreground absorption make near-infrared measurements better suited to accurate determinations of distance. Near-infrared imaging can probe low-mass stars in star clusters and nearby galaxies, and extend *Hubble*'s survey of galaxies at redshifts $6 < z < 8$, which is preparing the way for *WFIRST*/AFTA's survey. CLASH and the Frontier Fields offer a similar foretaste of *WFIRST*/AFTA's potential for galaxy cluster science.

Looking beyond *Webb*, the search for life beyond Earth stands out as the key challenge for 21st century science. This quest has been characterized as "finding Earth 2.0." Science is not, however, just the act of discovery, identifying "what is." Science also encompasses "how it came to be"—as well as, "when?", "where?", and "how often?" Searching for life within the current diversity of planets demands not only measurement of current conditions, but also mapping the past and the future. Astrophysics is crucial to understanding the formation and evolution of planetary systems throughout cosmic history. Thus, astrophysics sets the framework for understanding the development of other platforms for life.

Finding life beyond Earth and understanding its origins will require new initiatives to develop large space telescopes, and ongoing studies show a convergence of technical requirements.

A common theme in the *HST* IV presentations is that the community is pushing *Hubble* as far as it can go. The next scientific breakthroughs in the ultraviolet/optical domain will require a large-aperture, high-throughput telescope capable of multiplex observations—a "high-definition" space telescope. Thus, the 10–15 meter aperture required to characterize other Earths will also provide linear resolution better than 100 pc everywhere in the universe. AURA's Beyond *JWST* Committee has been established (**http://www.aura-astronomy.org/news/hdst.asp**) with the explicit charge of studying future space-based options for ultraviolet-optical-infrared astronomy that will significantly advance our understanding of the origin and evolution of the cosmos and the life within it.

In his introduction to the *HST* IV meeting, John Grunsfeld, the Associate Administrator for NASA's Science Mission Directorate, eloquently expressed NASA's mission as "Innovate, Discover, Explore and Inspire." In the 24 years since its launch, *Hubble* has risen to that challenge. Not only has *Hubble* enabled ground-breaking science and cemented itself as a public icon, but it has also highlighted the importance of multi-national co-operation as a path to addressing major scientific questions.

As noted by Fabio Favata, Head of ESA's Science Planning and Community Coordination Office, collaboration is more difficult than competition: in a competition, each participant goes his or her own way and accepts the eventual outcome; collaboration requires ongoing effort to build consensus and find a common direction. In a successful collaboration, moreover, the whole exceeds the sum of the parts. Collaboration between NASA and ESA, and between the North American and European astronomical communities, made *Hubble* possible. Continued collaboration, with the addition of CSA and Canadian astronomers, has enabled *Webb* to become a reality. Future collaboration will coordinate the relative roles of *Euclid* and *WFIRST*/AFTA, *TESS*, and *PLATO*. That same spirit of cooperation will be vital in stepping forward to tackle humankind's most pressing question: "Are we alone in the universe?"

Acknowledgement: the organizers wish to recognize Giancarlo Setti and Francesco Bertola for suggesting the beautiful venue and facilitating the organization of the conference. The *Accademia dei Lincei* provided a beautiful backdrop to *Hubble* science, and we are grateful for their gracious hospitality.

New Insights with WFC3 IR Observations

John W. MacKenty, *mackenty@stsci.edu*, **and Gabriel Brammer,** *brammer@stsci.edu*

Over the past several decades, astronomical observations at near-infrared wavelengths have become increasingly common. Access to this part of the electromagnetic spectrum provides multiple benefits, including the ability to observe dust-enshrouded sources, detect important spectral features in cooler objects, and measure rest-wavelength visible and ultraviolet light in distant (i.e., highly red-shifted) galaxies. Both technology and the nature of astronomical sources make the 1–2-micron-wavelength region suitable for such observations. Unfortunately for ground-based observations, the Earth's atmosphere in this range is plagued by strong and variable emission and absorption features, which interfere with observations of faint sources and molecular constituents that also occur in our atmosphere, such as water. For observations at wavelengths longer than ~2 microns, thermal emission from the Earth's atmosphere and from the telescope itself become the limiting factors. This situation has motivated multiple space missions with cold optics (e.g., *Infrared Astronomical Satellite*, *Infrared Space Observatory*, *Spitzer*, *Herschel*, *Wide-Field Infrared Survey Explorer*, and the upcoming *James Webb Space Telescope*).

Early in *Hubble*'s development, the value of including an infrared instrument was widely understood. The development of such an instrument for *Hubble* became an important driver of infrared-detector technology, with benefits accruing to other space missions as well as ground-based astronomy. The Near Infrared Camera and Multi-Object Spectrometer (NICMOS), which was installed in *Hubble* in 1997, defined a generation of ground-based detectors and validated *Hubble*'s potential for near infrared science. Today, Wide Field Camera 3 (WFC3), launched in 2009, includes an infrared channel for broad-band imaging and slitless spectroscopy limited primarily by the natural background in space.

Continued page 6

WFC3 IR from page 5

WFC3 incorporates the fruits of advancing detector technologies, offering 16 times the number of pixels of a NICMOS detector, greatly improved noise properties, and increased sensitivity.

Persistence

WFC3's infrared detectors have some known limitations, which we have strived to characterize and mitigate. Our initial expectation was that image persistence would be important, which has proven correct. In the *Institute Newsletter* (Vol. 29, Issue 1, **https://blogs.stsci.edu/newsletter/2012/07/30/persistence-and-after-images-in-wfc3ir-data/**), K. Long, S. Baggett, and K. Levay discussed image persistence and the strategies to cope with it. These strategies include careful planning of observation sequences (e.g., dithering multiple exposures), identifying the observations most likely to cause strong residual images and avoiding science observations for several hours after such observations, and developing a mechanism to track the exposure history of each pixel to predict persistence images. The implementation of spatial scanning (see *Institute Newsletter* Vol. 30, Issue 1, J. MacKenty, **https://blogs.stsci.edu/newsletter/2013/04/05/notes-from-the-wfc3-team/**) has opened the door for observations of targets brighter than ~10th magnitude. Spatial scanning creates very short *effective* exposure times as the source trails over a series of pixels. Combined with dispersion of the light using the slitless grisms, high signal-to-noise ratio observations of bright stars with transiting exoplanets are now possible. At the extreme, we have successfully measured Vega using these techniques and the grism in the –1st order.

Despite such advances, we have recently reached three interesting conclusions: (1) that the charge trapping causing persistence also has important consequences for the linearity and repeatability of short observations of bright targets, (2) that persistence from an intensive exposure of the detector may have effects that last many days, and (3) that subsequent exposure to moderate flux causes enhanced persistence. These phenomena represent a common theme: observers are pushing WFC3 to its limits and uncovering new factors to consider.

Zodiacal light

An original requirement on WFC3 stated that broad-band imaging and slitless spectroscopy must be limited by the zodiacal light. This requirement led to a design decision to limit the long-wavelength cutoff of the instrument to 1.7 microns, which avoided a dominant contribution from the thermal emission of the telescope. (This decision also had the consequence of permitting a straightforward and reliable approach to cooling the infrared detector.) Most WFC3 infrared observations encounter backgrounds of ~0.5 to 1.0 electrons per pixel per second. As a result, exposures longer than a few hundred seconds are background limited. Known exceptions include observing relatively close to the Sun, where the zodiacal light becomes much brighter, and in the rare circumstance that an observation skims along the bright limb of the Earth for a sustained interval.

Helium emission

Analysis of thousands of WFC3 infrared observations reveals a major exception to this background model. We sometimes encounter an excess background—by as much as five times—in two filters (F105W and F110W) and in both grisms (G102 and G141). Usually this excess is only present for part of an exposure. (WFC3 infrared exposures are obtained using multiple non-destructive readouts, so variations in the background during the exposure can be measured.) For the grisms, the two-dimensional structure of the observed background can vary, as well as the intensity within an exposure. These effects can become the limiting factor in analyzing such data.

We now understand that the source of this excess background is emission in the helium 1.0830 micron line from the terrestrial atmosphere. This emission is also observed from the ground during twilight—strong where the atmosphere is illuminated by the Sun, and vanishing inside the Earth's shadow.

Only these four grisms and filters in WFC3 transmit the helium wavelength.

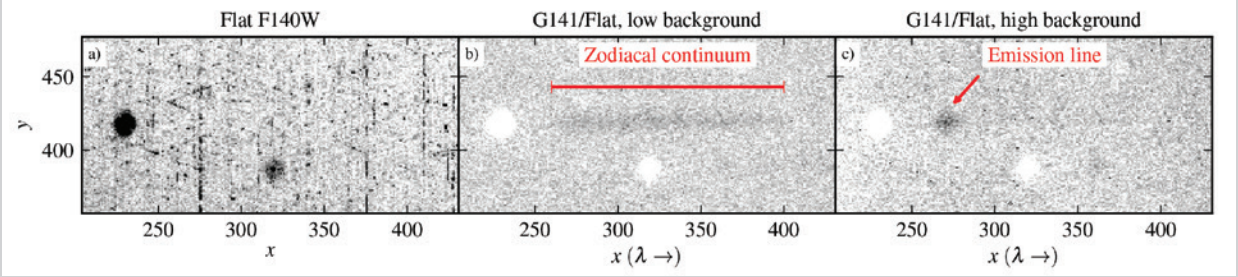

Figure 1: "Negative slit" spectra of the dust particles reveal the spectrum of a background source. (a) A flat field exposure using the F140W filter. (b) The smooth continuum of zodiacal light in observations taken when *Hubble* observes in the Earth's shadow. (c) Helium emission at 1.083 microns dominates spectra taken when *Hubble* observes the Earth's atmosphere illuminated by the Sun.

We have taken advantage of the presence of small particles on the mirror in the infrared channel that selects between the ultraviolet–visible and infrared channels. Its surface is nearly in focus on the infrared detector, and the particles appear as features in images. When the grisms are employed, however, each point within the field of view is dispersed as a spectrum. In this circumstance, particles act as "negative slits," producing a spectrum of the background (see Fig. 1). For the "normal" level of background, the negative spectrum is featureless, but when the helium emission is present, a strong emission feature is seen in the G102 and G141 grisms. Lesson: we can go to space, but cannot fully escape the terrestrial impacts on near-infrared observations in low-Earth orbit!

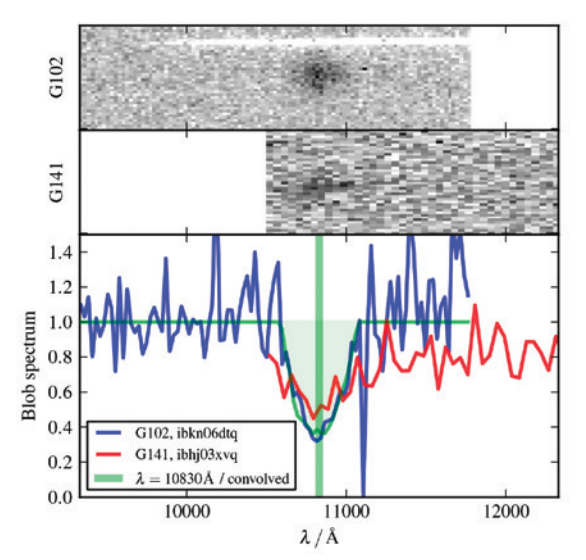

Figure 2: The emission-line component in the "negative slit" spectra occurs at the same wavelength—1.083 microns—in both the G102 and G141 grisms.

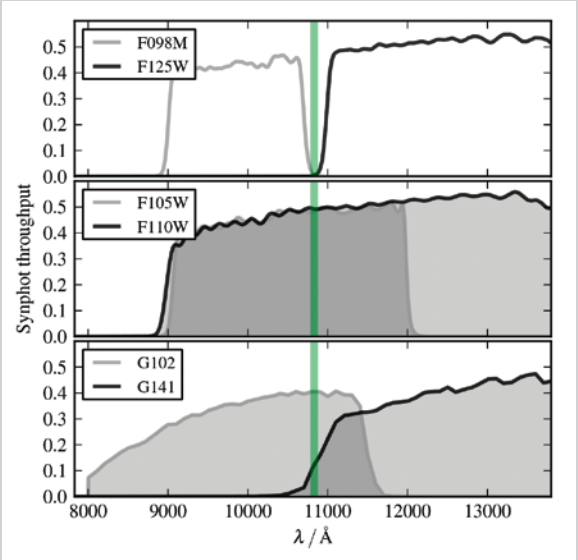

Figure 3: The F105W and F110W filters and both infrared grisms are sensitive to the He line at 1.083 microns. The F098M and F125W filters are not.

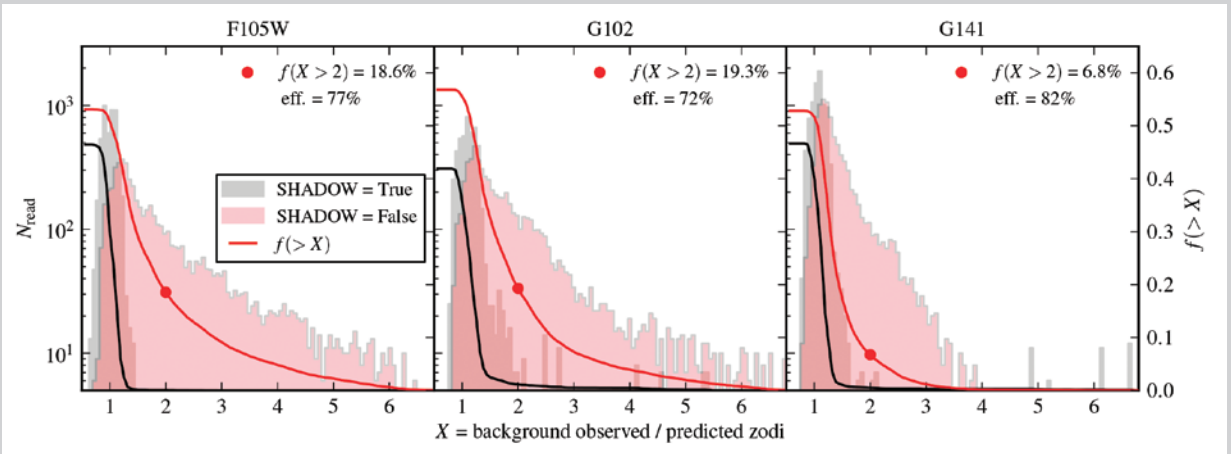

Figure 4: Distribution of background excess (over the nominal predicted zodiacal light) in individual WFC3/IR read-outs. The excess is caused by 1.0830-micron emission from helium in the illuminated Earth atmosphere. Nearly 20% of the WFC3/IR read-outs in the F105W filter and G102 grism show background levels more than twice the zodiacal "floor."

Pushing STIS Coronagraphy Deeper with New Coronagraphic Modes

John Debes, *debes@stsci.edu*, **Andras Gaspar,** *agaspar@as.arizona.edu*, **& Glenn Schneider,** *gschneider@as.arizona.edu*

The process of subtracting off or suppressing the diffracted and scattered light from a star is called "high-contrast" imaging. These techniques allow observers to detect circumstellar material and exoplanets in close proximity to stars. The starlight suppression required can be extreme: the light from exoplanets and dust structures can be as much as a thousandth or less than a billionth the brightness of their host star.

As detailed in a previous *Newsletter* article (Vol. 30 No 01; **https://blogs.stsci.edu/newsletter/2013/04/10/the-unique-coronagraphic-capabilities-of-stis-direct-imaging/**), the Space Telescope Imaging Spectrograph (STIS) possesses unique visible-light coronagraphic modes that keep the instrument at the forefront of exoplanet and debris-disk research. In Cycle 22, a new coronagraphic position is available that will push even closer to nearby bright stars. A damaged but now commissioned, coronagraphic, image-plane occulter in the 50CORON aperture is nicknamed "the bent finger."

The BAR5 aperture

Figure 1 shows a schematic of the 50CORON aperture of STIS, which includes two wedges, a large occulting bar, and the bent finger. Historically, this finger was named BAR5, which denoted the length of the bar, rather than its width. The second, larger occulting bar at the top of the detector is named BAR10, while the two wedges comprise the bulk of positions used for high-contrast imaging. Currently, the narrowest supported position in 50CORON is at WEDGEA0.6, corresponding to a minimum inner working angle of 300 mas.

BAR5 was damaged during the construction of the STIS instrument and thus was never activated as a usable coronagraphic position on the detector—primarily due to concerns that BAR5 might not be stable. After nearly two decades in orbit, BAR5 has not appreciably moved relative to the other occulting masks in the aperture. An outsourced calibration program 12923 (PI: Gaspar) in Cycle 20 was

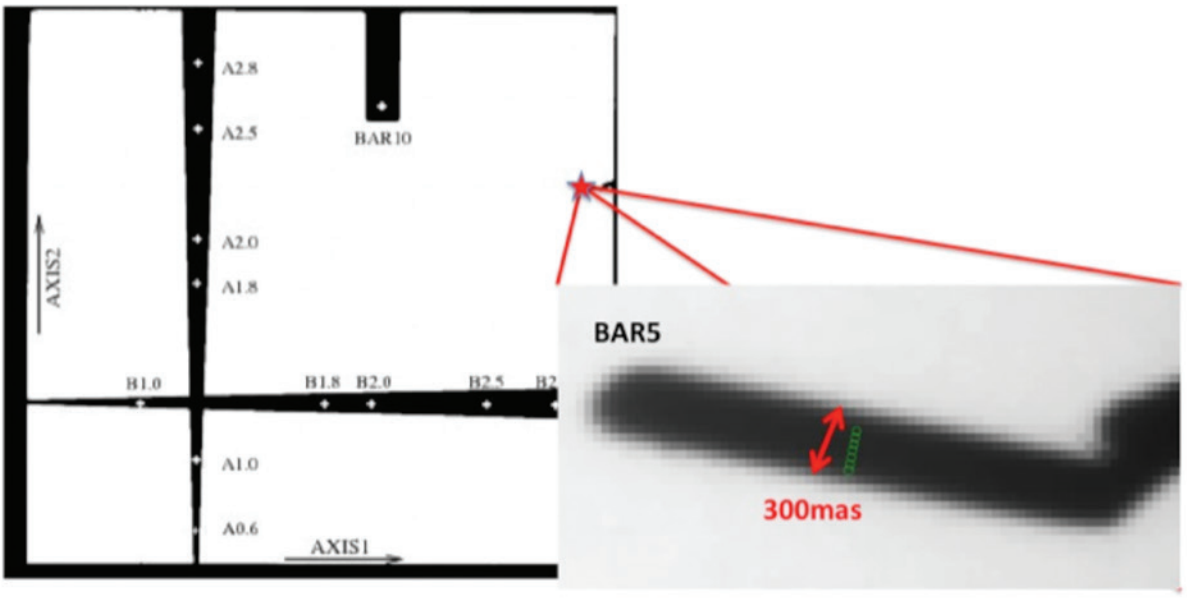

Figure 1: Full STIS 50CORON aperture including two wedges, a wide bar, and a coronagraphic finger that was bent during the assembly of STIS named BAR5. Due to its stability, BAR5 was investigated for a new coronagraphic position on the aperture that decreases the inner working angle to 150 mas, a factor of two smaller than the smallest wedge position, WEDGEA0.6. For a full listing of all supported positions, see (**http://www.stsci.edu/hst/stis/documents/handbooks/currentIHB/c12_special12.html**).

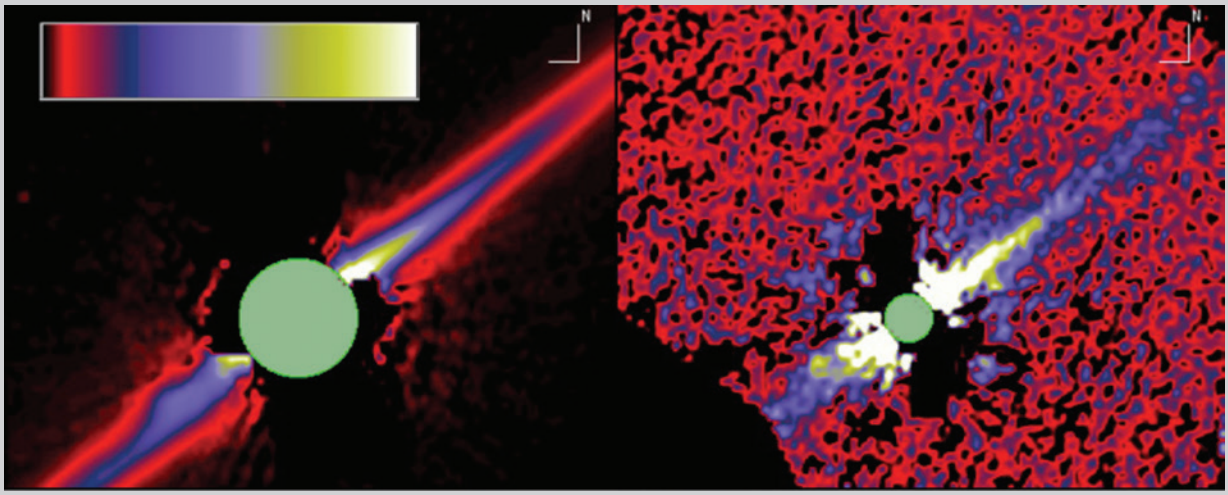

Figure 2: Comparing the AU Microscopii observations obtained in program 12228 (*left*: 12 ksec total integration time, inner working angle = 500 mas), with those obtained in program 12923 (*right*: 23 seconds total integration time, inner working angle = 200 mas). The images are on the same image flux and spatial scale, orientation, and linear display dynamic range: 0 to 15 counts/sec per pixel.

accepted to determine the positional offsets needed to reliably place stars behind the BAR5 mask, and to test its viability for starlight suppression at the smallest inner working angle ever offered by *Hubble*.

Pushing to smaller inner working angles

Program 12923 tested three separate positions on the detector that could allow inner working angles smaller than WEDGEA0.6: the middle of BAR5, and the lower left- and lower right-hand corners of the BAR10 mask. Such moves required a precise knowledge of how the plate scale of the detector and the geometric distortion were defined in the flight software and in the STIS space instrument aperture file.

The program was designed to take observations of four stars at the three new aperture locations. Two target stars, known to host debris disks, have very different spectral types and brightnesses: AU Microspii (M1) and β Pictoris (A6). The other two are reference stars for the point-spread function (PSF). Offsets relative to the BAR10 fiducial location placed the stars near the corners of the BAR10 mask and in the center of the BAR5 mask. To optimize contrast, small dithers mapped the edges of the mask at high precision. In addition, the dithers helped to further optimize for small, sub-pixel shifts that occur when the 50CORON focal plane masks are moved into the field of view.

Observations of the stars executed nominally, and initial results at all three positions succeeded in obtaining both raw and PSF-subtracted, high-contrast imaging at apparent separations <300 mas. Figure 2 shows PSF-subtracted images of AU Microscopii from program 12228 (PI: Schneider) obtained at six separate spacecraft orientations, with a combination of the WEDGEA1.0 and WEDGEA0.6 positions compared with the shallower, exploratory observations taken with 12923 at BAR5. The edge-on debris disk of AU Microscopii is recovered to ~200 mas, close to the limit of the BAR5 inner working angle and corresponding to a physical separation of 2 AU at AU Microscopii's distance of 10 pc.

A Visible Legacy for *Webb*

The availability of these new coronagraphic mask locations in the 50CORON aperture will provide a legacy of high-contrast, visible-light imaging for *Webb*. In particular, the 200 mas inner working angle obtained in program 12923 is similar to the offering of NIRCAM's coronagraphic occulting wedges (~4λ/D or 270 mas) at 2.1 microns. STIS's visible-light coronagraphy of circumstellar material and substellar objects will provide the contrast and spatial resolution for a range of targets at a level comparable to future observations with *Webb*, which will allow multi-wavelength studies spanning from the visible to the infrared.

Bruce Woodgate

Matt Mountain, mmountain@stsci.edu, Bill Oegerle, william.oegerle@nasa.gov, & Ken Sembach, sembach@stsci.edu

It is with heavy hearts that we pass along the sad news of the passing of Bruce Woodgate. Bruce was an exceptional man—kind, thoughtful, and generous with his time and his ideas. For those in our community who may not have personally known Bruce, you surely identify him as the principal investigator (PI) of the Space Telescope Imaging Spectrograph (STIS) and thereby recognize his profound impact on *Hubble*'s science program. Those of us who had the pleasure of working with him on various projects will always remember his clarity of vision and purpose, and his insatiable desire to innovate. Bruce's legacy to the field of astronomy is broad and enduring, represented not only by the scientific papers he authored, but also the research of the thousands of astronomers who have used—and continue to use—the instruments Bruce built to explore the universe. He was a master instrument builder on whose shoulders we stand. Bruce will be sorely missed.

Bruce Woodgate. (Photo courtesy of David P. Friedlander.)

Bruce had a remarkable career, spanning nearly 40 years as a civil servant at Goddard. He retired recently and was still working on ultraviolet detectors as an emeritus scientist. Bruce had very broad interests, in subjects ranging from earth science to stellar atmospheres to exoplanets to the large-scale structure in the universe—and of course, instrumentation of all sorts. We can't possibly list all his endeavors here, but here a few highlights.

In 1974, Bruce served as co-PI and experiment manager for the Ultraviolet Spectrometer and Polarimeter (UVSP) on the *Solar Maximum Mission* (*SMM*). In this capacity he was responsible for the design, development, testing and post-launch operation of the instrument. A number of important results were obtained with the UVSP. Bruce was also the *SMM* Project Scientist from 1983 to early 1986, leading the science team through the preparations for and aftermath of the 1984 *SMM* repair mission on STS-41C—NASA's first in-space satellite repair.

Bruce was probably best known as the PI for STIS, a second-generation instrument for the *Hubble Space Telescope*. In this capacity he led the design and development of the instrument, including preparation of flight-worthy large-format CCDs and Multi Anode Multi Array detectors. STIS dramatically advanced the state of the art over the previous *Hubble* spectrographs. STIS was installed on *Hubble* in 1997 and operated for seven years, until a power-supply failure occurred. STIS was repaired in 2009 during the final *Hubble* servicing mission, and it operates well to this day. STIS has proved to be a very versatile instrument and has played a key role in several of *Hubble*'s most famous discoveries, including (1) spatially resolved spectroscopy of the nuclei of galaxies, indicating the presence of supermassive black holes, and (2) the first detection of the atmospheric composition of a planet around another star (HD 209458), in which sodium, carbon, oxygen, and hydrogen were discovered. STIS has also enabled new discoveries about the nature of proto-planetary disks, supernova remnants, massive stars, and the intergalactic medium.

Bruce was also a tireless inventor of new technologies. Early in his career, he developed a technique for making conically shaped mosaics of thin crystals to produce large-area x-ray spectrometers. The two crystal-cleaving machines developed to produce thin crystal wafers are known worldwide. Bruce was co-inventor of the earlier of these two machines, holding a U. S. patent. More recently, he was developing a next generation photon-counting UV detector, employing advances in solid-state physics and nano-fabrication techniques.

A measure of Woodgate's research impact is his publication record: he has published 188 scientific and technical journal papers that have over 5300 citations. He has received Goddard's Award of Merit and the NASA's Distinguished Service Medal.

Descriptions of Bruce's scientific and technical accomplishments do not tell the whole story of his impact on the profession of astronomy. He mentored legions of students and young scientists and was a friend to everyone.

Bruce was born in Eastbourne, East Sussex, England and received his PhD from the University College London. After holding positions at Columbia University and Goddard Institute for Space Studies in New York, Bruce came to Goddard Space Flight Center in 1975, where he remained for the rest of his career. Bruce is survived by his wife, Patricia, and their two daughters, Cathy and Nina.

About the *Hubble* Cycle 21 TAC Ombudsperson Report

Neill Reid, inr@stsci.edu

Developing a time-allocation system that is both equitable and tuned to enable the highest-impact science is a key responsibility for every astronomical observatory. Like most observatories, the Space Telescope Science Institute employs a system based on community peer review; as at other observatories, those processes are reviewed periodically and, if necessary, modified to eliminate potential bias and better match community priorities. In that context, Matt Mountain, the Institute Director, decided to appoint an ombudsperson for the Cycle 21 Telescope Allocation Committee (TAC). The ombudsperson was asked to provide an independent review of the TAC process, and was also empowered to contact individuals in the community prior to the TAC meeting, to obtain a direct understanding of any issues that might have been raised with regard to the process. The conclusions and recommendations are summarized in a report submitted to the director, discussed with the Space Telescope Users' Committee (STUC), and released to the community. The ombudsperson's responsibilities do not extend beyond the TAC meeting; that is, s/he was not charged with contacting community members for feedback after the meeting.

Dr. Fred Lo, the former director of the National Radio Astronomical Observatory, agreed to serve as the Cycle 21 TAC ombudsperson. He attended the Cycle 21 TAC meeting held on 14–18 May 2013. The formal charge is given below, followed by his report, which was circulated to the STUC and discussed at their October 2013 meeting. Also below, we outline some of the actions taken in response to Dr. Lo's report to modify the procedures for the Cycle 22 *Hubble* TAC.

Actions

In consultation with the STUC, we have made a number of changes to the Cycle 22 TAC process to address the issues raised in the Cycle 21 report:

Workload – chairs

Both the ombudsperson and TAC members commented on the heavy workload for panel chairs. Panel chairs were required to submit preliminary grades for TAC proposals. They did not submit preliminary grades for panel proposals, but they participated in the review and grading of those proposals during the panel meeting. They were also asked to review a subset of the medium proposals. Separate panels initially reviewed the latter proposals, and only the highest ranked were put forward for TAC review. As a result, the panel chairs did not receive most of the medium proposals until midway through the TAC meeting.

In the future, we will employ a number of means to reduce the workload. Starting in Cycle 22, the chairs will be asked to run the panel meetings, but they will not vote on the proposals. This process is similar to that adopted in the current NRAO review, where panel chairs only vote on proposals if there are conflicts among panel members. We will also allow more time to review the medium proposals by using the preliminary grades to identify and circulate the top-ranked 40% prior to the TAC meeting. This will provide the chairs with more time to familiarize themselves with the proposals that are likely to be selected by the panels.

Workload – panelists

Some panels face heavy workloads, with between 80 and 90 submitted proposals.

We will reduce this workload by asking a subset of the panel to provide preliminary grades for each proposal. We are also advancing the deadline for submitting preliminary grades, which will enable us to construct and circulate the triage lists for each panel approximately one week before the meeting. All unconflicted panelists will discuss and vote on proposals at the panel meeting.

Schedule and panel seniority

A major reason given for declining service on the TAC is its coincidence with final examinations at many universities.

In an effort to improve the success rate in attracting more senior members of the community, we have adjusted the schedule by moving the Cycle 22 meeting to June. We note that the overall success rate for panelists' recruitment increased from 52% in Cycle 21 to more than 58% in Cycle 22. The success rate continues to be lower for more senior scientists.

Research areas

We recognize that certain sections of the community feel that they are at a disadvantage with the current TAC structure.

We are looking into how we can identify and mitigate such issues in an appropriate fashion.

Continued page 12

TAC Report from page 11

Triage

We have analyzed the distribution of preliminary grades for proposals that were ultimately recommended for acceptance in the Cycle 20 and 21 reviews. We found that 79% and 75%, respectively, of the accepted proposals were in the top 30% of the preliminary rankings. In both cycles, 95% of the accepted proposals were in the top 50% of preliminary rankings, with a further 3% between the 50th and 60th percentiles. Our current procedures are to flag the top 60% of proposals for discussion, and triage lower-ranked proposals. Thus, the overwhelming majority of proposals are initially ranked well above the triage cutoff, suggesting that the current approach is reasonable.

Expertise

The Hubble TAC assigns time and, for U.S. proposers, recommends grant funding. As a result, NASA's conflict-of-interest rules govern the process and limits which panelists may discuss and grade specific proposals.

We have mitigated the effects to some extent by defining separate categories for major and minor conflicts. Panelists with minor conflicts (institutional, close collaborator) may contribute to the proposal discussion but may not vote.

Conflicts are a particular problem on the super-TAC, where the extensive teams associated with large and Treasury proposals can lead to multiple institutional conflicts.

When those proposals are circulated to a subset of the panels and discussed by the panelists, the chairs are allowed to exploit their expertise.

Even so, it is possible that most of the relevant experts are not permitted to comment on a proposal.

We will address this issue by obtaining three written reviews from community experts for each proposal reviewed by the super-TAC. Those experts will be chosen to avoid conflicts, and, as with NSF proposals, will be asked to comment on the strengths and weaknesses of each proposal, not whether they believe a given proposal should be awarded time. We will collect those reviews and distribute them to the super-TAC members prior to their submitting preliminary grades before the TAC meeting.

Dr. Lo has agreed to return as TAC ombudsperson for the Cycle 22 TAC and provide his perspective on these procedural changes.

TAC Members

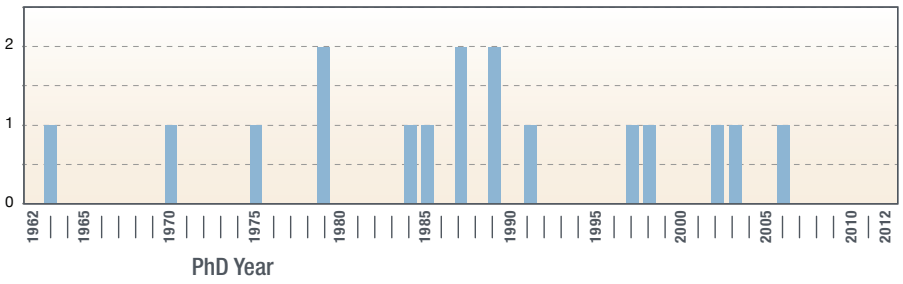

Panel Members

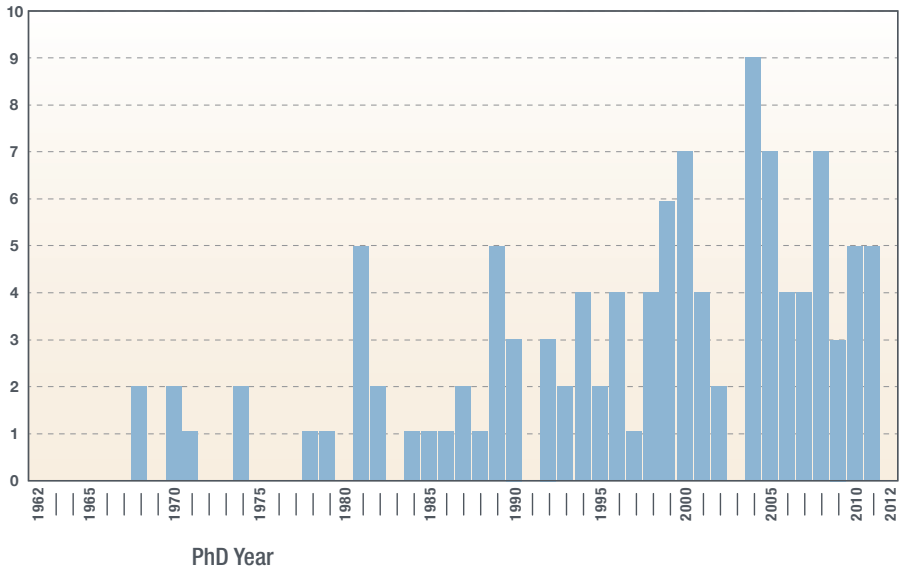

Report to the Space Telescope Science Institute Director

The Ombudsperson's View of the *HST* Cycle 21 Telescope Allocation Committee Process

Fred K. Y. Lo Distinguished Astronomer and Director-Emeritus, NRAO

June 2013

In response to some complaints and issues raised about the *Hubble Space Telescope* (*HST*) Telescope Allocation Committee (TAC) process, the Space Telescope Science Institute (STScI) Director, Matt Mountain, asked that I serve as an ombudsperson to observe the Cycle 21 TAC process and report my findings on the fairness of the process. Since I had gained some experience in this most important process of an observatory in my tenure as NRAO Director, via initiating an update of the NRAO TAC process and serving as Chair of the ALMA Board Subcommittee to formulate the ALMA TAC process, I agreed to serve, under a set of clearly defined charges to the ombudsperson (see Appendix).

Prior to attending the Cycle 21 TAC meetings in Baltimore, I talked on the phone to a number of *HST* users and to the relevant staff of the *Spitzer* and *Chandra* space telescopes about their TAC process, in order to gain the relevant perspective on the issues involved. I then attended in person a few panel meetings and essentially the entire TAC meetings, as an observer just watching and listening to the discussions.

Overall, I was very impressed by the dedication of the panel members and the chairs (who also constitute the TAC). I noted in particular the workload of the panel chairs was overwhelming, in my opinion. It was also clear the STScI staff very professionally organized the meetings.

Specific issues with the *HST* TAC process brought to the attention of the STScI Director included the following: (1) research areas that are not popular (in terms of proposal pressure) or topics that appeared to be old-fashioned (e.g., outstanding fundamental problems from years ago) had been overlooked by the TAC process, so that (2) astronomers in these areas have been "conditioned" and thus discouraged to submit *HST* proposals.

From my observations of the proceedings, talking to some panel members and users in these areas, I would judge these issues can be real. On the other hand, how much key science had been missed as a result was harder to tell. I believe these issues arose as unintended consequences of a process designed to address proposal pressure. Allocating time in proportion to proposal pressure is clearly the best way to satisfy the largest number of proposers. However, it is a reasonable question to ask whether responding to proposal pressure is the best or only way to elicit the best science. For example, should there be specific calls for "out of the box" proposals to use the Director's Discretionary Time or special orbit allocations?

Another concern raised was whether reviews of proposals were unduly influenced by the sociological factors of competing groups. Very importantly, I did not sense any egregious bias (scientific or otherwise) in the discussions of the scientific merit of the proposals in the TAC meetings and the panel meetings that I sat through. I did note a very few instances of personal scientific preference and undue (and even mistaken) concerns on scheduling practicalities getting in the way, but at a level that I deemed as par for course in any process that relies on personal judgment. A more proactive but appropriate monitoring of such exchanges by the panel and TAC chairs, and the STScI staff on technical and scheduling issues, should help confine the focus of the discussions mainly on scientific merits.

One concern that came up in my initial background check was the balance of the senior versus junior members on the panels and TAC. I could not judge the balance in the panels and how the balance affected the panel discussions, as I only sat in on only a few panels very briefly, but the TAC composition and the level of discussions appeared reasonable. I have since been provided with the distributions of PhD years of the panel and TAC members in Cycle 21, shown as Figure 1. The distributions indicate that the panel membership is somewhat skewed towards junior scientists, whereas the TAC membership is more evenly distributed.

Apparently, the success rate of recruiting senior astronomers to serve on the panels has become progressively lower over the years, and it is not for want of recruiting efforts by the STScI staff. This is a crucial community service issue that the STScI needs to address together with the Astronomy community at large.

Continued page 14

TAC Report
from page 13

From observing the TAC process, what became obvious very quickly was the very heavy workload on the panel chairs. The panel members had to review ~70 small proposals plus advise the panel chairs on ~7 medium and large proposals. On the other hand, the panel chairs had to review the small proposals in their panels plus ~90 medium and large proposals that cover all science categories. Getting all the evaluation and voting done during the week of meetings seemed especially daunting for the panel chairs/TAC members. While the TAC members discharged their duties admirably well, I wonder if this overwhelming burden can result in less than optimum evaluation of the large and medium proposals that asked for very significant resources from the *HST*.

Since all TAC members (chairs of the 14 panels of 6 scientific categories) voted on all the large and medium proposals, a significant fraction of the TAC may not have had the appropriate expertise on any given individual proposal. While two experts led the TAC discussions of each proposal, the non-expert TAC members tended to take part only by listening to the discussions of the experts. So, one could argue a significant fraction of the votes on the medium and large proposals may have been based largely on indirect assessment only. This potential problem can also be aggravated by a reduction of expert TAC members who could not vote due to potential conflict of interest.

Another issue that should be examined is the triage of the large proposals. Currently, the triage was based on preliminary grades by the panel chairs submitted within the first days of the TAC proceedings. While in principle the triaged proposals could be salvaged for further consideration by the TAC, in practice the TAC members were so busy that there was insufficient time and attention to examine the triaged proposals systematically for salvage. I had an uneasy feeling about whether the current triage process allowed the possibility of "throwing away the baby along with the bathwater."

To address the concerns noted above on the large and medium proposals, perhaps some variation of the following procedures should be considered for adoption by the *HST* TAC process: (1) asking the panels to review small, medium and large proposals within their scientific categories, but only recommend time allocation for small proposals, which would ensure the review and grading of large and medium proposals are by experts, (2) mailing out the large and medium proposals to additional expert referees for written reviews, which would ensure sufficient expertise for the review, minimize potential conflict of interest and engage more senior astronomers. Given the above, (3) the TAC should be able to focus more on the broader views and issues in combining and balancing the panel recommendations on the small, medium and large proposals, which would also make the job of panel chairs/TAC members more manageable and I suspect more satisfying.

Finally, one of my charges is to assess the utility of the ombudsperson and recommend how frequently such a position should be incorporated in the TAC process. As ombudsperson, I specifically watched for how the process itself worked and would question (in my mind) the established procedures, whereas the TAC and the panel members, rightly so focused solely on the scientific evaluation within the established TAC process. From the perspective of assessing the TAC process, the ombudsperson was necessary. If the TAC process will be changed significantly for Cycle 22, I would think it is important to have an ombudsperson to judge how well the revised process works. Once the TAC process is stabilized, it is perhaps not necessary to have an ombudsperson for every cycle.

Appendix: TAC Ombudsperson Charter

The Telescope Allocation Committee (TAC) ombudsperson is charged by the STScI Director to investigate issues and complaints brought forward by members of the astronomical community with regard to the allocation of telescope time by a TAC process supervised by STScI. The ombudsperson is encouraged to make direct contact with community members to obtain further information on specific issues as the need may arise. Any such interactions should be treated as confidential.

The ombudsperson will observe the TAC process and consult with the STScI Director or designate to clarify any issues that might arise. S/he will conduct an independent assessment of the fairness of the process, and advise the Director on potential improvements that could be adopted for future TACs.

In addition, s/he will provide the Director with an assessment of the utility of the role of "ombudsperson" within the TAC process, and will advise on how frequently such a position might be incorporated in future TACs.

The ombudsperson will produce a report for the Director on the TAC process. The report will be made available to the community.

Specific issues for *HST* Cycle 21: The ombudsperson is asked to pay particular attention to discussions of proposals for Solar System, AGN, deep field and IGM research.

Turning Up the Science When the Weather Gets Cold

Rachel Osten, *osten@stsci.edu*

This winter's frigid weather was not enough to dampen the enthusiasm of attendees of the 2014 winter meeting of the American Astronomical Society (AAS), held in National Harbor, Maryland. The meeting offered several opportunities for the community to learn about activities within the *Webb* development project and about the mission's science prospects.

A special session was devoted to the fields of science that will be advanced by *Webb*. Marla Geha (Yale) described how *Webb* will impact studies of galaxy formation by making direct measurements of the stellar initial mass function in galaxies different from the Milky Way. Matthew Tiscareno (Cornell) reported on the wealth of solar-system science to be done with *Webb*, commenting that *Webb* may be able to witness the birth of new moons in the solar system. He described solar-system science as the "ground truth" for studies of exoplanetary systems. Alicia Soderberg (Harvard) discussed supernova studies with *Webb* and the importance of multi-wavelength observations in interpreting and understanding the explosions. She introduced a "sonification" technique to study the intricacies of each stellar explosion. Mark Wyatt (Cambridge) described how debris disks give insight into the architecture of planetary systems, and how *Webb* results will constrain models of planet formation and evolution. John Johnson (Harvard) discussed exoplanet characterization using *Webb*—measurements of planet radii and spectroscopy of the atmospheres of Earth-like planets—which will complement *Kepler* results and research by other new missions and ground-based surveys (Figure 1). The presentation slides at the *Webb* special session are available at **http://www.stsci.edu/jwst/doc-archive/presentations**.

For the first time, the *Hubble* and *Webb* missions held a joint town hall meeting at the AAS, to apprise the community on the performance of *Hubble* and the progress on *Webb*. The Institute's Ken Sembach updated the audience on the health of *Hubble*, and noted that an overlap of one or more years of operations appears feasible. Eric Smith from NASA Headquarters described the achievements of the *Webb* project during 2013, including completion and delivery of numerous components of the observatory (see Figure 2). The

Figure 1: (*top*) John Johnson giving one of the talks in the *Webb* science session at the AAS meeting. (Photo courtesy of Jason Kalirai). (*bottom*) Photo montage of Google hangouts at the Institute booth. (Photos courtesy of Tony Darnell.)

JWST *AAS* from page 15

accompanying article by Scott Friedman and Randy Kimble discusses the first cryogenic tests of the integrated science instrument module. Adam Riess, of the Johns Hopkins University and the Institute, gave a science talk on narrow-field, precision cosmology with *Hubble* and *Webb*, describing how *Webb* can realize a one percent error on the Hubble Constant. (The town-hall presentations are also at the above web link.)

Webb was featured in talks at an exhibit about future missions organized by NASA Headquarters. The *Webb* team also arranged several field trips, on the last day of the meeting, for attendees to visit NASA's Goddard Space Flight Center, where several components of *Webb* (e.g., mirrors and instruments) are undergoing tests. The Institute also led several activities involving social media and public outreach related to *Webb*. Employing Twitter to communicate with the public, we promoted *Webb* opportunities, broadcast news items, and highlighted synergies with science presented at the meeting. We counted ~20,000 tweets during the AAS meeting, and "#JWST" was one of the most widely used hashtags.

The Institute also organized numerous Google hangouts, live from the AAS, which included interviews with NASA and community program scientists, students and postdocs, and even high school students who presented research at the meeting.

Scientists from the Institute interacted with other astronomers at the AAS about new developments in the *Webb* proposal-planning process. They gave demonstrations of the new planning tool for NIRSpec's multi-object spectroscopy (see article by Diane Karakla in this edition of the *Newsletter*). Institute scientists also sought community feedback in the form of user surveys, for example, about the vision for the *Webb* exposure time calculator, and about formats for disseminated documents and other information.

Figure 2: Photo montage of progress in 2013 on different aspects of the *Webb* mission. Photo courtesy of Eric Smith (NASA Headquarters).

Engaging the Science Community: the *Webb* Science Corner

Even though the launch of the *Webb* mission is still four years away, momentum is building in the astronomical community, anticipating the types of scientific advances *Webb* will make possible. Since the re-planning of the mission in 2011, an average of about 15 papers per month have appeared in the refereed scientific literature with a mention of how *Webb* will address the questions pertaining to a particular science topic. The Institute is harnessing this enthusiasm by organizing a "*Webb* Science Corner" (**http://www.stsci.edu/jwst/jwst-science-corner/**). To build the material available at this site, we canvass the current literature and invite authors to provide a short description of how *Webb* will advance their science. The response has

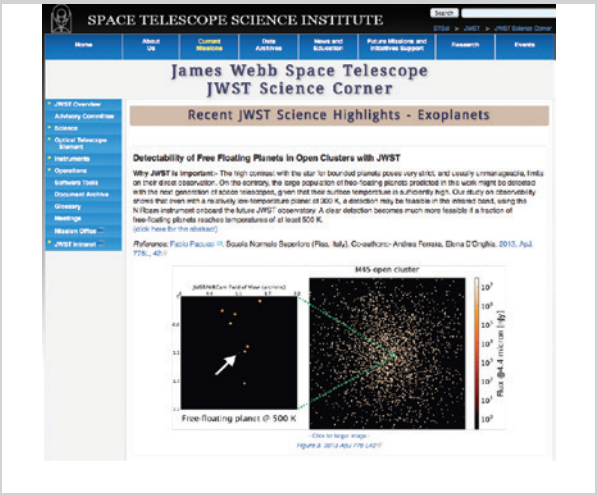

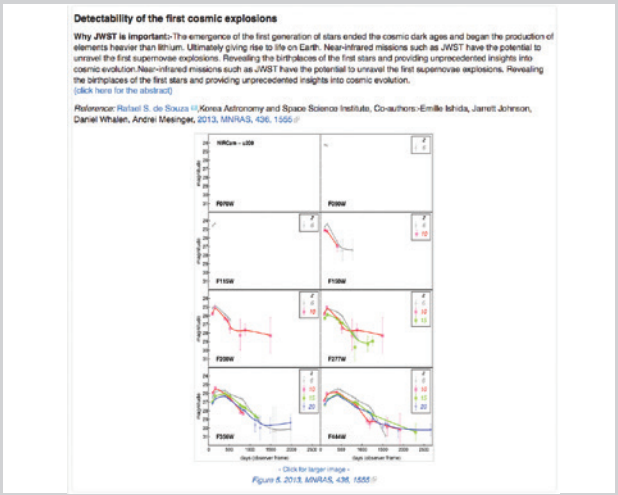

Figure 3: The *Webb* Science Corner features recent results from refereed science papers that discuss how *Webb* will advance the science in their field. These papers discuss, respectively, the detectability of free-floating planets in open clusters (*left side* of the figure) and the detectability of the first cosmic explosions with *Webb* (*right side* of the figure).

Figure 4: The Institute's Frank Summers discussing the *Webb* mission to attendees at the SXSW festival in Austin. The *Webb* 13-foot mirror display is visible to the left, and the interactive Microsoft screen is on the right. Image credit: Mike McClare.

been overwhelmingly positive, and to date, more than three-quarters of those approached have agreed. The science topics are diverse, covering the whole gamut from star formation to exoplanet science, to topics in the high-redshift universe.

As an example, Fabio Pacucci of Scuola Normale Superiore in Pisa, Italy, published a paper describing the detectability of free-floating planets in open clusters with *Webb* (2013 ApJ, 778, L42). The paper predicts that a large population of these exotic objects could be detected with near-infrared imaging with *Webb*—possibly planets as cold as 300 K, and certainly any planet as warm as 500 K. This research would explore diverse modes of planet formation and offer a unique insight into the dynamics of dense stellar systems.

Rafael de Souza of the Korean Astronomy and Space Science Institute recently wrote a paper discussing the detectability of the first cosmic explosions in the universe (2013 MNRAS, 436, 1555). The stars producing the first supernovae explosions signal the end of the cosmic dark ages and the beginning of heavy-element production. While these population III stars have eluded detection thus far, simulations of the death of massive, first-generation stars—coupled with a realistic observing strategy using *Webb*—have found that the brightnesses and detection rates are feasible. Locating the birthplaces of these first stars is important for understanding cosmic evolution.

If you have a paper that discusses the utility of *Webb* observations to tackle one of the broader current science questions, please consider contributing to the *Webb* Science Corner at **http://www.stsci.edu/jwst/jwst-science-corner/submit-information-jwst-science-corner**.

South by Southwest, Take Two

The Institute partnered with NASA Goddard, NASA Ames, Northrop Grumman and University of Texas (UT), Austin to bring *Webb* and *Hubble* back to the South by Southwest (SXSW) Festival in Austin, TX, from March 7–9, 2014. The team reached thousands in the general public with messages about *Webb*, *Hubble*, and *Kepler* in events ranging from public talks at UT Austin to the official SXSW interactive panel, "First Signs: Finding Life on other Planets." Social media reached millions more. During the festival, *Webb* and *Kepler* scientists also participated in a highly successful "Tweet Chat," where the general public asked science-related questions via Twitter; this interaction resulted in 9.8 million impressions. The booth featured the Institute's 13-foot mirror display and interactive Microsoft screens that allowed astronomers to engage the crowd through incredible, high-quality *Hubble* and *Kepler* imagery (see Figure 4).

SXSW brings together leaders in innovation from around the world, and the *Webb* and *Hubble* display fit right in among the festival highlights. One participant walked away from the booth telling his friend, "That was the best conversation I've ever had in my life!" Visitors at the exhibit spanned all ages, from children to adults—many remembering the *Webb* full-scale model display from the year before—and all sharing their enthusiasm to unlock the great mysteries of the universe when *Webb* launches in 2018.

Rachel Osten is the Institute's Deputy Project Scientist for the *James Webb Space Telescope.*

Aperture-Masking Interferometry with *Webb*'s NIRISS

Anand Sivaramakrishnan, *anand@stsci.edu*, **& Étienne Artigau,** *artigau@astro.umontreal.ca*

The *James Webb Space Telescope*'s Near Infrared Imager and Slitless Spectrograph (NIRISS) has a non-redundant mask (NRM) in its pupil wheel (Figure 1). This mask enables aperture-masking interferometry (AMI), a high-resolution, moderate-contrast imaging technique (e.g., Tuthill et al. 1999), which is gaining popularity in ground-based direct imaging of exoplanets and transition disks (e.g., Kraus & Ireland 2012). The 15% throughput, seven-hole mask offers simultaneous, multi-baseline interferometry with medium-bandwidth filters—F380M (5% bandwidth), F430M (5%), and F480M (8%)—and the broader F277W (25%) filter. Because NIRISS's 65-mas-square pixels satisfy the Nyquist criterion at 4 microns wavelength, the shorter-wavelength, F277W filter reduces AMI performance. Nevertheless, because F277W spans a deep absorption feature of water, its use with the NRM is still relevant for exoplanetary science.

When viewing a point source, the 21 unique (i.e., non-redundant) baselines—defined by pairs of holes in the mask—create a sharply peaked interferogram. This interferogram is actually just a point-spread function (PSF) with fine structure more than twice as sharp as the corresponding full-aperture PSF, but with much wider wings. The wings are imprinted with the fringe patterns created by the mask's multiple holes. These features of the NRM interferogram enable high-resolution imaging.

The AMI interferogram possesses certain observables—closure phases and amplitudes—which are used to remove instrumental effects by calibration. These observables allow the fitting of simple models, such as binary or triple point sources, at flux contrasts of up to about 10 stellar magnitudes. The search space of an NRM extends inwards to a separation of $\lambda/2B$, where B is the hole-to-hole length of the longest baseline. For fitting binary models as well as for true imaging—that is, not using closure relations or model-fitting—the NRM on NIRISS has an inner working angle (IWA) of about 70 mas.

Filter Name	80x80 subarray	2048x2048 full sensor
F480M	3.2	8.7
F430M	3.5	9.1
F380M	4.2	9.7
F277W	7	12.6

Table 1: NIRISS AMI point source saturation limits in Vega magnitudes for an AMI-specific 5.2 arcsec-square, 80-by-80 subarray, as well as the full 2 arcmin-square detector readout. The subarray readout enables AMI to follow up discoveries made by coronagraphic surveys using ground-based adaptive optics. The full detector readout is for high-resolution imaging of extended objects.

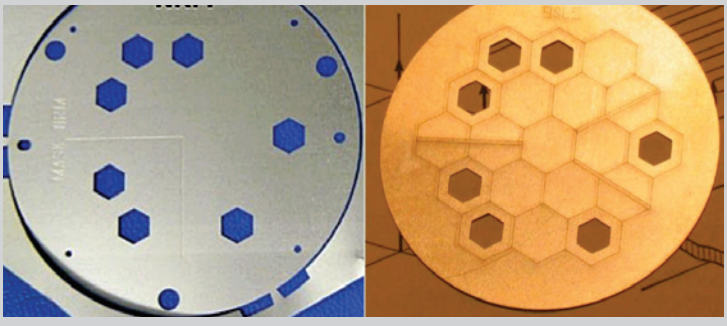

Figure 1: *Left:* NIRISS's titanium non-redundant mask (NRM) prior to blackening. No hole-to-hole, vector baseline is repeated. This ensures the non-redundancy of the mask's interferometric baselines. *Right:* A full-scale prototype NRM showing *Webb* primary mirror segments and secondary-mirror supports engraved on the part. In this re-imaged pupil plane, the diameter of the circumscribing circle of the full pupil is nominally 40 mm. The holes are undersized to allow for a pupil-placement error of up to 3.8% of the pupil diameter. Details on the design can be found in Sivaramakrishnan et al. (2009).

The performance of NIRISS AMI is complementary to the near-infrared coronagraphs on *Webb*, which offer higher dynamic range but larger IWAs, 400–500 mas in the 3–5 micron wavelength range. At these wavelengths, ground-based imaging and interferometry suffer from high thermal backgrounds and strong absorption by telluric steam. Ground-based adaptive optics systems in the *YJHK* bands are effective in stabilizing wavefront quality, but they do not stabilize transparency variations, which makes such imaging virtually impossible without the use of a simple prior model.

The science cases for NIRISS AMI include two types of follow-up observations of exoplanets: objects discovered by coronagraphic surveys using "extreme adaptive optics" (ExAO) at ground-based observatories, and massive planets discovered by astrometric and radial-velocity searches. The saturation limits of NIRISS AMI (Table 1) are bright enough to include most bright ExAO guide stars when a portion of the detector is read out rapidly.

AMI will also observe the close environs of the supermassive black holes (SMBHs) in brighter active galactic nuclei (AGNs), which should afford tests of cosmological theories and insights into galaxy evolution.

GPI and ESO SPHERE follow-up

Two ExAO, near-IR coronagraphs—the Gemini Planet Imager (GPI) and the European Southern Observatory

(ESO) Spectro-Polarimetric High-contrast Exoplanet REsearch (SPHERE)—will shortly commence ambitious surveys of young, nearby stars in order to directly detect and characterize massive, self-luminous planets. GPI, which saw first light at Gemini South in late 2013, will embark on a two-year, 900-hour survey (Macintosh et al. 2014). SPHERE will be used for a 500-night survey on the ESO Very Large Telescope (Beuzit et al. 2008). Both instruments are expected to find tens of self-luminous, gas-giant planets, and to follow up with low-resolution, 1–2.4 micron spectroscopy of the objects discovered. The spectroscopy will measure diagnostic spectral features, such as the molecular bands of CH_4 and H_2O. It will also probe gravity-sensitive features, such as the shape of the *H* band (Allers & Liu 2013).

A reliable measure of bolometric luminosity—for effective temperature and thermal history—calls for spectrophotometry at wavelengths longer than 2.5 microns, where giant planets emit most of their flux. NIRISS's moderate-contrast, AMI mode will enable four-filter photometry of planets between 2.7 and 4.8 microns. The majority of targets for GPI and SPHERE will be observable. AMI's multiple-point-source "sweet spot" is between 70 and 500 mas. At larger separations, the coronagraph in *Webb*'s NIRCam offers better performance (Beichman et al. 2010).

Figure 2 illustrates NIRISS AMI's limits in binary, point-source contrast, for a range of primary star brightness and a 5-σ detection threshold at 4.8 microns. Figure 3 shows the expected yield of the ground-based, GPI *YJHK,* Jovian-companion survey in a mid-infrared contrast-separation parameter space. The complementarity of NIRISS AMI and NIRCam coronagraphy is apparent.

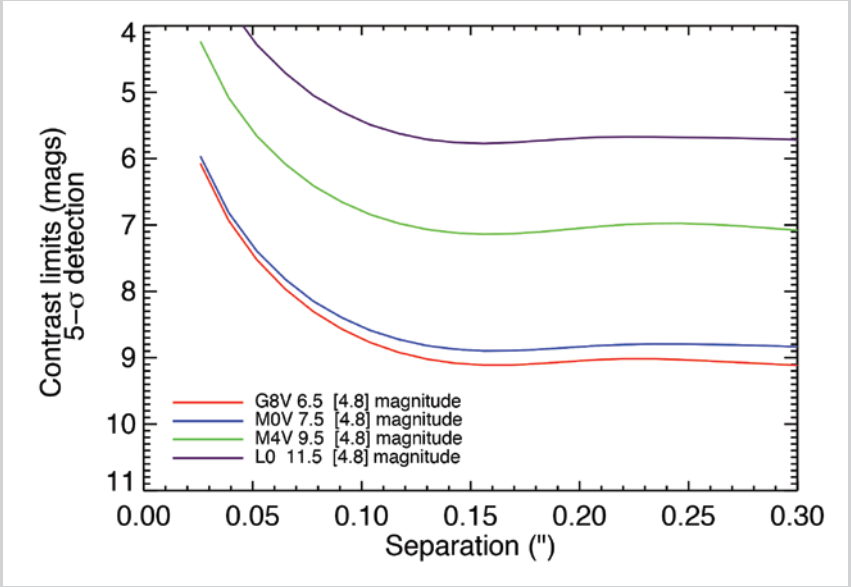

Figure 2: Contrast limits for 5-σ companion detection, for a range of [4.8] bandpass host star brightnesses that correspond to the indicated stellar types at a distance of 30 parsec.

High-contrast imaging of the kind performed on the HR8799 and Fomalhaut systems (Marois et al. 2008; Kalas et al. 2008), and even seeing-limited imaging (e.g., Ross 458c, GU Psc b; Goldman et al.

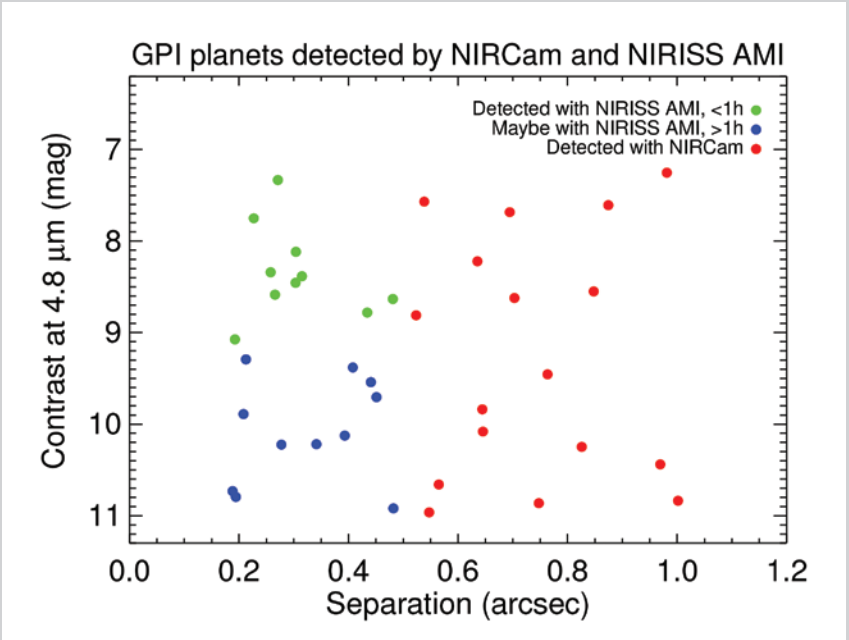

Figure 3: Mid-infrared contrast and separation of a sample of planets typical of the results expected from the GPI survey. Planets closer than 0.5 arcsec from their host will be followed-up with NIRISS AMI. Detection of the brightest planets should occur within 1 hour, while the remainder will require longer exposures.

Continued page 20

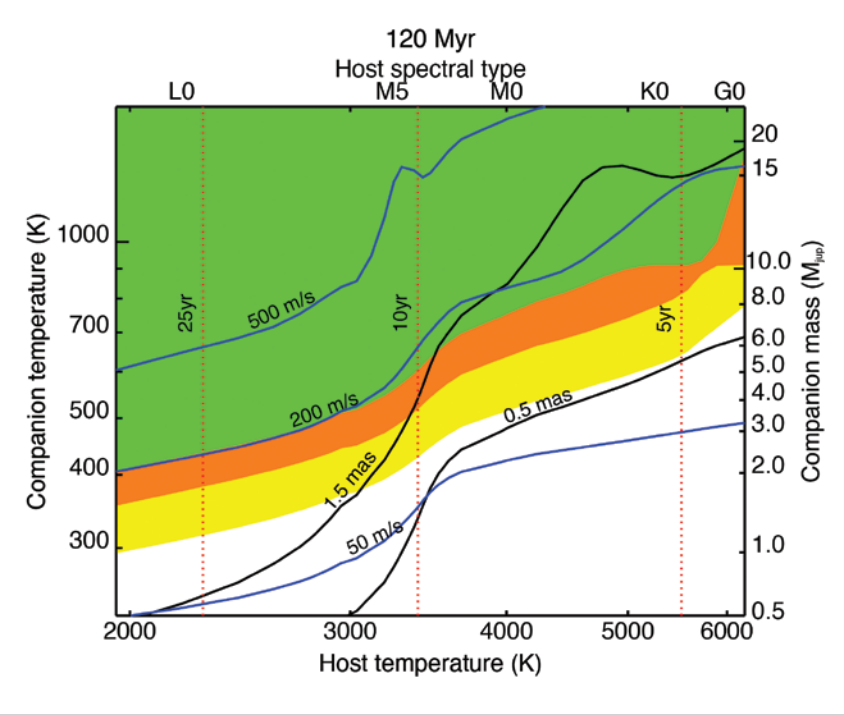

Figure 4: Planet detectability as a function of companion and host star temperature at 120 Myr, 30-pc distance, and 0.1 arcsec angular separation of the companion. These values correspond to a typical member of the AB Doradus moving group. The green region shows the parameter space where companions would have a >10-σ detection with a 1 hr integration, while orange and yellow contours give decreasingly significant detections down to 3-σ. Vertical lines give the orbital periods for such companions; for all stellar hosts earlier than spectral type ~L0 the orbital period would be shorter than 25 years. Lines indicating semi-amplitude of radial-velocity signal induced are shown, ranging between 50 m/s and 500 m/s. The astrometric signal is also shown.

2010; Naud et al. 2014), have so far been used only for about 30 of the thousand or so known exoplanets. Characterizing more of these objects will test models of planetary atmospheres. While the models have been applied to brown dwarfs, recent discoveries illustrate that planetary-mass companions differ from higher-gravity brown dwarfs, especially in the vertical extent of dust clouds in their atmosphere (Faherty et al. 2013). Various chemical species in brown dwarf and exoplanet atmospheres have gravity-sensitive absorption depths. Such a collisionally-induced H_2 absorption feature occurs in *K*. The depths of these features can be compared with models to constrain the mass and radius of a planet. These parameters can also be estimated using interior evolutionary models and age constraints inferred from their host star's properties, providing much needed cross-calibration. This cross-calibration is key to understanding field objects in both planetary-mass and brown dwarf mass regimes.

Small stars, big planets

Current estimates of mass for directly imaged exoplanets are derived from models that depend on an assumption about the host star's age. Obtaining a *direct* measurement of mass requires a planet with a short orbital period—less than 10–20 years—a reasonable timeframe for radial-velocity or astrometric monitoring to yield a result. To date, however, directly imaged planets have periods ranging from 50 yr (HR8799e) to tens of millennia, and none has afforded a direct mass measurement.

In the future, we expect the *combination* of indirect mass measurements and direct spectrophotometry to provide useful tests of both atmospheric and evolutionary models. The best bet may be nearby young M dwarfs showing astrometric acceleration or a trend in radial velocity. Within the next few years the *Gaia*'s data on M dwarfs within 50 pc is expected to discover every Jovian-mass planet within a few AU of these stars. Since the primaries are faint, modest-contrast imaging at 4 microns should detect low-mass planetary companions younger than 120 Myr. These planets are inaccessible to GPI and SPHERE because their adaptive-optics systems require guide stars brighter than any M dwarf.

Webb instruments should be able to detect exoplanets around M dwarfs, but high angular resolution is at a premium. A planet orbiting a 0.4 $M_{\odot}$ M dwarf with a 3 AU semi-major axis at 30 pc from the Sun—an angular separation of 100 mas—has a period of eight years. Kepler's Laws restrict the search space to within roughly 150 mas of the host star. At 4 microns, *Webb*'s coronagraphs cannot reach the

small separations available to NIRISS AMI, albeit at moderate—but sufficient—contrast. As shown in Figure 4, NIRISS AMI will be able to detect planets down to 2–3 Jupiter masses around late-type (M and L) dwarfs in nearby young associations.

AGN science with interferometric imaging

Accretion onto SMBHs (10^6–10^9 $M_\odot$) at the centers of AGNs is believed to play a key role in Lambda-Cold Dark Matter (ΛCDM) cosmology and galaxy formation (Silk & Nusser 2010). However, the extreme luminosities of AGN—10^{10}–10^{16} $L_\odot$ (Kauffmann & Heckmann 2009)—make imaging a challenge. The problem is exacerbated by the small angular size of the parsec-scale accretion flows at typical AGN distances, often more than 10 Mpc.

Ford et al. (2014) demonstrate that true imaging at 4–5 microns will enable NIRISS AMI to study of the environments of accreting SMBHs. After including realistic NIRISS and *Webb* noise sources and operational plans, Ford et al. report that AMI will map extended structure at 70 mas angular resolution and a dynamic range of 100:1 (Figure 5). Such data can test models of AGN binarity, feedback, fueling and structure, and will complement longer wavelength observations of the same targets by the Atacama Large Millimeter/submillimeter Array.

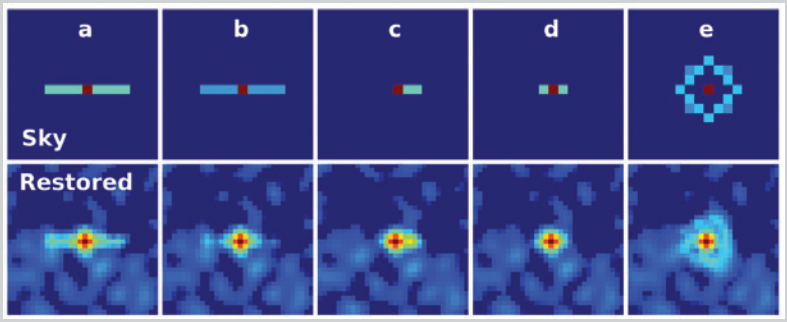

Figure 5: Synthesis imaging of Active Galactic Nuclei (AGN) environs using NIRISS AMI (after Ford et al. 2014). Simple AGN models consisting of a point-source nucleus and fainter extended structure—very thin bars and rings—are shown in the *top row,* on the NIRISS 65-mas pixel scale. At a distance of 10 Mpc one detector pixel spans 3.2 pc. The corresponding restored images (*bottom row*) combine two observations oriented perpendicularly. Such orientations would be spaced by about a quarter of the *Webb* orbital period. The restoration process utilizes a finer pixel scale than the detector pixels. The Multichannel Image Reconstruction Image Analysis and Display (MIRIAD) software package's CLEAN algorithm was used for these image reconstructions. This simulation suggests that a 100:1 pixel-to-pixel contrast is well within the reach of NIRISS AMI with expected levels of noise. Explanations: (a) The integrated flux from the bar is 1 magnitude fainter than the point source. (b) The bar is 2 magnitudes fainter than the point source. (c) An asymmetric 3-pixel bar with the same surface brightness as the bar in (a), and (d) a similar symmetric bar. (e) A 5-pixel diameter circular ring with integrated flux 1 magnitude fainter than the point source.

Comparable high-resolution imaging of AGN is not possible with any ground-based infrared interferometer or telescope for at least three reasons: (a) thermal background on ground-based telescopes limits them to a handful of bright targets, (b) fluctuating amplitude and phase error due to atmospheric variability hamper credible image reconstruction unless a prior model of the object is invoked, and (c) good adaptive-optics compensation is limited to the brightest few targets. NIRISS AMI can complete a survey of a dozen bright AGNs with a total of about 200 minutes of exposure, in spite of the non-redundant mask's 15% throughput.

The cosmological model of hierarchical galactic mergers predicts an abundance of SMBH mergers. If merging black holes continue to accrete, then binary AGN in galaxies should be commonplace. Nevertheless, very few such nuclei have been observed to date (Liu et al. 2010). NIRISS AMI will resolve binary AGN as close as 70 mas—17 pc at a distance of 50 Mpc. This performance improves upon current ground-based optical or IR interferometry, especially when dust obscures the AGN in the shorter *JHK* near-infrared bandpasses.

NIRISS is provided to the *Webb* project by the Canadian Space Agency (**http://www.asc-csa.gc.ca/eng/satellites/jwst/contribution.asp**). René Doyon (Université de Montréal) is the principal investigator, and COM DEV Canada is the prime contractor. More information about NIRISS is available on the NIRISS website at the Institute: (**http://www.stsci.edu/jwst/instruments/niriss**).

References

Allers, K. N., & Liu, M. C. 2013, ApJ, 772, 79
Beichman, C. A., et al. 2010, PASP, 122, 162
Beuzit, J.-L., et al. 2008, Proc. SPIE 7014
Faherty, J. K., et al. 2013, AJ, 145, 2
Ford, K. E. S., et al. 2014, ApJ, 783, 73
Goldman, B., Marsat, S., Henning, T., Clemens, C., & Greiner, J. 2010, MNRAS, 405, 1140
Kalas, P., et al., 2008, Science, 322, 1345
Kauffmann, G., & Heckman, T. 2009, MNRAS, 397, 135
Kraus, A. L., & Ireland, M. J. 2012, ApJ, 745, 5
Liu, X., et al. 2010, ApJ 715, L30
Macintosh, B. A., et al. 2014, PNAS; accepted
Marois, C., et al. 2008, Science, 322, 1348
Naud, M.-E., et al. 2014, ApJ, 787, 5
Silk, J., & Nusser, A. 2010, ApJ, 725, 556
Sivaramakrishnan, A., et al. 2009, Proc. SPIE 7440
Tuthill, P. G., Monnier, J. D., & Danchi, W. C. 1999, Nature, 398, 487

Introducing the NIRSpec Planning Tool for Multi-Object Spectroscopy

Diane Karakla, *dkarakla@stsci.edu*, **Alexander Shyrokov,** *shyrokov@stsci.edu*, **Klaus Pontoppidan,** *pontoppi@stsci.edu*, **Jason Tumlinson,** *tumlinson@stsci.edu*, **Tracy Beck,** *tbeck@stsci.edu*, **Susan Kassin,** *kassin@stsci.edu*, **Karoline Gilbert,** *kgilbert@stsci.edu*, **and David Soderblom,** *drs@stsci.edu*

The Near-Infrared Spectrograph (NIRSpec) will be the workhorse instrument on the *James Webb Space Telescope* for near-infrared spectroscopy. It will offer three spectral bands with spectral ranges from 1.0 to 1.8 microns, 1.7 to 3.0 microns, and 2.9 to 5.0 microns, with a choice of both medium ($R \sim 1000$), and high ($R \sim 2700$) resolution gratings. A low-resolution prism ($R \sim 100$) operating over the full spectral range from ~0.6 to 5 microns will also be available.

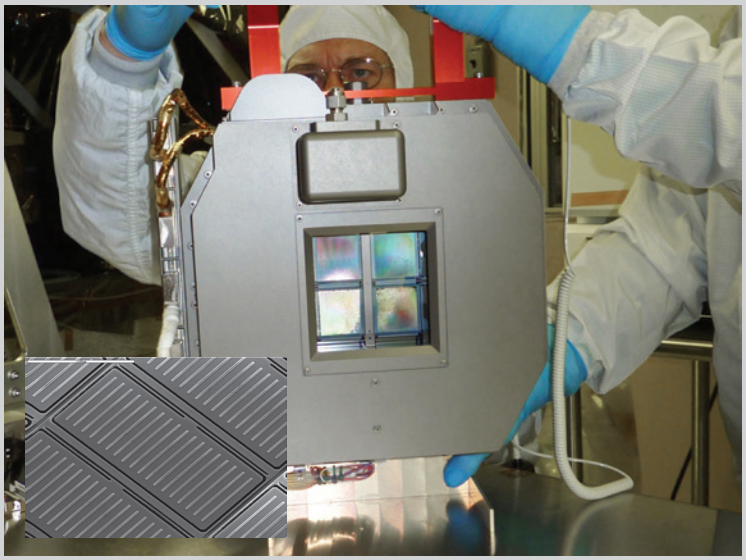

Figure 1: The four-quadrant MSA is shown above. The inset image shows a close-up view of the shutters of the MSA. A white bar indicating a length of 100 microns in the image is shown at the upper left. The MSA bars surrounding the shutters can be seen in the inset image, as well as the shutter hinges. (Images courtesy of NASA.)

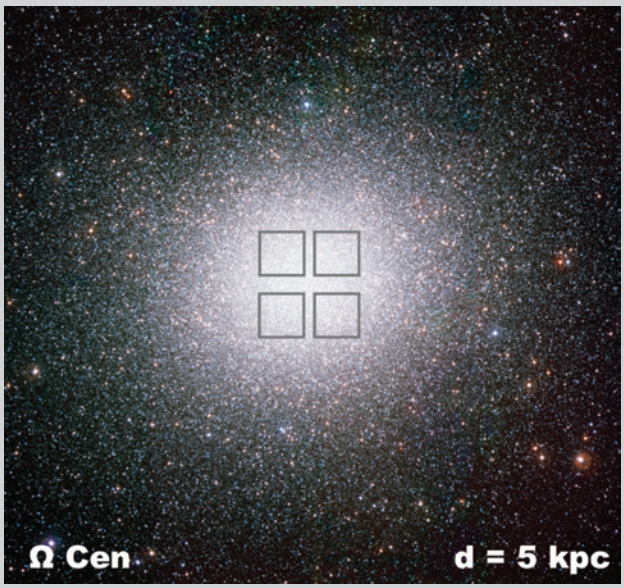

Figure 2: Ω Cen overlaid with the footprint of the MSA. The MSA field of view is about 3.4 arcmin^2.

NIRSpec will feature astronomy's first space-based, multi-object spectroscopic (MOS) capability, using micro-shutter arrays (MSAs). Each shutter is about 100 × 200 microns and covers an area of just 0.2 × 0.46 arcseconds on the sky. The shutters can be configured into small slits to simultaneously observe up to ~200 targets. Working with software developers, the Institute's NIRSpec team is creating a software tool for optimizing observations with the MSAs, which will be challenging due to the unusable area between the open shutters, and because of optical distortions across the field. The Institute's NIRSpec team developed the algorithms necessary for planning MOS observations, and implemented those algorithms in the Astronomer's Proposal Tool (APT).

The team debuted the MSA Planning Tool (MPT) at the winter 2014 American Astronomical Society (AAS) meeting. We engaged interested scientists in one-on-one demonstrations, and discussed their particular science cases to evaluate the implications to the tool's algorithms and usability. The latest public release of APT contains the MSA Planning Tool (**http://apst.stsci.edu/apt/external/downloads/installers/install.html**).

The NIRSpec MSA

The MSA is composed of four quadrants, each with about 62,000 shutters separated by small bars (Figure 1). The bars act as a support structure for the shutters that are hinged to them. To observe with the MSAs, users must create MSA configuration files that are similar to slit masks used in ground-based MOS observing. MSA configuration files contain a map of open and closed shutters for each exposure that are used to create small slits at the location of each target in the field. After each exposure, the MSA can be re-configured to observe other targets, or to re-observe the same targets at different positions in the MSA after performing a pointing dither. We expect that observers will want to perform such dithers to improve spectral or spatial resolution, or simply to mitigate the effects of detector artifacts. The MPT was designed to assist users in planning MSA observations.

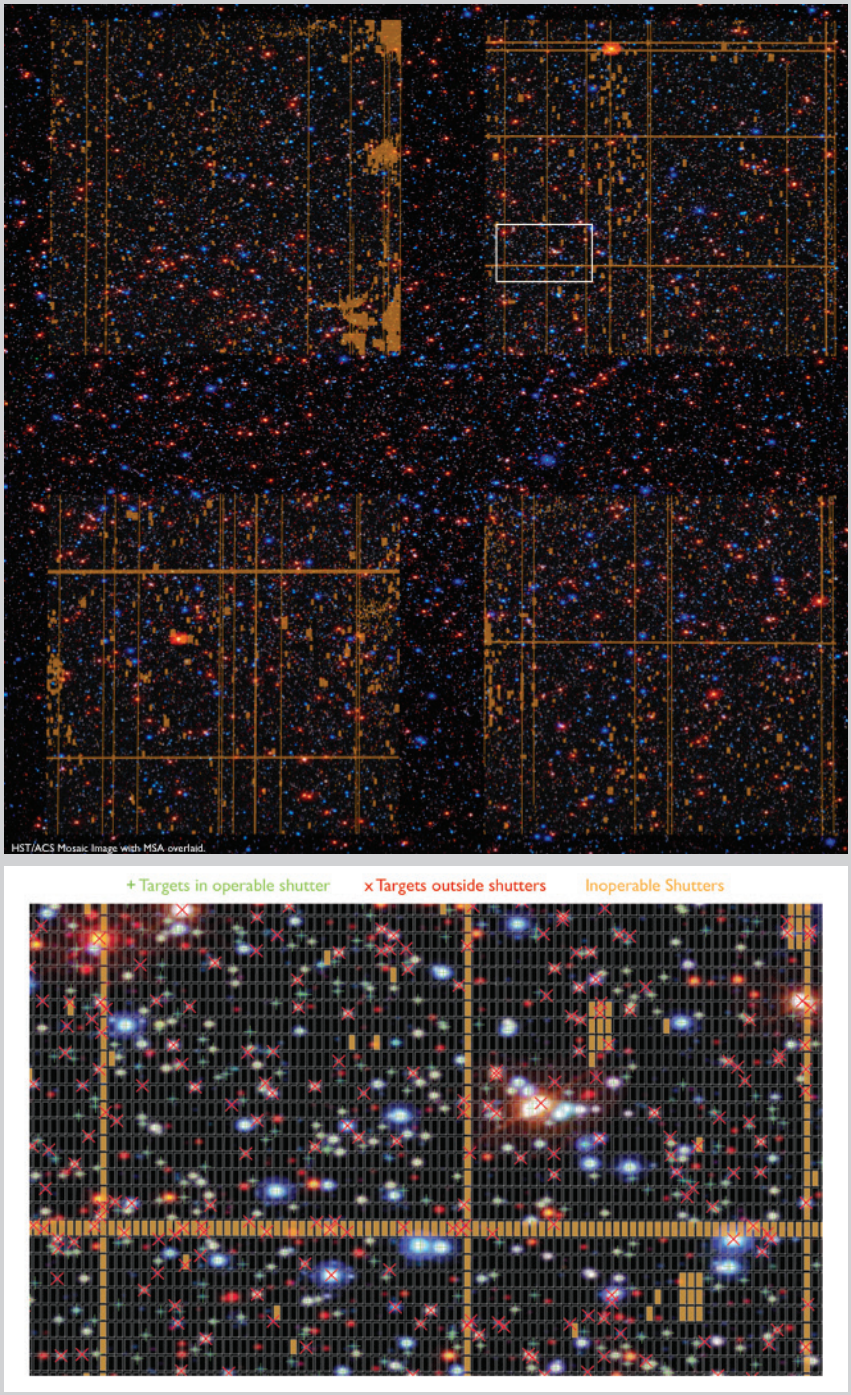

Figure 3: The current MSA is shown projected onto an ACS image at one pointing in Ω Cen. The *lower* image, extracted from the area represented by the white box in the *upper* image, shows a sample of the many targets that are accessible to the MSA at a single pointing (sources marked with green plus symbols). Because of spectral overlap by targets in the same row of the MSA, many different MSA configurations would be required to obtain spectra of all accessible targets. Small dithers would further enable observation of the inaccessible targets shown in red.

Science with the MSA

Dense fields of stars are seen in Galactic globular clusters, the bulge, and many star-forming regions. These special places are challenging for spectroscopy, but they are places where stellar kinematics and abundances could be crucial to unraveling the origins and fate of the stars. The galactic globular cluster Omega Cen is hotly debated—it may be a true globular cluster or the surviving core of a stripped dwarf galaxy. NIRSpec will enable intensive spectroscopy of thousands of Omega Cen stars with its unique

Continued page 24

NIRSpec
from page 23

MSA (Figures 2 and 3). The MSA covers a field of 3.4 arcmin on a side, an area in which Omega Cen has 10,000 stars down to 20th magnitude. NIRSpec's 250,000 individually configurable microshutters are denser still, enabling spectroscopy of thousands of stars—limited only by the available time and not by field crowding. These spectra will measure kinematics and elemental abundances, and constrain the chemodynamical history of this enigmatic cluster with unprecedented statistical precision.

Benefits of the MSA Planning Tool

The MPT performs several functions: finding an optimal set of telescope pointings to observe a large number of sources at once; ensuring as many targets as possible can be observed at all dither positions; and deriving the required MSA configurations.

The MPT optimization algorithms work with a number of constraints posed by the MSA that together complicate the manual planning of efficient observations for all but the simplest observing cases.

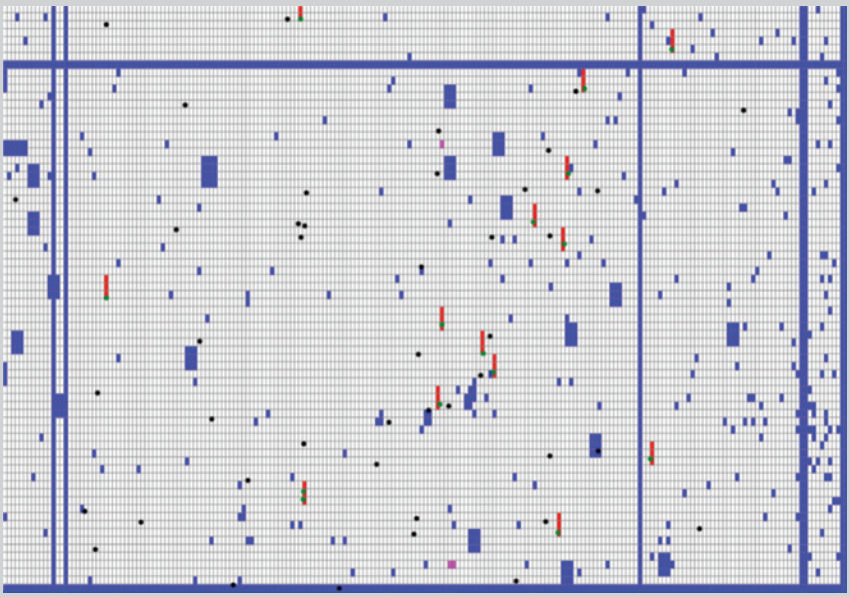

Figure 4: A close-up view of a small portion (~5%) of the area of the MSA. This is one of the views provided by the MPT for planning MOS. The dots are sources in our test catalog. Dots in red slits are sources that can be observed in a set of planned dithers. Failed closed shutters and plugged shutters are shown in blue. Blue rows and columns are inoperable due to shorts. The small magenta boxes are stuck open shutters.

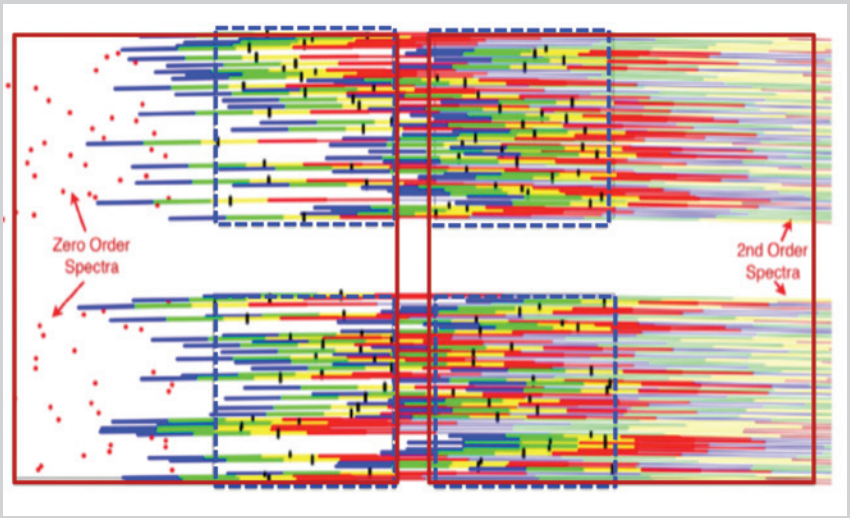

Figure 5: Model spectral traces for the G235M grating ($R \sim 1000$) shown as rainbow lines dispersed across two NIRSpec detectors (large red rectangles). Dashed blue squares are the MSA quadrants projected onto the field. When using medium- and high-resolution gratings, a portion of each spectrum falls into the gap between the chips.

- The MSA is a fixed grid. Even the best pointing cannot perfectly center each source in its respective shutter. Nevertheless, sources must be well centered in an open shutter to avoid slit losses, and to improve photometric accuracy.
- Field distortion is significant. Because of optical distortions across the MSA, after a large dither, a new MSA configuration will be required to re-observe many of the same targets.
- During fabrication and testing, it is inevitable that a few shutters are rendered inoperable in various ways—stuck open or stuck closed shutters, or shorted rows and columns (Figure 4). These limit the options for placing targets on the MSA. It should be noted that new MSA quadrants with reduced numbers of failed shutters are currently being fabricated. Still, planing around any failed shutters is important to improving the multiplexing efficiency of this instrument mode.
- A gap exists between the two detectors (Figure 5). This requires at least one large dither to recover the wavelengths that fall into the gap.
- Due to the dispersion of spectra along the MSA rows (Figure 5), only one target per row is allowed when using the medium- and high-resolution gratings. This restriction—familiar to ground-based MOS observers—prevents overlapping spectra.

Community Outreach

Educating future users is a high priority. Even observers familiar with ground-based MOS instruments will be unfamiliar with some of the challenges posed by the MSAs on NIRSpec. In designing the MPT interface, we sought to strike a balance between the tool's usability and the complexity required to enable most science observations. The 2014 AAS meeting in Washington DC presented an opportunity to get the perspective of the community to be sure we are striking that balance appropriately.

In preparation for the AAS meeting we created a public web page (**http://www.stsci.edu/jwst/instruments/nirspec/msa-planning-tool**) hosting a user's guide and videos demonstrating the use of the MPT. We also conducted live in-house demonstrations with Institute science staff, which allowed us to collect early feedback, and gain experience training users and demonstrating the tool.

During the AAS meeting, NIRSpec team members gave targeted one-on-one demonstrations of the MPT. We sought community input on the tool's algorithms, its usability, and the usefulness of the results presented to the user. This targeted outreach proved to be valuable for all participants. Members of the MOS community, many of whom were unfamiliar with NIRSpec, began to think about the science they could propose with the MSAs. The feedback we received has helped us prioritize our future work. We are now in a position to better assess the variety of MOS science scenarios users are considering, and are more confident that we are designing a tool that best meets the community's needs.

ISIM Cryo-Vacuum Test #1

Scott D. Friedman, *friedman@stsci.edu*, **& Randy A. Kimble,** *randy.a.kimble@nasa.gov*

The components of the *James Webb Space Telescope* undergo tests at many levels as they are assembled into an increasingly complex system. These tests, which culminate in a fully qualified astronomical observatory, involve a variety of hardware, including assemblies of detectors; mechanisms for filters, pupils, and focus; optical elements, such as filters and gratings; and myriad electronics boards. These are a few examples of the subsystems that were tested in the assembly of the *Webb* science instruments (SIs)—Near Infrared Camera (NIRCam), Near Infrared Spectrometer (NIRSpec), Mid-Infrared Instrument (MIRI), and Fine Guidance Sensor/Near Infrared Imager and Slitless Spectrograph (FGS/NIRISS).

The SIs were extensively—but not completely—tested in a cryogenic environment, and verified by the development teams at their integration facilities, in California, Germany, the United Kingdom, and Canada. The four SIs were delivered to the Goddard Space Flight Center, where they have been assembled into the Integrated Science Instrument Module (ISIM). As the test program was originally conceived, the ISIM was to have undergone two extensive cryo-vacuum (CV) test campaigns to verify that its performance meets requirements. The campaigns were to have been separated by a series of ambient environmental tests, including acoustic and vibration, electromagnetic interference, and gravity release tests.

Continued page 26

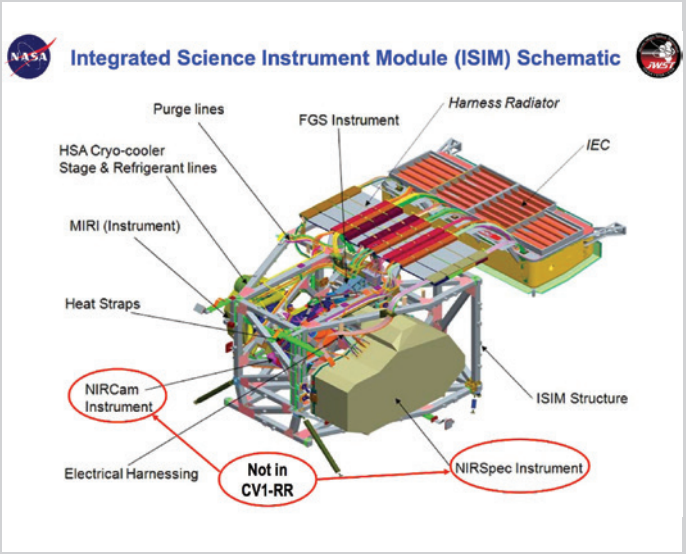

Figure 1: A schematic diagram of the ISIM with the thermal panels and blankets removed. This shows the locations occupied by NIRCam and NIRSpec although they were not present for CV1RR. All instruments will be in place for CV2 and CV3.

Figure 2: The SES Integration Fixture. ISIM is in the central region, surrounded by silver-colored thermal blankets enclosing its sophisticated thermal management system. The IEC is at the upper-right side and contains electronics that operate at room temperature.

A variety of circumstances forced a considerable modification to this plan, however. For example, a design flaw in the detectors for the near-infrared instruments, which caused long-term degradation, requires that they be replaced with new, robust detectors in which the defect is eliminated. The performance of the microshutter array (MSA) assembly for NIRSpec was found to be unacceptable: an excessive number of shutters became immovable after acoustic testing, which requires replacement of at least some of the MSA quadrants. In fact, all SIs have some components that need to be replaced, either in their optical module or warm electronics boxes. The long lead times for such replacements have dictated that this work must be done well after the SIs were delivered to Goddard. Additional modifications of the testing plans were required by the fact that MIRI and FGS/NIRISS arrived considerably earlier than NIRCam and NIRSpec. Note that these are not new developments; the need for making these hardware changes—and the budget and schedule changes they precipitated—have been known for quite some time. For example, the decision to procure new NIR detectors was made in 2011 and new MSAs in 2012.

Rather than delay CV testing until all SIs arrived and all components and subassemblies were replaced, the ISIM project at Goddard scheduled a preliminary test using the hardware in hand. It recognized that the ISIM-level CV tests are complex and challenging in many ways, even beyond verification of ISIM performance.

The thermal and mechanical performance of ISIM and its extensive ground support equipment (GSE) had been modeled in detail, but had not been verified with the SIs. The Optical Telescope Element (OTE) Simulator (OSIM), which provides point-source and extended-source light to ISIM during CV testing, had been verified in two CV campaigns of its own, but it had not yet been used with the SIs. The data flow through the ISIM command and data handling system and the GSE data recorders had not been exercised with multiple SIs in a flight-like configuration. The system for rapidly re-planning the optical tests, which is always needed in such a complicated program, had not yet been operated in a true test environment. Even the way the personnel interact—test director, SI teams, and test operators—had never been exercised as a group before. Therefore, an additional CV campaign was inserted before the two already planned. The goal of this new campaign—CV1RR—was not to verify requirements, but to reduce risk by gaining experience with the hardware on hand.

The high-level objectives of CV1RR were:

- To demonstrate that the test configuration, which includes large amounts of new GSE, is able to support the test requirements of the ISIM verification program and to identify any hardware fixes needed before CV2.
- To dry-run critical test procedures, to learn how to formulate and execute the procedures most efficiently, and to analyze the results and identify any necessary improvements to procedures and test logistics before CV2.

These objectives demonstrate that CV1RR is as much of an engineering test of both the flight and ground support hardware as it is a performance test of ISIM with these science instruments. CV2 and CV3, of course, will have a heavier emphasis on performance and verification of requirements.

The CV1RR Test Campaign

All ISIM CV testing takes place in Goddard's largest vacuum tank, the 9-meter diameter, 13-meter tall cylindrical Space Environmental Simulator (SES). In addition, enormous preparation was required well before CV1RR was ready to begin, much of which took place after the SIs were delivered to the nearly 37,000 m^3 high-bay cleanroom at Goddard. In summer 2013, multiple hardware components—the ISIM, the ISIM Electronics Compartment (IEC), the electrical harness radiator, a flight-like MIRI heat exchanger

stage assembly (the flight unit will be installed at a later date), and other associated hardware (Figure 1)—were installed into the SES Integration Fixture (SIF). The SIF is a truss-like structure that also contains a sophisticated GSE thermal management system to simulate the thermal environment of the observatory (Figure 2).

On August 10, 2013, the SIF was carefully lifted and placed into the SES tank. Figure 3 shows the arrangement of the test hardware. As an example of the thermal engineering challenges, the electronics in the IEC, running at room temperature, are separated by only a couple of meters from FGS/NIRISS, operating at less than 45K, and from MIRI, actively cooled to just 6.7K!

CV1RR began on August 29 and the test ran largely as planned through pump-down, cool-down, and initial testing. Mechanisms and electronics were checked. Dark exposures and exposures with internal lamps verified that the instruments were performing as they did prior to delivery to Goddard. The testing team was eagerly anticipating the first illumination with the external OSIM sources on October 1, 2013, when the federal government shut down, and the team was required to put the hardware into a safe-hold configuration. No testing was permitted during this frustrating period until the furlough ended on October 17. To preserve the overall schedule, *Webb* management directed that CV1RR must end at about the same time as it would have without the furlough. Therefore, the team developed an abbreviated test plan, preserving the highest priority tests, including the critical risk-reduction activities. CV1RR ended on November 11, 2013.

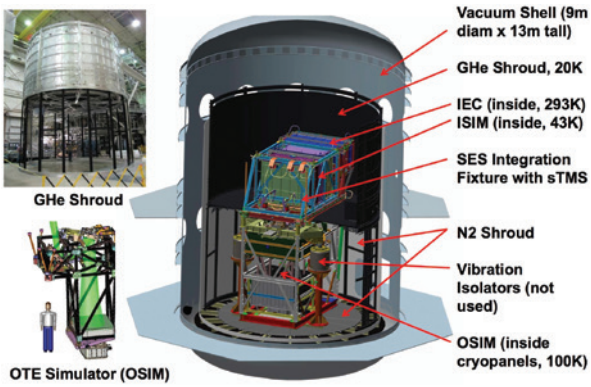

Figure 3: A schematic diagram showing the ISIM test configuration inside the SES thermal-vacuum chamber. The top of this tank is removed to install ISIM and OSIM. OSIM, which provides the external light sources to the instruments, is in the bottom half of the chamber and is cooled to 100K. The SES Integration Fixture, which contains ISIM, the IEC, and other hardware, sits atop OSIM. It is cooled with a shroud containing gaseous helium to less than about 45K. MIRI is further cooled to 6.7K with a dedicated cryo-cooler. The photograph at the *top left* shows the helium shroud before it was inserted into the SES chamber. The diagram on the *bottom left* shows the scale of a person standing next to OSIM. The SES chamber is 9 meters in diameter and 13 meters tall.

Despite the shortened duration, the team ran many important tests in CV1RR, including:

- Functional testing with ISIM systems in vacuum at room temperature.
- Functional and performance testing with ISIM systems in vacuum at the nominal cryo operating temperature.
- OSIM+SI checkout. The ability of OSIM to place point sources at the desired locations in the SI fields of view was demonstrated. The OSIM light-source intensities were calibrated, although more time will have to be devoted to this task early in CV2.
- Optical baseline, consisting of external flat fields, a through-focus exposure sweep, and a measurement of the pupil alignment of the SIs. This test will be repeated in future CV campaigns to identify trends in performance.
- A variety of thermal tests to measure the heat load into the instruments, particularly MIRI, and for correlating these measurements with the ISIM thermal model.
- Preliminary assessment of SI alignment and image quality at the ISIM level, including phase-retrieval analyses of wave-front error.
- NIRISS performance characterization. Due to a rather late change in the design of this instrument, NIRISS was never operated in its current end-to-end optical configuration in SI-level cryogenic testing. Therefore, this “first light” test measured the NIRISS image quality, plate scale, wave-front error, ghosting, vignetting, stray light, and the orientation and location of grism spectra on the detector.
- Operations script subsystem (OSS). In ground testing, the SIs can be commanded with low-level scripts or with the Python-based OSS. In flight, only the OSS will be used for normal operations, and some test time was therefore devoted to this method of commanding.
- ASIC tuning. Application Specific Integrated Circuits (ASICs) perform two tasks: driving the NIR detectors and doing initial processing of detector output signals. Each ASIC must be tuned to its specific detector, and since all NIR detectors will be replaced, ASIC tuning will be an important activity in upcoming CV campaigns. CV1RR provided the first opportunity to practice ASIC tuning.
- Electromagnetic interference from the MIRI cryo-cooler. While the NIR instruments are passively cooled to below 45K in flight, MIRI has an active cooler so that it can operate at about 6.7K. This test was to demonstrate that the cooler does not introduce noise into the sensitive signal outputs from the detectors.

Continued page 28

ISIM
from page 27

Institute personnel fully participated in CV1. Approximately 20 scientists and engineers provided a wide variety of support functions including serving as test conductors and operators, providing quick-look data analysis for all three instruments, and preparing and running OSS tests. Their subsequent activities include more detailed analyses of test data and working with the SI teams and the Goddard optics team to define the tests to be executed in CV2.

CV1RR Results

By almost any measure, CV1RR was a great success. Referring to the test objectives listed above, the test configuration was shown to be fully capable of supporting CV2 and CV3, when ISIM performance will be verified. Many test procedures were successfully run, despite the government shutdown. The team gained valuable experience crafting the tests, modifying them in real time, and learning which areas of staffing need augmentation. Along with these successes it is not surprising that some problems were discovered and must be addressed. Examples of each include:

- Safe cool-down, warmup, and the ability to achieve thermal balance were demonstrated.
- The six-degrees-of-freedom alignment and pupil alignment of the SIs were measured to be within requirements.
- The image quality was good in all SI channels. This was particularly important for the MIRI medium-resolution spectrograph, because image quality was not well measured during SI-level testing in England. Phase-retrieval analysis performed on focus sweep data demonstrated the ability to precisely determine wave-front errors in both SIs (Figure 4), which were excellent.
- Demonstrated satisfactory stray-light background for conducting the ISIM-level optical test program. This was viewed as a high risk going into this test because of the difficulty of shielding so many warm components, which emit strongly, especially at mid-infrared wavelengths.
- Data acquisition and processing methods to improve signal-to-noise performance in the MIRI detectors. Unexpectedly low signal-to-noise levels were observed during SI level testing due to detector drifts. The detector team developed mitigation strategies on flight-like hardware at JPL. These methods were successfully demonstrated with the flight instrument, closing out the problem report that had been generated at SI-level testing.
- Demonstrated acceptable contamination control through a full CV test cycle.
- Externally induced mechanical jitter was acceptably low. Based on previous jitter measurements during OSIM cryo-testing, the use of a floating vibration isolation system was removed from CV1RR because of the concern that it might introduce more risk of optical misalignments than it would reduce in the case of jitter; the low jitter observed validated that decision.
- The most serious problem with the SIs was an occasional but recurring communication dropout with both FGSs and NIRISS. This problem has been traced to a coding problem in the SI's field-programmable gate arrays (FPGA). The instrument team is building new FPGA boards to eliminate this problem.

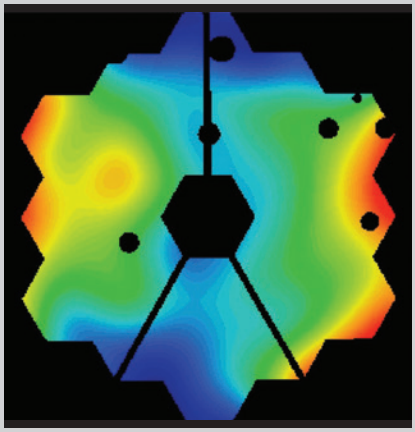

Figure 4: A map of the optical wave-front error (WFE) of NIRISS after the effects of the OSIM have been removed, using the method of phase retrieval. The measured WFE is 48 nanometers rms, fully consistent with requirements for this portion of the total optical error. This was measured close to the center of the NIRISS field. In CV2 and CV3 the WFE will be measured at multiple field locations. The dark circles are artifacts arising in the OSIM illumination system. (Courtesy of D. Aronstein, GSFC.)

- Significant ghosting was observed with the NIRISS GR700 grating. This effect was modeled by the Goddard optics team and the source is now well understood. A fix has already been identified and will be implemented before CV3.
- The NIRISS and FGS best-focus positions (Figure 5) were not at the expected locations. The offsets are well within the range of their focus mechanisms. Nevertheless, the team members want to be sure they understand the origin of this discrepancy.
- The SES helium cooling system had several brief (approximately one hour) failures during the test, which caused frozen N_2 and O_2 to sublimate and possibly (temporarily) condense on MIRI optics. This constitutes a contamination risk. The faulty parts have been identified and will be replaced prior to CV2.
- The GSE cryo-cooler measured an unexpectedly high heat load into MIRI. This heat load is scrutinized carefully because of the importance of maintaining sufficient performance margin for the flight MIRI cryo-cooler. Therefore, any unexplained heat load is a cause for concern. The cooler team at JPL and the ISIM team at Goddard are examining this excess to ascertain whether it represents an actual, flight-relevant load or a parasitic load caused by the test configuration.

In summary, despite the issues encountered, CV1RR was very successful. It served its purpose in significantly reducing risk heading into CV2 and CV3, and has prepared the team well for those even more ambitious tests.

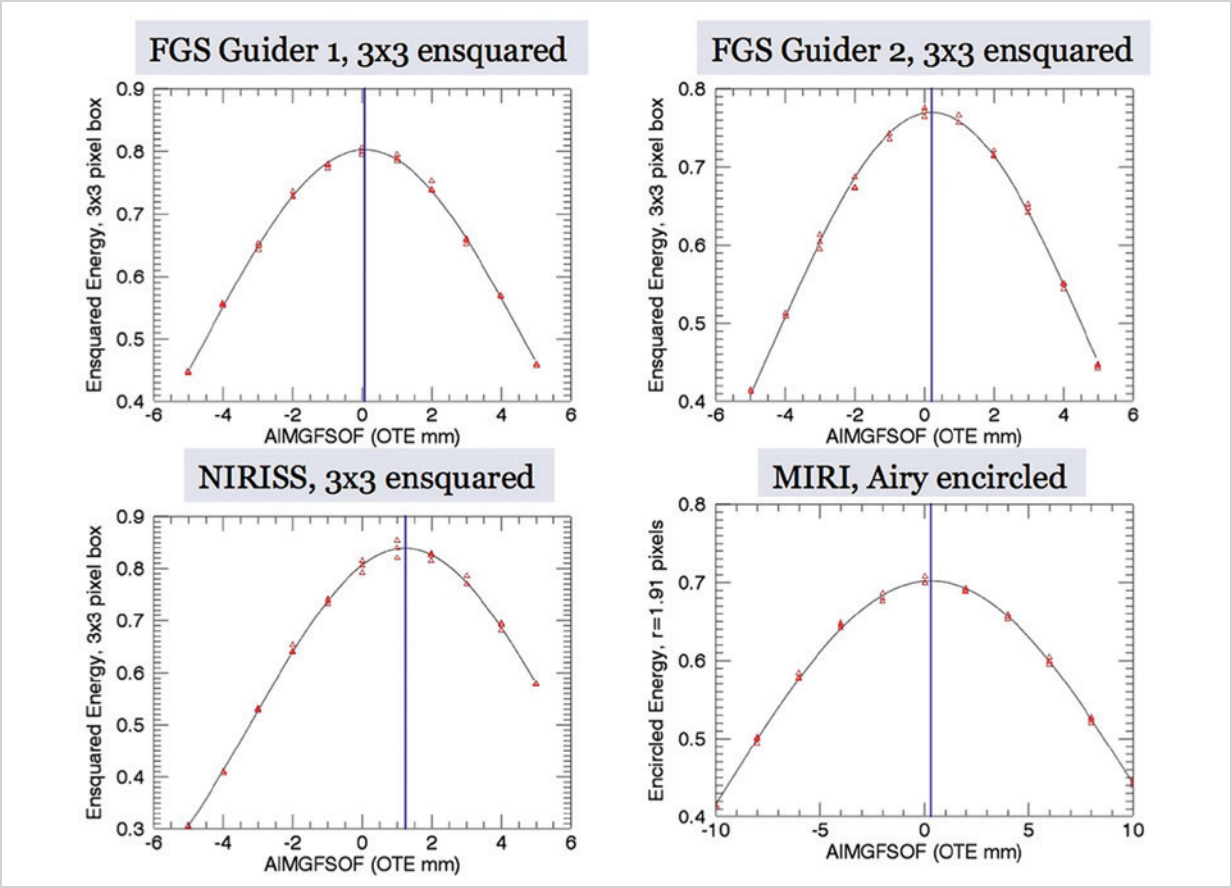

Figure 5: Energy contained in the brightest 3 × 3 pixel region as a function of focus position for the two FGSs and NIRISS, and the encircled energy within the first dark Airy ring for MIRI. The X-axis label AIMGFSOF is a telemetry mnemonic meaning the actual image focal surface offset, which is to say the OSIM focal position relative to the focal plane of the Optical Telescope Element. All best focus locations are well within the range of the focus mechanisms for the NIR instruments. MIRI has no focus adjustment mechanism so it is particularly important to verify that it is in proper focus during ground testing. (Courtesy of R. Telfer, GSFC.)

A Look Ahead

As this article is being written, NIRCam and NIRSpec have just completed electrical testing and optical metrology in preparation for their installation into ISIM, which will then house all *Webb* science instruments for the first time. A very fortunate development is the faster-than-expected production of replacement NIR detectors. As a result, the full complement of ten detector arrays has already been installed into NIRCam heading into CV2, which is currently scheduled to begin in late spring or early summer of 2014, and to last about 100 days, about 60 of which will be at a stable, cryogenic operating temperature.

After CV2 a considerable amount of hardware will be replaced:

- The remaining NIR detectors (two arrays in NIRSpec, three arrays in FGS/NIRISS).
- Some or all of the NIRSpec microshutter assembly quadrants.
- A new, more efficient NIRISS GR700 grating, to be installed in a rotated position to eliminate the ghosting problem.
- NIRCam, FGS/NIRISS, and MIRI electronics boards, to address some shortcomings observed at SI-level or ISIM-level testing.

CV3 is scheduled to begin in mid-2015 and represents the final test of ISIM at Goddard. It will then be integrated with the OTE in the Goddard cleanroom. The full-up telescope and instrument suite will then travel to Johnson Space Center for end-to-end optical and thermal testing, and then to Northrop Grumman for integration and testing with the spacecraft and sunshield.

The extensive test program, at ever-increasing levels of complexity, is designed to discover and correct problems early, when they are easier and less expensive to fix, in both time and dollars. We are now seeing the benefits of this approach with SI-level testing and with CV1RR. This approach gives us high confidence that the *Webb* observatory will perform as designed when it is launched in 2018.

Selecting Targets for *Webb*

Margaret Meixner, meixner@stsci.edu

Twelve years ago, when I proposed to use *Webb*'s Mid-InfraRed Instrument (MIRI) to study the Magellanic Clouds and dust disks around forming stars, the launch of *Spitzer Space Telescope* and all its discoveries were still in the future. Even so, MIRI's unparalleled sensitivity made it easy to describe fascinating investigations that it alone would enable. *Webb* will observe objects typically an order of magnitude fainter than any recent and current observatories (Figure 1). *Webb*'s 6.5-m diameter primary mirror, which is the reason for this tremendous sensitivity increase, also permits superior angular resolution in the infrared compared to *Spitzer.* So, we will get *Hubble*-like infrared images from *Webb*. Furthermore, *Webb*'s lower flux-saturation limits mean that many *Spitzer* and *Hubble* targets will be too bright for *Webb*, and will require vetting with current facilities. So, we are talking about whole new target lists for MIRI and the other *Webb* instruments. It's not just more of the same; *Webb* performance is a whole new realm!

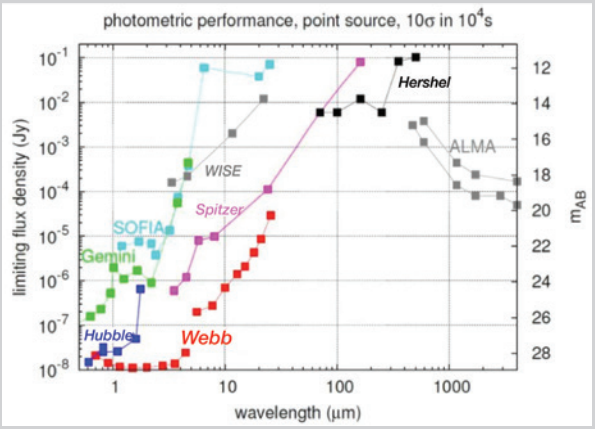

Figure 1: The limiting flux density of a point source, measured at 10σ in 10,000 seconds of integration for some current, past, and future observatories. Lower values mean better sensitivity. This plot is from the *Webb* sensitivity website: **http://www.stsci.edu/jwst/science/sensitivity**.

Figure 2: The *Spitzer* SAGE image of the Large Magellanic Cloud (Meixner et al. 2006). The picture shows dust at its three main cosmic hangouts: around the young stars, where it is being consumed (red-tinted, bright clouds); scattered about in the space between stars (greenish clouds); and in expelled shells of material from old stars (blue old stellar population and embedded old stars as red dots).

Webb overlaps the spectral ranges of *Spitzer* and *Hubble*, but its science operations will be more like *Hubble*. *Webb* is big, and its great inertial mass means that it will be more efficient for pointed, small-field observations than for large-area surveys. Fortunately, the space observatories that precede it—*Spitzer*, *Herschel*, and to some extent, *Hubble*—produced major surveys, which are helping to select targets for *Webb*.

LMC & SMC

In my own research area—the life cycle of dust in galaxies—the Large and Small Magellanic Clouds (LMC, SMC; Figure 2) are ideal sources of suitable targets for *Webb.* They are close enough that we can separate the stars from the interstellar medium and study how they interact, but they are also far enough away that we were able to survey them with *Spitzer* and *Herschel*. The metallicities of the LMC and SMC fortuitously bracket the mean metallicity of the universe at the time of peak star formation. Furthermore, they have been surveyed with many ground- and space-based observatories, notably including *Spitzer* and *Herschel*, which performed a photometric survey from 3.6 to 500 microns, as well as a spectroscopic follow-up in a series of projects called "Surveying the Agents of Galaxy Evolution" (SAGE).

YSOs

To provide some examples of the ideas and issues at play in *Webb* target selection, let's drill down on young stellar objects (YSOs). Thousands of YSOs have been discovered in the LMC and SMC, including some of the most dust-enshrouded (Stage 0, I, II) and highest mass (>1–4$M_{\odot}$; Whitney et al. 2008; Gruendl and Chu 2009; Sewiło et al. 2013; and Carlson et al. 2012). The *Spitzer/Herschel* surveys show where to point *Webb* to study the active star formation. One idea is to image these regions with *Webb*/MIRI and the Near Infrared Camera (NIRCam) to study the less dusty (Stage III) and the less massive (<1 $M_{\odot}$) YSOs. For example, N113 in the LMC is a compact, high-intensity region of star formation (Figure 3). The dust remaining in the disks of these more-evolved YSOs is the birthplace of planets. It will be interesting to see if the amounts of dust found in these disks are comparable to that of galactic sources—hence having the same potential to create planets, despite their low metallicity.

Figure 3 shows a potential tiling of the NIRCam fields of view (2.2 × 2.2 arcmin) over the N113 region; the MIRI fields of view are slightly smaller (1.9 × 1.3 arcmin) and would require a bit more tiling. Using six filters of NIRCam and MIRI (0.7, 1.77, 1.5, 3.56, 5.6, and 21 microns), it would take 10.3 hours[1] to image these fields deeply enough to be sensitive to the thermal emission from the dust disk of a classical

[1]You can estimate observation times for some Webb modes using the exposure time calculator online at: **http://jwstetc.stsci.edu/etc/.**

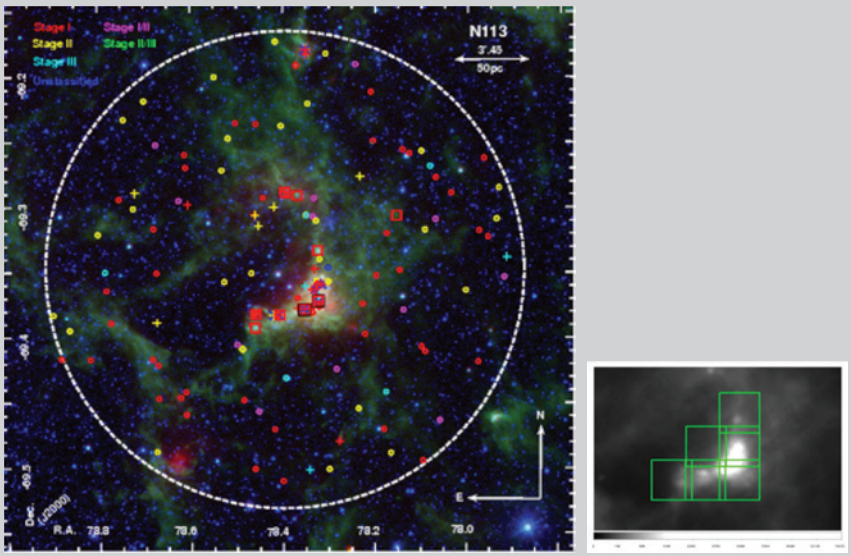

Figure 3: N113. *Left*: This detailed *Spitzer* study by Carlson et al. (2012) of the N113 region extended our census of the YSOs in this region to lower masses as low as 1.5 $M_{\odot}$ from ~4 $M_{\odot}$ based on the galaxy-wide massive YSO searches. These new candidates are shown as circles, whereas the massive YSO candidates found earlier are shown as "+" signs. The *Herschel*-identified YSOs are shown as squares (Sewiło et al. 2010). *Right*: An approximate tiling of six NIRCam fields of view necessary to image the less dusty, lower-mass YSOs.

Figure 4: *Hubble* image of NGC 602, showing amazing clarity. Carlson et al. (2011) used this image to detect young solar-mass stars with planet-forming disks, shown here as the faint blue points of light near the bright stars in the center of this star-formation region. *Webb* will have a similar clarity as *Hubble* in the infrared bands covered by *Spitzer*. This greater clarity will enable us to detect, for the first time, the planet-forming dust disks around these solar-mass stars at the distance of the LMC. We will be able to address questions such as: can planets form in lower-metallicity environments?

T-Tauri star of 2 $M_{\odot}$ appearing in these images of N113. The exposure time for characterizing the dust is quite quick with NIRCam—only 2 hours—and for MIRI it is 8.3 hours. Such investigations of the dust disks in the LMC and SMC are impossible with current facilities. Nevertheless, to prepare for such *Webb* observations, *Hubble* is needed to identify the location of these classical T-Tauri stars, using *V*, *I*, and Hα photometry. An example is the *Hubble* image of NGC 602, which is an active star-formation region in the SMC (Figure 4; Carlson et al. 2011). This picture demonstrates the type of image quality we expect from *Webb*, with its filters for thermal emission from dust.

A second idea on follow-up observations of YSOs is to use spectroscopy by *Webb*/MIRI and Near-Infrared Spectrograph (NIRSpec) to understand the chemistry of the planet-forming YSOs at lower

Continued page 32

Webb *Targets*
from page 31

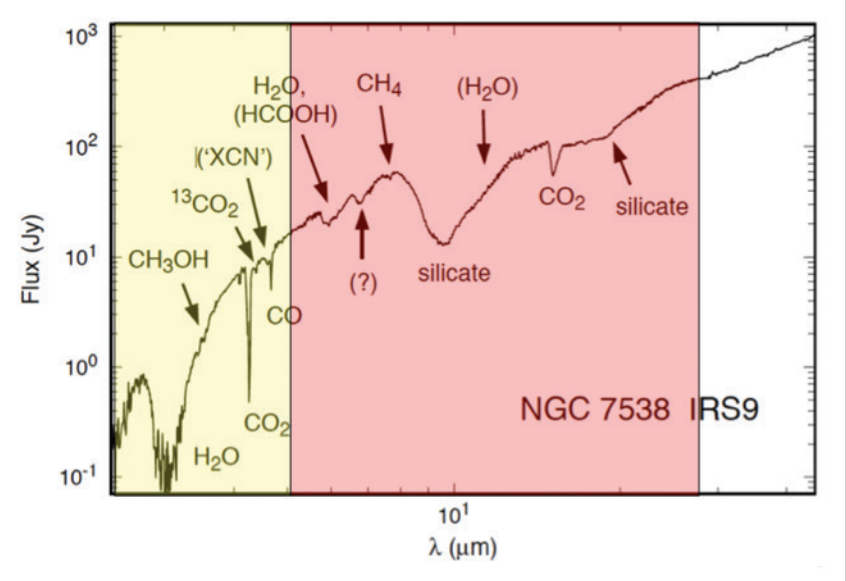

Figure 5: The *ISO*/SWS spectrum of the Galactic embedded YSO NGC 7538 IRS 9 by Whittet et al. (1996) reveals many ice features and silicate dust in absorption. With NIRSpec and MIRI on *Webb*, we will be able to obtain similar spectra of YSOs, but in the Magellanic Clouds.

metallicities. The spectral resolutions of MIRI and NIRSpec will be close to that of the *Infrared Space Observatory*'s Short Wavelength Spectrometer (*ISO*/IRS), which obtained many interesting spectra of Galactic targets, including NGC 7538 IRS 9, the embedded YSO in Figure 5. This spectrum by Whittet et al. (1996) revealed many ice features, as well as silicate dust in absorption, and shows the type of information we expect to derive for the embedded YSO targets in the Magellanic Clouds. NIRSpec will be able to complete the shorter wavelengths ranges, up to 5 microns. MIRI will cover the remaining part of the spectrum, up to ~28 microns. Combined, these observations will provide a complete census of the ices in such objects. Will we find the same inventory of ices like NGC 7538 or will they differ in the low-metallicity environment?

For a total time of 3.8 hours, we could obtain full spectral coverage of a single YSO in the Magellanic clouds using both NIRSpec and MIRI. MIRI's and NIRSpec's spectral resolution, which is better than that of *Spitzer*'s Infrared Spectrograph by a factor of 10, will allow us to better constrain the chemistry of the ice—H_2O, CO, and CO_2—as well as complex organic compounds like methanol and methane. The shape of the absorption profile will change, depending on the precise composition/mixture of ices on dust grains. High resolution will be required to define this shape. Also, we expect ionized jets of gas at velocities >100 km s^{-1}, which may be resolved, allowing us to constrain outflow velocities.

When *Webb* is in full operation, we will be able to study star formation in the Magellanic Clouds on a par with current-day studies in our Galaxy.

References

Carlson, L. R., Sewiło, M., Meixner, M., et al. 2011, "A Panchromatic View of NGC 602: Time-resolved Star Formation with the Hubble and Spitzer Space Telescopes," ApJ, 730, 78

Carlson, L. R., Sewiło, M., Meixner, M., Romita, K. A., & Lawton, B. 2012, "Identifying young stellar objects in nine Large Magellanic Cloud star-forming regions," A&A, 542, A66

Gruendl, R. A., & Chu, Y.-H. 2009, "High- and Intermediate-Mass Young Stellar Objects in the Large Magellanic Cloud," ApJS, 184, 172

Meixner, M., Gordon, K. D., Indebetouw, R., et al. 2006, "Spitzer Survey of the Large Magellanic Cloud: Surveying the Agents of a Galaxy's Evolution (SAGE). I. Overview and Initial Results," AJ, 132, 2268

Sewiło, M., Carlson, L. R., Seale, J. P., et al. 2013, "Surveying the Agents of Galaxy Evolution in the Tidally Stripped, Low Metallicity Small Magellanic Cloud (SAGE-SMC). III. Young Stellar Objects," ApJ, 778, 15

Whitney, B. A., Sewiło, M., Indebetouw, R., et al. 2008, "Spitzer SAGE Survey of the Large Magellanic Cloud III. Star Formation and ~1000 New Candidate Young Stellar Objects," AJ, 136, 18

Whittet, D. C. B., Schutte, W. A., Tielens, A. G. G. M., et al. 1996, "An ISO SWS view of interstellar ices: first results," A&A, 315, L357

Star Formation in Nearby Galaxies: The Role of *Webb*

Daniela Calzetti, *calzetti@astro.umass.edu,* **Jennifer E. Andrews,** *jandrews@astro.umass.edu*, **& Alison F. Crocker,** *alison.crocker@utoledo.edu*

The hallmark high angular resolution and infrared capabilities of the *James Webb Space Telescope* will usher in a new epoch for studies of star formation in nearby galaxies. Decades of observations in the infrared and at other wavelengths, using both space- and ground-based facilities, have vastly increased our understanding of how star formation evolves in galaxies, and how it is related to a galaxy's general characteristics. Nevertheless, key questions remain unanswered. These include but are not limited to: (1) the physical link between local (molecular-cloud-level) and global (galaxy-scale) star formation; (2) the origin of the stellar Initial Mass Function (IMF); (3) the nature of correlation between central black holes and the host galaxy's bulge mass; and (4) the formation and evolution of dust, which is often used to trace star formation itself.

Answers to these questions can only come from *Webb* in combination with existing facilities offering high angular resolution, like *Hubble* and the Atacama Large Millimeter Array (ALMA). Those answers will provide the interpretative foundation for two of *Webb*'s core science goals: understanding the history of galaxy assembly, from the early phases of the universe to the present day, and studying the light from the first stars and galaxies.

Schmidt-Kennicutt Law

In the past several years, the connection between star formation and the gas supply in galaxies has been revealed by uniform surveys of nearby galaxies using a variety of telescopes: *Spitzer Space Telescope* and the *Herschel Space Observatory* in the infrared; *Galaxy Evolution Explorer* in the ultraviolet (UV); ground-based optical telescopes for nebular line emission; and HI and CO lines using ground-based radio and millimeter facilities. While the infrared, UV, and optical observations are used as diagnostics of current star-formation rate (SFR), the observations of HI and CO are tracers of atomic and molecular gas, respectively.

The now-standard formulation for connecting the SFR to the gas supply, also known as the Schmidt-Kennicutt Law (SK Law; Kennicutt 1998, Kennicutt & Evans 2012) is expressed as:

$$\Sigma_{SFR} = A\,(\Sigma_{gas})^{\gamma}$$

where is Σ_{SFR} is the SFR surface density of a galaxy, Σ_{gas} its gas surface density, A is a scaling constant (i.e, the star formation efficiency if γ =1), and γ is an exponent expected to be in the range ~1–2, and includes most of the physical information. The SK Law has been tested in many different environments and galaxies (Figure 1). So far, the results have been contradictory and non-conclusive; they disagree on whether such a relation is universal, what its physical underpinnings might be, and whether the law holds on all spatial scales, from individual molecular clouds to whole galaxies. The contradictions stem from the generally non-intersecting samples and the diverse observational strategies employed by studies on different scales. The dust-enshrouded early stages of star formation, which are the most closely related to the natal gas cloud and are traced via the emission from young stellar objects (YSOs), have been studied only in the Milky Way and its closest companions, the Magellanic Clouds. The reason is the limited angular resolution—2 arcsec or worse—of the infrared facilities that have been available so far (e.g., Shimonishi et al. 2010; Heiderman et al. 2010; Gutermuth et al. 2011; Sewilo et al. 2013).

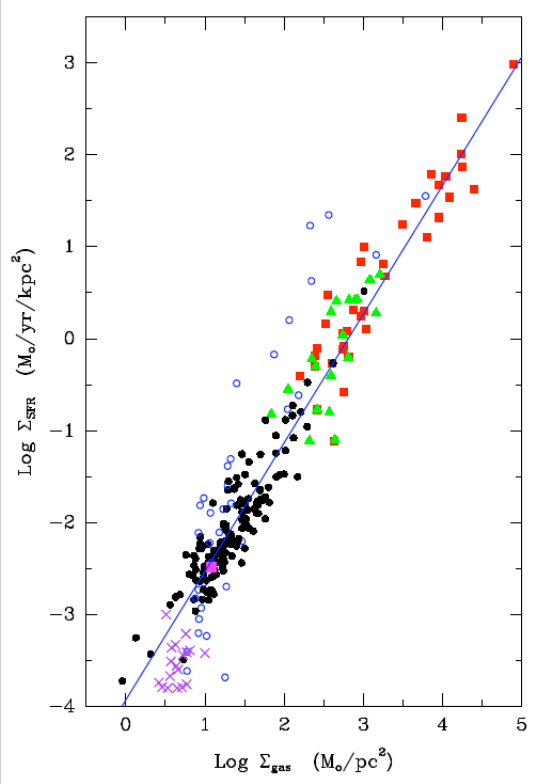

Figure 1: The relation in galaxies between the surface density of the star-formation rate surface density, Σ_{SFR}, and gas (atomic plus molecular) surface density, Σ_{gas}. Each data point is one galaxy. Black symbols are normal spiral and irregular galaxies; red squares are infrared-bright galaxies; green triangles are circumnuclear starbursts; purple crosses are galaxies with low surface brightness; blue circles are irregular and starburst galaxies with low metallicity and low mass. The magenta square is the Milky Way. The blue line has slope γ = 1.4. (From Figure 11 of Kennicutt & Evans 2012; reproduced with permission from the authors.)

With its sub-arcsecond capability in the mid-infrared, *Webb* will resolve individual YSOs in galaxies up to ~10 times the distance of the Magellanic Clouds, or about 0.5–1 Mpc. The integrated light of dust-enshrouded star formation in regions the size of molecular clouds (~15–40 pc) will be measured up to distances of ~10 Mpc. To gain a quantitative appreciation of how large a volume *Webb* will probe, consider that today we can only study up to about 1 Mpc—roughly the distance of M33—with the same spatial resolution. This small volume contains only two massive galaxies (M33 and M31) in addition to the Milky Way. However, massive galaxies are where most of the star formation takes place, and they

Continued page 34

Star Formation from page 33

are some of the key test beds for investigating the SK Law. Within the local ~10 Mpc, 85% of the total SFR is contained in the ~80 galaxies more massive than the Large Magellanic Cloud, and only 15% is contained in the remaining ~400 galaxies.

The powerful combination of *Webb*, tracing dust-enshrouded star formation, and ALMA, tracing the molecular gas, will provide stepping stones on multiple fronts: (a) quantifying the duration of the dust-enshrouded phase of star formation and its dependence on local and global galactic conditions; (b) a solution to the diffuse/clustered star-formation dichotomy, whether it is an actual, physical separation or whether it is artificial, with star formation proceeding on a continuum of clustering scales; (c) the dependence of star-formation efficiency (the rate at which gas is converted into stars) on the local physical parameters; (d) an understanding of potential mediating mechanisms (e.g., stellar feedback; Hopkins et al. 2013) on the SFR–gas relation that separates different regimes and scales; and (e) ultimately, the physical underpinning of the SK Law as a function of spatial scale, from the molecular clouds within galaxies to the global galaxy population. Point (e) is fundamental for developing predictive theories of galaxy formation and evolution.

Stellar IMF

The variety of conditions under which stars form in gas clouds provides an uneasy basis for a "universal" stellar IMF, meaning invariant as a function of location and time. Much debate still surrounds the stellar IMF, including whether or not it is universal (see Bastian et al. 2010 for a recent review). Theories of star formation lack the predictive power to inform observations, due to the intrinsically complex physics involved. As a result, both universal and variable IMFs are supported by models (e.g., Krumholz et al. 2010; Shadmehri & Elmegreen 2011). In the now-widely used formulations of the IMF by Kroupa (2001) and Chabrier (2003), 44% of the mass is contained in the 89% of stars with mass below 1 $M_{\odot}$.

As a rule-of-thumb, any quantity related to SFRs, short-timescale (<500 Myr) star-formation histories, feedback, or chemical enrichment of galaxies, will involve the high-end of the IMF. This is because stars above a few solar masses emit, via stellar winds and supernovae explosions, virtually 100% of the ionizing photons, over 80% of the non-ionizing UV photons, and provide the vast majority of the energy, momentum, and chemical output from stars.

Conversely, the low-end of the IMF impacts the masses of galaxies and traces their star-formation histories on long timescales, as the low-mass stars—below 0.9–1 $M_{\odot}$—accumulate throughout the Hubble time. Variations both at the high and low end of the IMF can have a major influence on the interpretation of galaxy evolution, as they affect measurements of galaxy masses and SFRs, for example, by factors 2 to 5, depending on the strength of the variation and the range of stellar masses considered. This impact can, additionally, be non-uniform across galaxy populations.

Direct measurements of the IMF, both at the low and high end, are available only for limited and less-crowded environments in the Milky Way and the Magellanic Clouds (Bastian et al. 2010). The same is true for a few low-density, faint galaxies near the Milky Way (e.g., Geha et al. 2013; using *Hubble*). The latter finding tentatively indicates a systematic variation at the low end of the IMF with galactic environment (Figure 2).

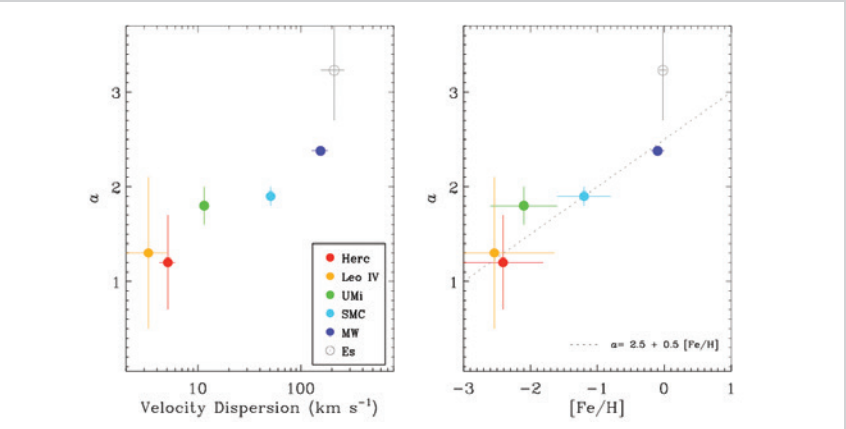

Figure 2: Variations in the power law slope α (where $dN/dm \sim m^{-\alpha}$) of the low end of the stellar IMF, in the mass range ~0.5–0.8 $M_{\odot}$, as determined from direct star counts in a handful of nearby (<40 kpc) galaxies and the Milky Way (color circles). The indirect measure for elliptical galaxies is shown as the empty black circle. The slope is plotted as a function of the velocity dispersion (*left* panel) and the metal abundance (*right* panel) of the galaxy. In the *right* panel, the dotted line is from a model suggested by Kroupa (2001). (From Figure 5 of Geha et al. 2013; reproduced with permission from the authors.)

Far more abundant are the indirect measures of the IMF, using integrated light from galaxies. At the high end of the IMF, results are controversial (compare Andrews et al. 2013 with Lee et al. 2009 and Meurer et al. 2009), owing to the degeneracies involved, mainly between IMF and the star-formation history. Conversely, the mass-to-light ratios of elliptical galaxies (e.g., Cappellari et al. 2012) indicate variations for the low end of the IMF consistent with the results of Geha et al. (2013). Far from settled, these results are still tentative, and, in the case of the direct measures, based on small-number statistics.

Webb will be key for addressing the low end of the IMF through direct measures. Star counts in the near-IR will be possible in a ~500 times larger volume than is currently possible with *Hubble*. The observations will extend out to the virial radius of the Milky Way (~300 kpc), improving the statistics more than five-fold from the current handful of galaxies to >25, (Geha 2014). These observations will produce tight constraints on IMF theories (Offner et al. 2013).

Black holes & bulge velocity dispersion

There is a tight relation between black-hole mass and the velocity dispersion of the bulge, which related to the bulge mass (e.g., Gultekin et al. 2009). This tightness suggests the presence of a regulating mechanism in the growth of black holes that efficiently couples with the bulge's stellar properties. Any coupling, however, must be effective over a significant range of spatial scales, from a black hole's accretion disk (<~0.1 pc) to a bulge (several kpc). This spatial range corresponds to a range of timescales. One scenario suggests the existence of multiple black-hole feedback mechanisms that cause gas removal from the black hole's surroundings, effectively quenching star formation. When coupled with ineffective cooling, these mechanisms provide a channel for black-hole self-regulation (Hopkins et al. 2009; Roth et al. 2012). Another scenario prescribes a connection between black holes and bulge mass via gas stabilization in pressure-supported bulges (Martig et al. 2009). This "morphological quenching" predicts an overall low efficiency of star formation in early-type galaxies. Current observations cannot uniquely resolve the tension between "normal" and "reduced" star-formation efficiency in the central regions of early-type galaxies, owing to the contamination of star-formation tracers by the emission from active galactic nuclei (AGNs) in low-resolution infrared data (Crocker et al. 2012; Martig et al. 2013). This will be prime territory for the *Webb*: the integral field unit in the Mid-Infrared Instrument will be able to identify the key line diagnostics for star formation and AGN gas excitation—and to separate the emission from the two components—at unprecedented resolution in the local early-type galaxies in the iconic surveys (e.g., ATLAS3D; Cappellari et al. 2011). In combination with ALMA, *Webb* will determine the efficiency of star formation in these systems, and establish whether reduced star-formation efficiencies are tied to the relation between the mass of black holes and the velocity dispersion in the bulge.

Dust emission

The dust emission from galaxies, and from star-forming regions within galaxies, is used as a tracer of dust-enshrouded star formation at all redshifts. The spectral range shortward of the peak of the infrared emission, including thermal and non-thermal continuum and the emission features of the polycyclic aromatic hydrocarbons (PAHs), has been calibrated as a SFR indicator in a number of papers, using data from a variety of space facilities (e.g., Calzetti et al. 2007, 2010; Kennicutt et al. 2009; Rieke et al. 2009; Liu et al. 2011). Longward of the infrared peak, the strongest correlations are found with the dust and cold-gas content of galaxies. Despite the global-scale proportionality between infrared emission and SFR, important deviations are observed when looking closely at the galaxies. For instance, significant fractions of the emission in the Wien tail of the dust thermal continuum (~20–30 microns), and in the region of the PAH emission features (~8 microns), have been found to be due to dust heated by old stellar populations, rather than by young, star-forming regions. These fractions vary from galaxy to galaxy, but are generally around 30%–60% for the thermal continuum of the dust, and about 40%–80% for the PAH features (e.g., Verley et al. 2009; Crocker et al. 2013; Calapa et al. 2014). Equally important is the fact that the PAH emission features—some of the key SFR tracers for high-redshift galaxy populations—are depressed both in low-metallicity environments (Engelbracht et al. 2005, 2008; Draine et al. 2007; Smith et al. 2007) and within regions of active star formation (e.g., Helou et al. 2004; Bendo et al. 2008; Relano & Kennicutt 2009). This is possibly an effect of dust processing (Madden et al. 2006; Gordon et al. 2008). One detailed study of the Small Magellanic Cloud at spatial scales of <1 pc finds that the PAH emission is both depressed in HII regions, confirming previous findings, and enhanced in molecular clouds (Sandstrom et al. 2010). Overall, we still have poor constraints on the life cycle of the dust components within galaxies, mainly because detailed studies have been limited to the cases of the Milky Way and the Magellanic Clouds, with only lower-resolution analyses in more distant galaxies.

Understanding dust formation is as important as understanding the processing of dust. Dust production in core-collapse supernovae (CCSNe) is an open question that has fundamental implications for interpreting high-redshift galaxies. Dust masses as large as 10^8 $M_\odot$ are observed in the host galaxies of quasi-stellar objects at $z \sim 6.5$, when the universe is <800 Myr old (Bertoldi et al. 2003). Such large dust masses require a fast and efficient channel of dust production. The short-lived CCSNe are

Continued page 36

Star Formation from page 35

candidates for quickly returning material back to the interstellar medium. In the local universe, however, dust yields from CCSNe have been measured to be generally a few orders of magnitude less than the 0.1–1 $M_{\odot}$ per CCSN needed to account for the dust masses observed in high-redshift galaxies (e.g., Nozawa et al. 2003; Cherchneff & Dwek 2010). Only recently, ALMA observations of SN 1987A in the Large Magellanic Cloud (Indebetouw et al. 2014) have revealed that at least 0.2 $M_{\odot}$ of cool dust has formed in the inner ejecta. Nevertheless, it is still unclear what fraction of that dust will survive. These studies are still hampered by small-number statistics, together with the difficulty of separating intervening dust from the dust produced by the SN itself.

Webb's mid-infrared imaging and spectroscopic capabilities will extend analyses of dust emission at spatial scales of 1–10 pc to a volume of space 1,000 times larger than that probed so far, extending all the way to 10 Mpc distance and probing the full range of global and local-galaxy properties. The investigation of dust formation in CCSNe will be extended to distances well beyond 10 Mpc, with detailed analyses of the mid-IR spectral diagnostics that trace newly formed dust and its composition. This increased diversity of galaxies will enable the study of the mechanisms that form and process the different dust components across all galactic environments, and over the spatial scales of star-forming regions, gas clouds, and supernova remnants. Understanding the life cycles of the different dust components under varying conditions will provide the physical grounding for extrapolating the locally calibrated dust-enshrouded SFRs to the conditions of the early universe, and for pinning down the nature of the dust at high redshift.

In summary, *Webb*'s capabilities will provide answers to fundamental open questions on the physical processes that govern star formation in galaxies. Nearby galaxies offer the best locales for exploring these processes at the spatial scales relevant for star formation itself, namely those of star-forming regions and gas clouds. The answers to those questions will provide the foundation for transforming measurements of distant galaxies into physical quantities, and interpreting those quantities within the framework offered by theoretical models of galaxy evolution.

References:

Andrews, J. E., Calzetti, D., Chandar, R., et al. 2013, ApJ, 767, 51
Bastian, N., Covey, K. R., & Meyer, M. R. 2010, ARAA, 48, 339
Bendo, G. J., Draine, B. T., Engelbracht, C. W., et al. 2008, MNRAS, 389, 629
Bertoldi, F., Carilli, C. L., Cox, P., et al. 2003, A&A, 406, L55
Calapa, M., Calzetti, D., Draine, B. T., et al. 2014, ApJ, submitted
Calzetti, D., Kennicutt, R. C., Engelbracht, C. W. et al. 2007, ApJ, 666, 870
Calzetti, D., Wu, S.-Y., Hong, S., et al. 2010, ApJ, 714, 1256
Cappellari, M., Emsellem, E., Krajnovic, D., et al. 2011, MNRAS, 413, 813
Cappellari, M., McDermid, R. M., Alatalo, K., et al. 2012, Anture, 484, 485
Chabrier, G. 2003, PASP, 115, 763
Cherchneff, I., & Dwek, E. 2010, ApJ, 713, 1
Crocker, A. F., Calzetti, D., Thilker, D., et al. 2013, ApJ, 762, 79
Crocker, A. F., Krips, M., Bureau, M., et al. 2012, MNRAS, 421, 1298
Draine, B. T., Dale, D. A., Bendo, G. et al. 2007, ApJ, 633, 866
Engelbracht, C. W., Gordon, K. D., Rieke, G. H., et al. 2005, ApJ, 628, 29
Engelbracht, C. W., Rieke, G. H., Gordon, K. D., et al. 2008, ApJ, 685, 678
Geha, M. C. 2014, BAAS, 223, 314.03
Geha, M. C., Brown, T. M., Tumlinson, J., et al. 2013, ApJ, 771, 29
Gordon, K. D., Engelbracht, C. W., Rieke, G. H., et al. 2008, ApJ, 682, 336
Gültekin, K., Richstone, D. O., Gebhradt, K., et al. 2009, ApJ, 698, 198
Gutermuth, R. A., Pipher, J. L., Megeath, S. T., et al. 2011, ApJ, 739, 84
Heiderman, A., Evans, N., Allen, L. E., et al. 2010, ApJ, 723, 1019
Helou, G., Roussel, H., Appleton, P., et al. 2004, ApJS, 154, 253
Hopkins, P. F., Murray, N., & Thomson, T. A. 2009, MNRAS, 398, 303
Hopkins, P. F., Narayanan, D., & Murray, N. 2013, MNRAS, 432, 264
Indebetouw, R., Matsuura, M., Dwek, E., et al. 2014, ApJ, 782, L2
Kennicutt, R. C. 1998, ApJ, 498, 541
Kennicutt, R. C., & Evans, N. J. 2012, ARAA, 50, 531
Kennicutt, R. C., Hao, C., Calzetti, D., et al. 2009, ApJ, 703, 1672
Kroupa, P. 2001, MNRAS, 322, 231
Krumholz, M. R., Cunningham, A. J., Klein, R. I., & McKee, C. F. 2010, ApJ, 713, 1120
Lee, J. C., Gil de Paz, A., Tremonti, C., et al. 2009, ApJ, 706, 599
Liu, G., Koda, J., Calzetti, D., et al. 2011, ApJ, 735, 63
Madden, S. C., Galliano, F., Jones, A. P., & Sauvage, M. 2006, A&A, 446, 877
Martig, M., Bournaid, F., Teyssier, R., & Dekel, A. 2009, ApJ, 714, L275
Martig, M., Crocker, A. F., Bournaud, F., et al. 2013, MNRAS, 432, 1914
Meurer, G. R., Wong, O. I., Kim, J. H., et al. 2009, ApJ, 695, 765
Nozawa, T., Kozasa, T., Umeda, H., et al. 2003, ApJ, 598, 785
Offner, S. R., Clark, P. C., Hennebelle, P., et al. 2013, in *Protostars and Planets VI*, University of Arizona Press (2014), eds. H. Beuther, R. S. Klessen, C. P. Dullemond, and Th. Henning
Relano, M., & Kennicutt, R. C. 2009, ApJ, 699, 1125
Rieke, G. H., Alonso-Herrero, A., Weiner, B. J., et al. 2009, ApJ, 692, 556
Roth, N., Kasen, D., Hopkins, P. F., & Quataert, E. 2012, ApJ, 759, 36
Sandstrom, K. M., Bolatto, A. D., Draine, B. T., et al. 2010, ApJ, 715, 701
Sewilo, M., Carlson, L. R., Seale, J. P., et al. 2013, ApJ, 778, 15
Shadmehri, M., & Emegreen, B. G., 2011, MNRAS, 410, 788
Shimonishi, T., Onaka, T., Kato, D., et al. 2010, A&A, 514, A12
Smith, J. D. T., Draine, B. T., Dale, D. A., et al. 2007, ApJ, 656, 770
Verley, S., Corbelli, E., Giovanardi, C., & Hunt, L. K. 2009, A&A, 493, 453

The Galactic Center through the Eye of *Webb*

Jessica R. Lu, *jlu@ifa.hawaii.edu*, **Jay Anderson,** *jayander@stsci.edu*, **Tuan Do,** *do@dunlap.utoronto.ca*, **Andrea Ghez,** *ghez@astro.ucla.edu*, **& Mark Morris,** *morris@astro.ucla.edu*

The center of our Milky Way is a unique environment when compared with the rest of the Galaxy. The central 400 pc defines a Central Molecular Zone (Figure 1) that contains 10% of all the molecular gas in our Galaxy in only 0.02% of the volume (Morris & Serabyn 1996 and references therein). The high stellar densities also make the Galactic Center an excellent place to study extremely rare stellar populations. There are several very active and massive star-forming regions, such as Sagittarius B2, and at least three young star clusters over 10,000 solar masses: the Arches, Quintuplet, and Young Nuclear Cluster. At the very heart of the Galactic Center lies a supermassive black hole of 4 million solar masses that sputters along in a fairly under-luminous state, given the amount of gas we think it consumes. Occasionally, as will be the case this spring, the black hole may disrupt a passing star or cloud and activity levels may rise. Other physical conditions that make this environment unique include higher magnetic fields, higher ambient ultraviolet and X-ray radiation fields, and molecular clouds that are denser, hotter, and more turbulent than their counterparts in the Galactic disk. Taken all together, the Galactic Center represents one of the most extreme environments in the Galaxy.

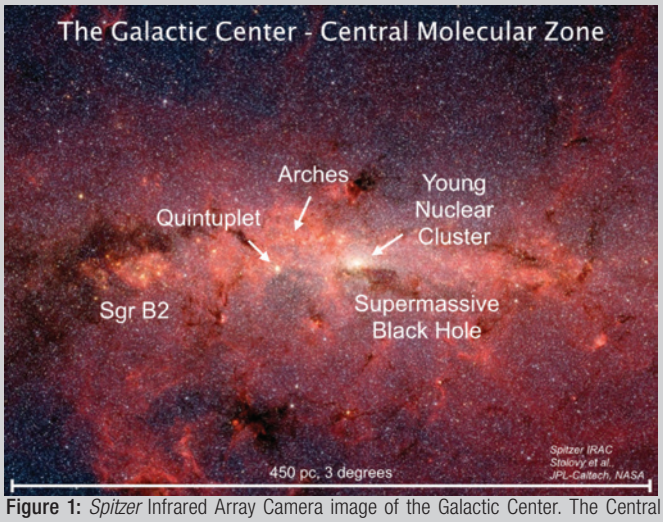

Figure 1: *Spitzer* Infrared Array Camera image of the Galactic Center. The Central Molecular Zone is ~400 pc across and contains 10% of the Milky Way's molecular gas in just 0.02% of the volume. This region also hosts three young star clusters over 10,000 solar masses (Arches, Quintuplet, Young Nuclear Cluster), several actively star-forming giant molecular clouds (e.g., Sgr B2) and the supermassive black hole at the very center.

Webb can address a number of fundamental questions through studies of the Galactic Center. First, we can investigate how supermassive black holes grow and influence their environment at a level of detail that is not possible in other galaxies. We can learn how nuclear star clusters form, and whether their growth is related to the growth of the black hole in some fashion. Last, we can investigate how the extreme conditions in this region affect the star-formation process.

One of the key advancements for Galactic Center studies is *Webb*'s increased spatial resolution over *Hubble*. Figure 2 shows an image of the Galactic Center taken with *Hubble*'s Wide Field Camera 3, compared with *Webb*'s Near Infrared Camera at infrared wavelengths. *Webb* can easily overcome the crowding seen in the *Hubble* image. The Galactic Center stars are bright, and *Webb*'s narrow-band filters are essential for obtaining deep images without saturating the brightest stars ($K = 9$). With *Webb*'s imaging capabilities, we will routinely detect emission from the black hole's accretion and watch individual stars orbit around the black hole—something that has thus far been possible only with the largest ground-based telescopes equipped with adaptive optics. Simultaneously, *Webb*'s large imaging field of view will allow us to measure the precise brightness, color, and motion of half a million stars in order to reconstruct the star-formation history and dynamical evolution of the surrounding nuclear star cluster.

With *Webb*'s integral-field unit on the Near Infrared Spectrograph, we can measure the fundamental properties of stars (temperature, metallicity, luminosity) at the Galactic Center down to stellar masses that are ten times lower than can be observed today (1 $M_{\odot}$ vs. 10 $M_{\odot}$). In addition to the stars, we can also trace the flow of gas as it makes its final journey from the inner parts of the Central Molecular Zone, through the central parsec, and possibly into the black hole. Figure 3 shows velocity slices of hot-hydrogen-gas emission in the vicinity of the Galactic Center (from a mosaic of star-subtracted integral-field spectra). The reservoirs and streams of gas that *Webb* will find can be modeled to estimate the rate at which gas accretes at different spatial scales. *Webb*'s 3D spectra will cover larger areas far more efficiently and with a wider range of gas emission lines as a result of *Webb*'s combination of high spatial resolution and high sensitivity over a large range of infrared wavelengths.

For more Galactic Center information, animations, and figures, see:

http://www.galacticcenter.astro.ucla.edu
http://www.mpe.mpg.de/ir/GC

Morris & Serabyn 1996, Annual Review of Astronomy & Astrophysics, 34, 645
Genzel, Eisenhauer, & Gillessen 2010, Reviews of Modern Physics, 82, 3121

Continued page 38

Galactic Center
from page 37

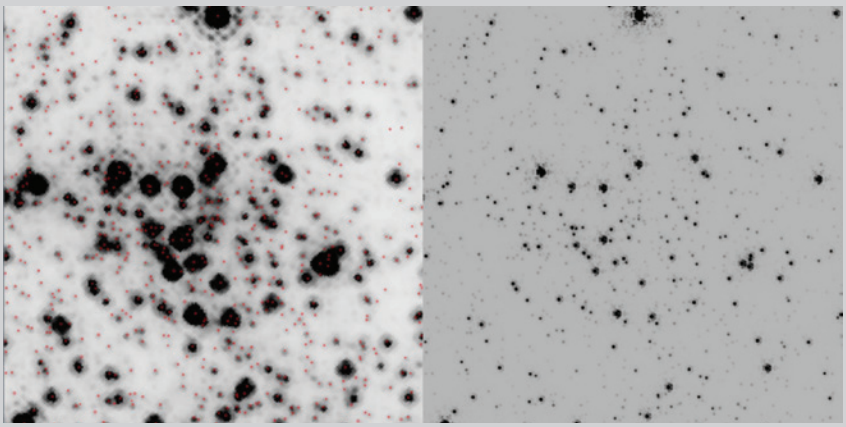

Figure 2: Images of the central 0.4 pc of the Galactic Center from *Hubble*'s Wide Field Camera 3 (observed) and *Webb*'s Near Infrared Camera (simulated). *Webb* will provide enormous gains in spatial resolution, which is essential for resolving the crowded region immediately around the supermassive black hole located at the center of the image. *Webb*'s resolution and sensitivity in the infrared will allow us to measure the precise brightness, color, and motion of half a million stars in order to reconstruct the star-formation history and dynamical evolution of the surrounding nuclear star cluster. The red points on the left are the stars used in the simulation on the right.

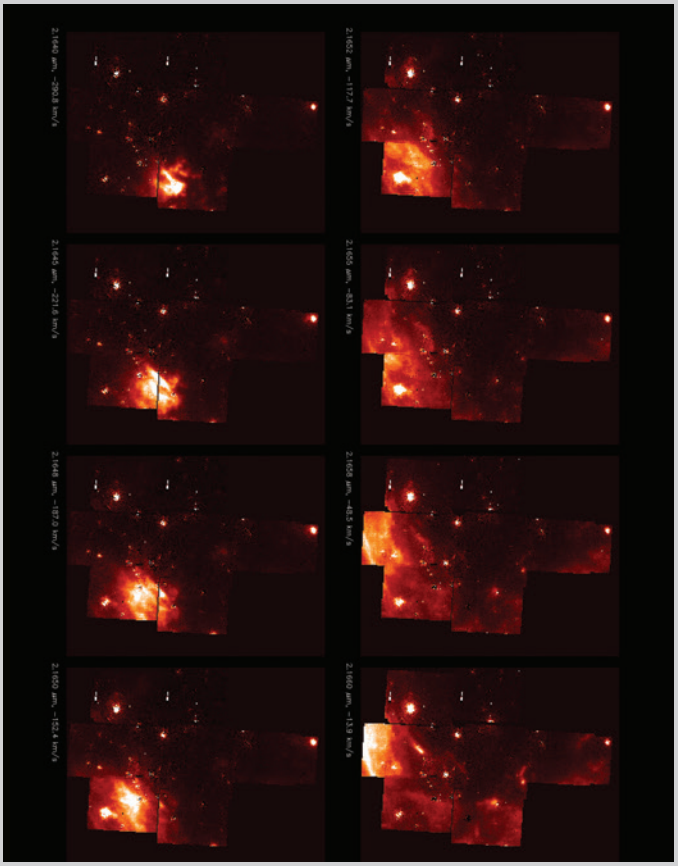

Figure 3: Snapshots of hot hydrogen gas emission (Brackett gamma) at various line-of-sight velocities as the gas orbits around the supermassive black hole. Similar measurements by *Webb* over a larger field and for different gas emission lines will allow us to constrain the physical mechanisms that drive gas in to the black hole or expel gas out into the rest of the Galaxy. Velocities increase from top to bottom in the first column and continue in the second column. This 10 × 7 arcsec mosaic was constructed with the OSIRIS instrument (OH-Suppressing Infrared Integral Field Spectrograph) at the W. M. Keck Observatory, which produces a spectrum at each pixel in the image. *Webb* will produce these types of measurements more efficiently, and for many different gaseous emission lines.

Barbara A. Mikulski Archive for Space Telescopes

Anton Koekemoer, koekemoer@stsci.edu, for the MAST team

The Barbara A. Mikulski Archive for Space Telescopes (MAST) is one of NASA's premier astronomy data centers, along with the High Energy Astrophysics Science Archive Research Center (HEASARC) and the NASA/IPAC Infrared Science Archive (IRSA). MAST is the primary archive repository for data from several large, active space missions (*Hubble*, *Kepler*, *XMM*-OM and *Swift*-UVOT), legacy data from past missions (*GALEX*, *FUSE*, *IUE*, *EUVE*, and others), planned data from future missions, such as *James Webb Space Telescope*, and all-sky surveys such as VLA-FIRST, GSC and DSS.

MAST supports the scientific research carried out by the astronomical community by facilitating access to its collections, offering expert user support and software for calibration and analysis, and providing value-added scientific data products. These include high-level science products (HLSPs) such as mosaics, catalogs, and spectra delivered to MAST by science teams, as well as enhanced products accessible via the *Hubble* Legacy Archive (HLA). As of March 2014, the total volume of MAST's data holdings was approximately 296 terabytes (TB), with an average of 18 TB of data downloaded per month. Current MAST news and updates are continuously posted on our main archive site (**http://archive.stsci.edu**) and on social media, including Facebook (**https://www.facebook.com/MASTArchive**) and Twitter (**https://twitter.com/MAST_News**).

Hubble Frontier Fields high-level science products available in MAST

The *Hubble* Frontier Fields Team has completed observations and delivery of HLSPs for the first epoch of each of the first two clusters, Abell 2744 and MACS J0416.1-2403. For Abell 2744, five weekly releases of v0.5 mosaics were delivered to the community during October–November 2013, followed by the full-depth v1.0 release on December 17, 2013. Subsequently, for MACS J0416.1-2403, four weekly releases of v0.5 mosaics were delivered to the community during January 2014, followed by the v1.0 release on February 28, 2014. For each cluster, the v1.0 release consists of full-depth combined mosaics in all the Frontier Fields program filters for ACS (F435W, F606W, F814W) and WFC3/IR (F105W, F125W, F140W, F160W), also including all archival data, to produce the deepest possible images of these fields. These full-depth mosaics have been produced by the Frontier Fields Implementation Team at the Institute, who have carried out extensive scientific value-added processing beyond standard calibration, to address instrumental effects such as bias de-striping, time-variable sky background, persistence, flat-fielding, and a variety of other calibration effects, all of which are described in more detail in the documentation that is released together with the mosaics.

Initial science results related to data from the Frontier Fields program are already being published by several different teams in the community on a variety of topics, including newly discovered high-redshift galaxy candidates (e.g., Atek et al. 2014; Laporte et al. 2014; Schmidt et al. 2014; Vanzella et al. 2014; Zheng et al. 2014), high-redshift supernovae (Rodney et al. 2013; Brammer et al. 2014), spectroscopic catalogs (Ebeling et al. 2014), dark matter and lensing (e.g., Bayliss et al. 2014; Schultz et al. 2014), and Spitzer observations (Bradač et al. 2014). In addition, for each of the six Frontier Fields clusters, MAST has publicly released gravitational lensing models that had been constructed and delivered by several independent teams in the community (led by M. Bradač, J.-P. Kneib, P. Natarajan, J. Merten, A. Zitrin, K. Sharon, and L. Williams). These models have been made available through a web-based interface at MAST, enabling their direct use by the community to estimate magnification parameters at any location on the cluster fields. All these products may be accessed directly from the MAST Frontier Fields website: **http://archive.stsci.edu/prepds/frontier/**.

Hubble Legacy Archive Star Clusters Project

The *Hubble* Legacy Archive Star Clusters Project (Whitmore et al. 2014) presents compact star cluster catalogs for 20 nearby, star-forming galaxies using observations from the Advanced Camera for Surveys (ACS) and source lists generated by the HLA. A typical cluster luminosity function can be approximated by a power-law, with an average value for the index of –2.37 and r.m.s. scatter = 0.18. The uniform database provided by these HLA catalogs results in a small scatter (0.5 magnitude) in the correlation between the magnitude of the brightest cluster ($M_{\rm brightest}$) and log of the number of clusters brighter than $M_{\rm I} = -9$ (log N). The images and catalogs are all available for download from the HLA Star Cluster project website: **http://archive.stsci.edu/prepds/hlastarclusters/**.

Multi-Cycle Treasury programs complete

All observations are now complete for the three Multi-Cycle Treasury (MCT) programs, namely CANDELS (P.I.: S. Faber and H. Ferguson; see Grogin et al. 2011, Koekemoer et al. 2011), CLASH (P.I.:

Continued page 40

MAST
from page 39

M. Postman; see Postman et al. 2012), and PHAT (P.I.: J. Dalcanton; see Dalcanton et al. 2012), and the teams have delivered all the associated products to the archive. As of March 2014, more than 59 TB of mosaics and HLSPs created by these teams have been downloaded by the community, to over 3500 unique IP addresses. A total of 166 science papers have been published to date using data from these programs, covering topics from high-redshift supernovae, galaxy evolution in the early universe, black holes, lensed high-redshift galaxies, physical properties of clusters, the dynamics and structure of M31, and the properties of its stellar populations. More details about these programs, as well as all the data, are available at: **http://archive.stsci.edu/prepds/candels/, http://archive.stsci.edu/prepds/clash/, and http://archive.stsci.edu/prepds/phat/**.

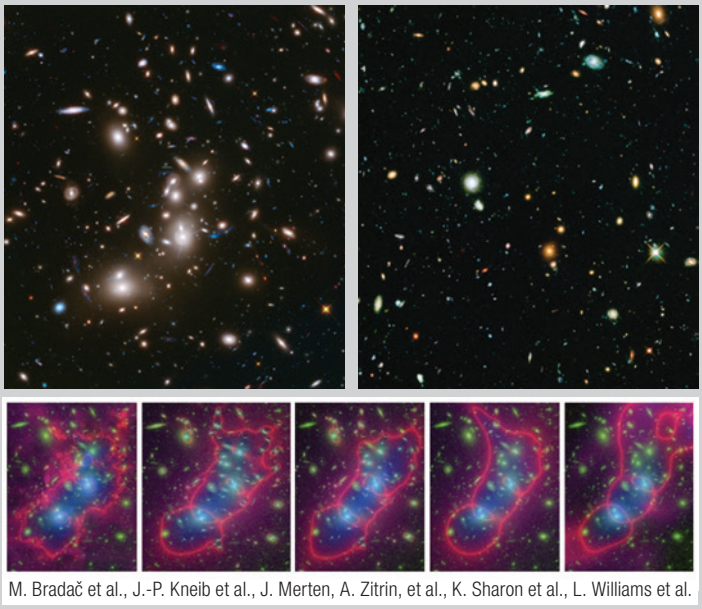

Figure 1: The first Frontier Fields cluster, Abell 2744. *Top left*: 70 orbits of WFC3/IR F105W, F125W, F140W, F160W. *Top Right*: Abell 2744 parallel field (70 orbits of ACS F435W, F606W, F814W); image credits: J. Lotz, M. Mountain, A. Koekemoer, and the HFF team. *Bottom panels*: Gravitational lensing models for Abell 2744 delivered to MAST by several independent teams (M. Bradač et al., J.-P. Kneib et al., J. Merten, A. Zitrin, et al., K. Sharon et al., L. Williams et al.), with the red overlays indicating the degree of lensing magnification. Differences in the detailed structure of the models reflect different approaches used by the different teams, while their overall similarity across the cluster field is highly encouraging for their use in determining the properties of lensed background galaxies.

Hubble Space Telescope 24th anniversary image and associated products

To commemorate the 24th anniversary of the launch of *Hubble*, the *Hubble* Heritage Team has carried out observations of a dramatic dust pillar in NGC 2174, using the WFC3 infrared camera. This new view is strikingly different than previous *Hubble* images obtained in visible light with the Wide Field Planetary Camera 2 (Proposal 9091, PI: Hester). The new WFC3 observations were obtained in February 2014, and include four tiles in a 2 × 2 mosaic pattern, where a small shift between tiles allows for the removal of detector artifacts (see proposal 13623, PI: Z. Levay, for details). The broad-band F105W, F125W, and F160W filters highlight unique physical processes occurring in and around the nebula, and they combine to produce a dramatic new color image. Parallel observations with the ACS Wide Field Channel were also obtained to create an H-alpha mosaic of the "horizon" feature just north of the target. The two sets of observations (ACS/WFC and WFC3/IR) showcase the ongoing multi-wavelength capabilities of the observatory and provide a preview of the capabilities of the *James Webb Space Telescope*. All the reduced mosaics are available at: **http://archive.stsci.edu/prepds/heritage/ngc2174/**.

Survey of the Low-Redshift Intergalactic Medium with *Hubble*/COS

A survey of the low-redshift intergalactic medium (IGM) has been performed by Danforth et al. (2014). Using *Hubble*/COS spectra of 75 UV-bright active galactic nuclei, several thousand absorption lines were identified from 2,518 distinct redshift systems at $z < 0.723$. The spectral features were selected and measured using a semi-automated analysis to minimize bias in line identification. For each of the 75 sightlines, a co-added, continuum-fitted spectrum is provided in FITS format. Two catalogs for each sightline are presented: one catalog lists the identified spectral features sorted by wavelength, while another lists the absorption features associated with IGM systems sorted by redshift. Finally, preview plots of each sightline's spectrum are provided, complete with line identifications. For convenience, we also provide machine-readable versions of tables from Danforth et al. (2014). All the data are available at: **http://archive.stsci.edu/prepds/igm/**

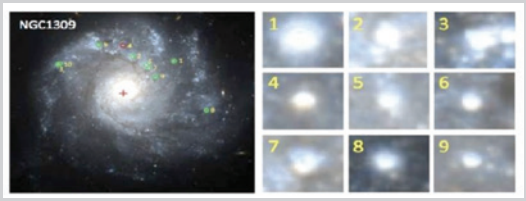

Figure 2: Example dataset from the HLA Star Clusters project (Whitmore et al. 2014), showing the multi-band ACS F555W and F814W imaging for NGC 1309, including close-ups of several of the star clusters for which photometric properties are presented in this project.

Catalogs of unique *GALEX* sources from Bianchi, Conti & Shiao (2014)

The *GALEX* spacecraft operated for over 10 years and surveyed nearly the entire sky during its lifetime. The telescope observed in both the far ultraviolet (FUV; 1344–1786 Å) and near ultraviolet (NUV; 1771–2831 Å) simultaneously until May 2009, when the FUV detector failed. The NUV detector continued to operate until June 2013, when *GALEX* was retired and the mission ended. The standard *GALEX* data products at MAST include visit and coadd image files, as well as a source catalog produced by the *GALEX* reduction pipeline called the "MCAT." The MCAT consists of over 200 million source measurements, but since it was run on each tile, there are multiple measurements of the same source due to tile overlaps and different surveys (AIS, MIS, DIS, Guest Investigator, etc.) To rectify the situation, Bianchi et al. (2014) have constructed catalogs of unique sources: one based on

All-Sky Imaging Survey (AIS) tiles, and another based on Medium-Sky Imaging Survey (MIS) tiles. These catalogs (BCS AIS and BCS MIS, respectively) are homogeneous in depth and quality, and are optimal for cross-matching *GALEX* UV fluxes with data in other bands (e.g., for source selection combining optical or IR data), or for Galactic and extragalactic population studies. All the catalogs, together with interactive interfaces to query them, are available here: **http://archive.stsci.edu/prepds/bcscat/**.

Hubble Legacy Archive (HLA)

The HLA has made available Data Release 7.2, which includes improved source lists for WFC3, totaling 85% completion of approved source lists for all image products. We are also pleased to announce the Beta 0.3 release of the *Hubble* Source Catalog (HSC—**http://archive.stsci.edu/hst/hsc/**). The goal of the HSC is to combine the tens of thousands of visit-based *Hubble* Legacy Archive source lists into a single master catalog. The primary improvements in Beta 0.3 are the inclusion of WFC3 source lists from the HLA, and improvements to the matching algorithms that result in an increase of "good" catalog regions from about 70% in Beta 0.2 to about 95% in Beta 0.3.

For further details, please see the HLA page (**http://hla.stsci.edu/**) where updates continue to be posted as they become available.

Kepler updates

All Q17 data are now available as batch downloads through the search interface, online for both light curves and target pixel files, and as tar files (for light curves only). See the webpage (**http://archive.stsci.edu/kepler/**) that explains ways to retrieve data other than via batch requests. In addition, the tar files containing light curves for targets labeled *Kepler* Objects of Interest (KOI) have been recreated to reflect the newly updated list. Finally, the Ecliptic Plane Input Catalog (EPIC) for the proposed K2 mission has also been made available; please see the K2 webpage at MAST for further details (**http://archive.stsci.edu/k2/**).

As always, please feel free to contact the MAST help desk (**archive@stsci.edu**) with questions, or contact us through Facebook (**MASTArchive**) or Twitter (**@MAST_News**) to provide suggestions on how we can improve our sites and services.

References

Atek, H., et al. 2014, ApJ, 786, 60
Bayliss, M. et al. 2014, ApJ, 783, 41
Bianchi, L., et al. 2014, Ad.Sp.R., 53, 900
Bradač, M. et al. 2014, ApJ, 785, 108
Brammer, G. et al. 2014, ATel 5728
Dalcanton, J., et al. 2012, ApJS, 200, 18
Danforth, C. W., et al. 2014, arXiv:1402.2655
Ebeling, H. et al. 2014, ApJS, 211, 21
Grogin, N. A., et al. 2011, ApJS, 197, 35
Koekemoer, A. M., et al. 2011, ApJS, 197, 36
Laporte, N., et al. 2014, A&A, 562, L8
Postman, M., et al. 2012, ApJS, 199, 25
Rodney, S. et al. 2013, ATel 5496
Schmidt, K. et al. 2014, ApJ, 782, L36
Schultz, C. et al. 2014, arXiv:1401.3769
Vanzella, E. et al. 2014, ApJ, 783, L12
Whitmore, B., et al. 2014, AJ, 147, 78
Zheng, W., et al. 2014, arXiv:1402.6743

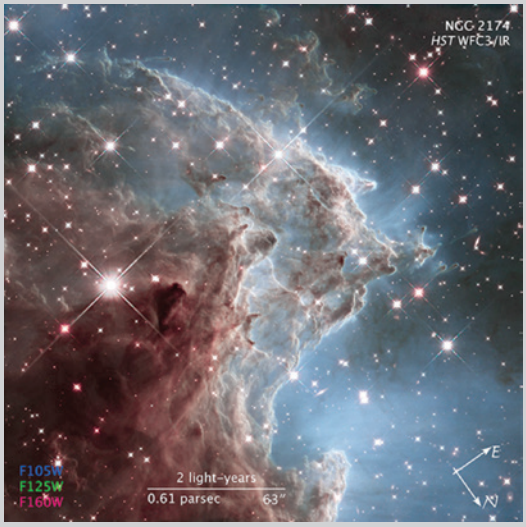

Figure 3: Commemorating the 24th anniversary of the launch of *Hubble*, a new image of the dust pillar in NGC 2174, obtained using WFC3 with the F105W, F125W, and F160W filters (see proposal 13623, PI: Z. Levay, for further details).

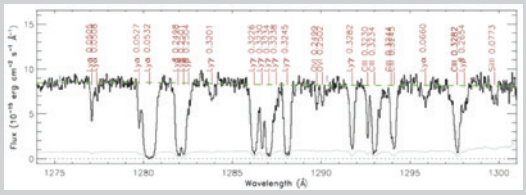

Figure 4: Example subsection of a spectrum for the IGM sightline 3C57. Features marked in red are intergalactic absorber lines from systems at various redshifts (see Danforth et al. 2014).

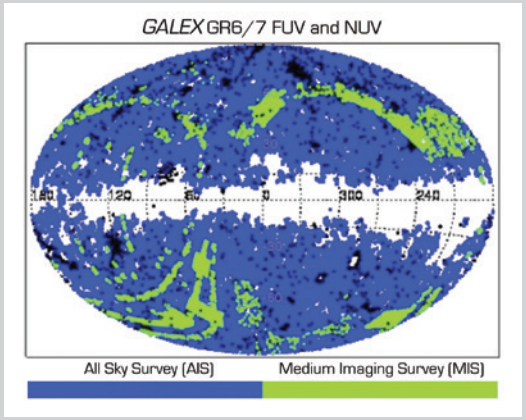

Figure 5: Coverage map of the BCS catalog in Galactic coordinates. Blue are AIS tiles, green MIS tiles, and black are from other surveys (DIS, GII, etc., but are not included in the BCS catalog). For further details, see Bianchi, Conti & Shiao (2014).

Continued page 42

Cosmic Reionization and Early Galaxy Formation

Brant Robertson, *brant@email.arizona.edu*, **& Richard S. Ellis,** *rse@astro.caltech.edu*

One of the final frontiers in assembling the full story of cosmic history relates to the period 200–800 million years (Myr) after the Big Bang, when early galaxies first bathed the universe in starlight. When did this happen, and were those sources the principal agent responsible for transforming hydrogen in the intergalactic medium from a neutral to ionized state? To address these fundamental questions requires observations of faint galaxies that probe into the heart of the reionization era, at redshifts up to $z = 10$.

The *Hubble* Ultra Deep Field 2012 campaign (UDF 2012; GO 12498, PIs: Ellis & McLure; Koekemoer et al. 2013), which executed in August and September 2012, adopted a filter-deployment strategy aimed at creating the first representative sample of galaxies in the redshift interval $6 < z < 10$, building on earlier campaigns in this well-studied field obtained by the Advanced Camera for Surveys (ACS) and the Wide Field Camera/Infrared Channel (WFC/IR). We used over half of the 128-orbit allocation to create an ultra-deep F105W image, which was essential for rejecting candidates with photometric redshifts $z < 6$. We employed an additional F140W filter to improve the fidelity of photometric redshifts for the most distant sources and to measure their intrinsic colors.

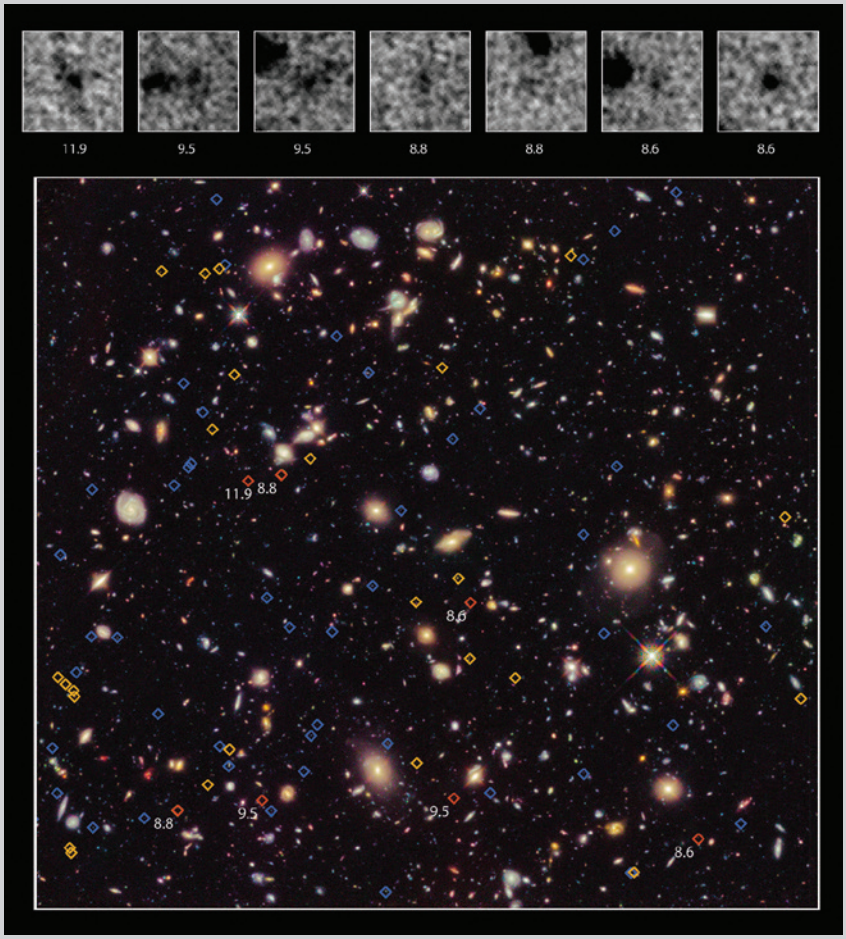

Figure 1: The distribution of faint galaxies in the redshift intervals $6.2 < z < 7.3$ (blue), $7.3 < z < 8.5$ (yellow) and $z > 8.5$ (red, *top panel* with redshifts indicated) from the UDF 2012 campaign (Schenker et al. 2013, McLure et al. 2013). The ultra-deep F105W exposure doubled the number of known $z \sim 7$ galaxies in the field, most of which are intrinsically faint. This provided a more robust measure of the faint-end slope of the luminosity function at $z \sim 7$–8, the contribution of feeble galaxies to the reionization process, and the first census of galaxies beyond $z \sim 8.5$ (Ellis et al. 2013).

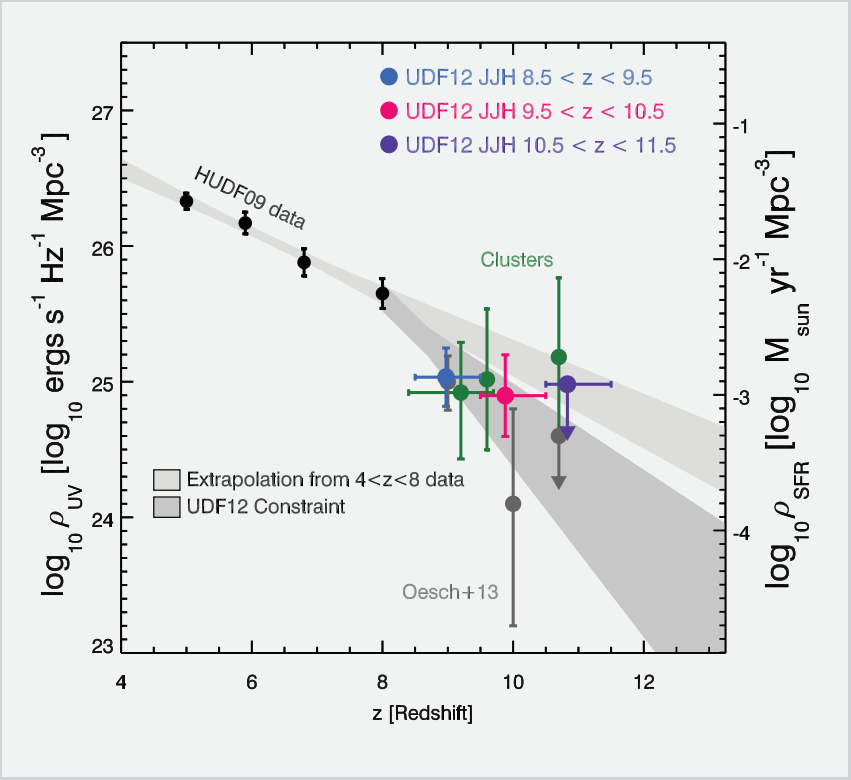

Figure 2: Luminosity and star-formation-rate density versus redshift inferred from the UDF 2012 campaign. Data over $5 < z < 8$ are based on earlier ACS and WFC3/IR campaigns (Bouwens et al. 2007, 2011). Estimates from the CLASH lensing campaign are shown in green (Bouwens et al. 2012). Luminosity densities for the four $8.5 < z < 9.5$ and two $9.5 < z < 10.5$ sources are shown in blue and magenta, respectively. The potential candidate at $z = 11.9$ is not shown (see Ellis et al. 2013). The dark gray points represent an independent analysis incorporating CANDELS data (Oesch et al. 2013). The gray shaded areas illustrate extrapolations of the linear trend over $4 < z < 8$ and the formal uncertainty arising from the UDF 2012 campaign.

We combined the new, deep WFC3/IR data with all earlier UDF and related exposures. We released the coadded images on both the Institute's archive web pages[1] and a public UDF 2012 web page at the University of Arizona.[2] The release included the combined 128-orbit, full-depth, ACS, parallel mosaic and an improved reduction of the WFC/IR F125W mosaic taken in 2009 (GO 11563, PI: Illingworth).

The primary advance of the UDF 2012 campaign is an enlarged and more robust catalog of galaxies in the redshift range $6.2 < z < 10$, specifically addressing the role of galaxies in cosmic reionization and the implications for galaxy searches beyond redshift $z = 10$ with future facilities, particularly *Webb*. The ultra-deep F105W image reaches an impressive 5σ limit of $AB = 30.0$ (0.4 arcsec aperture) providing a gain of 0.7 magnitudes over earlier data. Most of the newly discovered sources—twice as many as in the 2009 campaign at $z \sim 7$—are intrinsically faint, corresponding to absolute magnitudes as faint as $M_{UV} < -17$ (Figure 1). The improved count of these feeble sources is key to constraining the shape of the luminosity function of star-forming galaxies at early times. The superb spatial resolution also enables detailed studies of galaxy sizes at unprecedented distances (Ono et al. 2013).

The UDF 2012 campaign also provides a valuable "ultra-deep tier" for the wedding cake of WFC3/IR surveys, building on the wider and shallower CANDELS Deep and Wide programs (GO 12060, PIs: Ferguson, Riess & Faber; Grogin et al. 2011; Koekemoer et al. 2011). As an ultra-deep blank field, it also complements the CLASH (GO 12065, PI: Postman; Postman et al. 2012) and Frontier Fields[3] lensing programs.

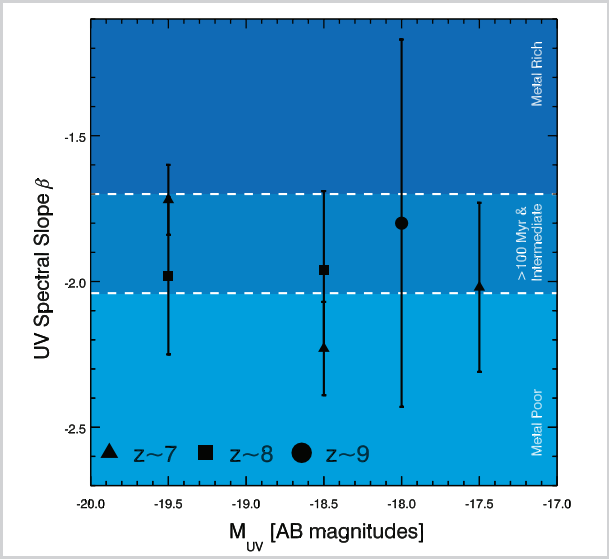

Figure 3: The rest-frame UV continuum slope parameter β for UDF 2012 galaxies with $7 < z < 9$ down to luminosities of $M_{UV} = -17.5$ (Dunlop et al. 2013). Shaded regions show predictions for various metallicities and ages. The data is most consistent with >100-Myr-old stellar populations implying earlier sources with $z > 10$.

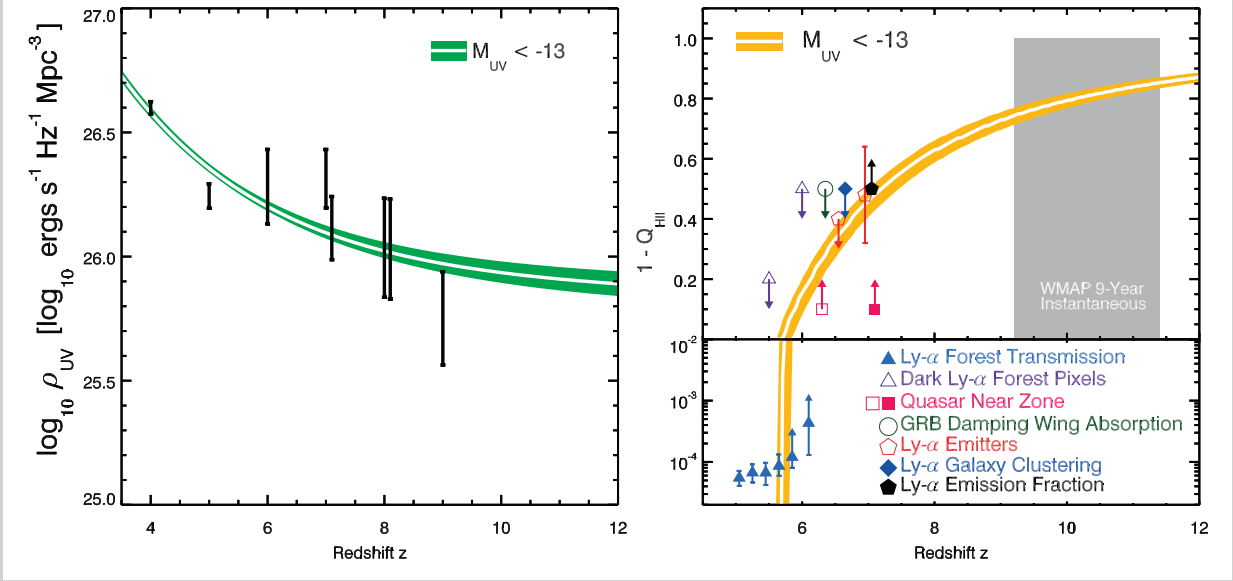

Figure 4: Star-forming galaxies are capable of reionizing the universe if the volume-averaged star-formation history extends beyond $z \sim 10$ (see Figure 3) and the luminosity functions observed (Figure 2) extend down to $M_{UV} = -13$ (*left panel*). For an escape fraction of ionizing photons of 20%, the history of the reionization process, calculated in terms of the neutral fraction ($x_{HI} = 1 - Q_{HII}$) is compared with independent estimates (*right panel*).

The gain in depth afforded by stacking the WFC3/IR F160W, the new F140W, and earlier F125W images (each limited at $AB = 29.5$, 5σ) provided the first census of galaxies beyond $z = 8.5$. Seven galaxies were located with photometric redshifts $z > 8.5$ using both color selection and methods for fitting spectral energy distributions. The ultra-deep F105W filter and the stacked ACS BViz data from the 2004 UDF campaign (GO 9998, PI: Beckwith) were key to refining photometric redshifts for sources claimed to lie above $z = 8.5$ based on earlier, shallower data. In fact, all but one of the earlier sources claimed to lie at $z > 8.5$ were found to be at lower redshift. The remaining earlier candidate is an intriguing, single-filter detection, which could be an intense line emitter at $z = 2.4$. Regardless of this uncertainty, the UDF 2012 census indicates that the decline in the star-formation density over $5 < z < 8$ extends 180 Myr earlier, to $z \sim 10$ (Figure 2). A similar trend has been suggested by independently discovered gravitationally lensed $z > 8.5$ sources from the CLASH program (STScI *Newsletter* Vol. 30, Issue 02).

The gradual decline in star-formation density suggests the presence of yet earlier, $z > 10$ sources, beyond the reach of *Hubble* but within the grasp of *Webb*. This presence can also be deduced from the rest-frame-ultraviolet colors of the large sample of $z \sim 7$–8 galaxies within the UDF 2012 sample. Earlier work suggested the faintest $z \sim 7$ galaxies were unusually blue, such as might be the case if they were extremely metal poor or recently formed. With only two filters to estimate the color, however, the analysis was prone to a bias to bluer colors as one approached the limiting depth. By selecting sources in the newly added F140W filter and measuring the rest-frame-ultraviolet color using the independent F125W and F160W filters, such a bias can be avoided. The $z \sim 7$–8 galaxies have colors no bluer than the bluest star-forming galaxies found locally (Figure 3), consistent with mature (>100-Myr-old) systems with either solar or modestly sub-solar metallicities, and little dust. The absence of extremely young systems at $z \sim 7$–8 (to $M_{UV} \sim -18$) provides further evidence for earlier populations at $z > 10$.

So, what did we conclude from the UDF 2012 campaign about the role of early galaxies in cosmic reionization? Three findings—the dominant population of feeble sources (Figure 1), the smooth decline in the cosmic star-formation history (Figure 2), and the nature of the stellar populations that govern the output of energetic, ionizing photons (Figure 3)—permit us to address this fundamental question. We conclude that star-forming galaxies did provide the primary source of ionizing photons (Figure 4). The caveats—discussed in detail in Robertson et al. 2013—are: galaxies must populate the faint end of the luminosity function to $M_{UV} \sim -13$ (4 magnitudes below the UDF 2012 detection limit), and the redshift distribution extends smoothly beyond $z \sim 10$, as predicted from the mature UV colors studied at $z \sim 7$–8. The most uncertain assumption is a 20% fraction of ionizing photons escaping from a typical galaxy into the intergalactic medium. Deep absorption-line spectra of lensed sources may ultimately trace the covering fraction of neutral and cold gas, and provide a valuable constraint on this assumption. Although some may be disappointed that *Hubble* has not yet found a truly primeval

stellar population, the good news is that we have the first empirical constraints on the history of the reionization process (Figure 4), and there is every prospect for locating and studying sources in the all-important period $10 < z < 20$ with *Webb*.

References

Bouwens, R., et al. 2007, ApJ, 670, 928
Bouwens, R., et al. ApJ, 737, 90
Bouwens, R., et al. 2012, ApJL, 752, 5
Dunlop, J., et al. 2013, MNRAS, 432, 3520
Ellis, R., et al. 2013, ApJL, 763, 7
Grogin, N., et al. 2011, ApJS, 197, 35
Koekemoer, A., et al. 2011, ApJS, 197, 36
Koekemoer, A., et al. 2013, ApJS, 209, 3
McLure, R., et al. 2013, MNRAS, 432, 2696
Oesch, P., et al. 2013, AJ, 773, 75
Ono, Y., et al. 2013, ApJ, 777, 155
Postman, M., et al. 2012, ApJS, 199, 25
Robertson, B., et al. 2013, AJ, 768, 71
Schenker, M., et al. 2013, ApJ, 768, 196

[1]**http://archive.stsci.edu/prepds/hudf12/**
[2]**http://udf12.arizona.edu/**
[3]**http://www.stsci.edu/hst/campaigns/frontier-fields/**

Orion Nebula Workshop

Massimo Robberto, robberto@stsci.edu

The Institute hosted a mini-workshop titled "The Orion Nebula Cluster as a Paradigm of Star Formation" on October 13–16, 2013. Over 60 participants, including the majority of the leading experts in the field, came to discuss the current understanding of what is probably the best studied star-forming region in the sky. Continuing a tradition of influential conferences on Orion—from the 1982 Draper Symposium in New York to the 1996 Ringberg Castle Workshop in Germany—this meeting commemorated the completion of the *Hubble* Treasury observing program on the Orion Nebula Cluster (ONC).

In her introductory talk, Hillenbrand illustrated how the Orion region plays a paradigmatic role in our understanding of star and planet formation. As the nearest young cluster dominated by massive OB stars, the ONC allows the study of thousands of newborn stars across the full electromagnetic spectrum, from giant O stars to brown dwarfs and planetary mass objects. Understanding the ONC represents a necessary step to eventually gain knowledge of the more distant and energetic star-forming regions like the Galactic Center and starburst regions in other galaxies. As Bally said in the conference's summary talk, Orion is the "atom" of star formation, the fundamental quantum.

The wealth of recently acquired information on the ONC reveals deeper levels of complexity that continuously pose new scientific questions. The fundamental problem of the age of the Orion Nebula's cluster provides a clear example. In his review, Jeffries showed that the cluster is young—with an average stellar age of about 2 Myr—as derived from a comparison with theoretical isochrones in the HR diagram. The spread of stellar ages, however, is substantial. While several factors, both observational and intrinsic to the stars, affect the apparent position of stars in the HR diagram, the most accurate analysis supported by other age indicators seems to confirm that at least part of the spread in age is real.

If one assumes that at least the relative ages are somewhat reliable, then evolutionary effects, such as the evolution of disks and mass accretion rate with time, can be probed (Manara). Since Orion offers the richest sample of sources, it is statistically possible to derive robust relations between, for example, mass accretion

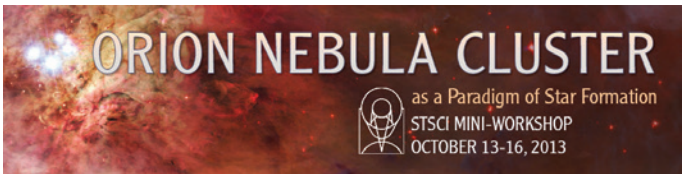

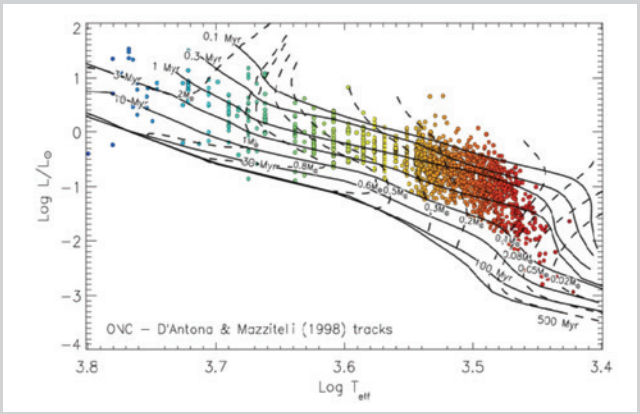

HR diagram of the Orion Nebula Cluster (from Da Rio et al. 2012). With more than 1800 sources, the ONC provides the richest sample of young stars with known physical parameters. The color of the circles encodes the effective temperature of each source. The density of points provides a graphic representation of the Initial Mass Function, peaking around 0.1–0.2 $M_{\odot}$ (according to D'Antona and Mazzitelli tracks).

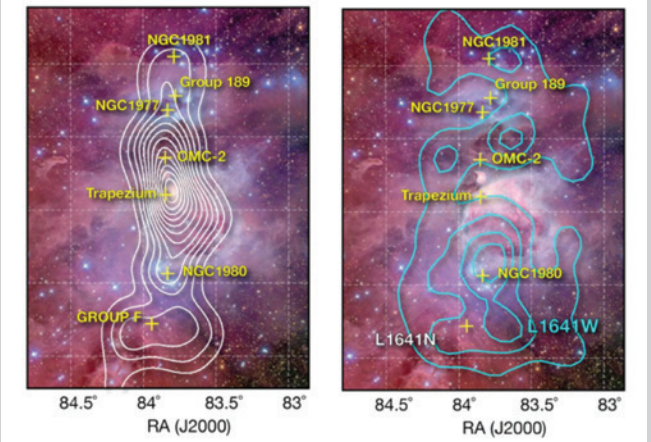

The Orion Nebula Cluster ("Trapezium" in this figure from Bouy et al. 2013) represents the most recent major event of star formation; however, older, more dispersed clusters like NGC 1980, are diffused through the entire region. Their members may contaminate the observed ONC population. *Left*: spatial density of X-ray sources from Alves and Buoy (2012); *right*: spatial density of foreground population from Buoy et al. (2014).

and stellar age and mass, paying attention at the substantial correlations introduced deriving these quantities (Da Rio). Stassun indicated that eclipsing binary stars in the Orion Cluster allow us to directly measure masses and radii of stars. They show anomalies (larger radius and therefore colder temperatures) correlated to the chromospheric activity. Theorists are producing a new generation of evolutionary models accounting for these effects, which may reconcile some of the problems encountered when stellar ages are derived from isochrones.

Cody showed how one of the many contributions of the Young Stellar Object Variability (YSOVAR) program carried out with *Spitzer* was the discovery of six more eclipsing binaries in the region—a major addition to this elusive but crucial class of stars. Rice presented the results of the near-IR variability monitoring campaign performed at the United Kingdom Infrared Telescope, complementing YSOVAR findings. Bally pointed out that the Atacama Large Millimeter Array (ALMA) is also starting to enable direct measures of the mass of young stellar sources in Orion using the keplerian rotation curves of their circumstellar disks. Great progress in this field is expected from ALMA in the next few years.

From an observational point of view, source multiplicity, contamination from foreground and (especially in the infrared) background stars, and variability are all sources of noise and opportunities for new discoveries. Thanks to the exquisite spatial resolution of the *Hubble*, complemented by ground-based adaptive optics, it has been possible to study in great detail the frequency of binary stars in Orion, which turns out to be about the same as in the field population (Reipurth). This result is in contrast to findings for less densely populated star-forming associations, which have many more binaries, suggesting that the initial multiple population of the ONC has already been significantly altered. If, in dense environments like the ONC, high-order multiples tend to evolve more rapidly in hierarchical systems, we may be facing an early evolution of the Initial Mass Function.

Regarding contamination, Alves showed evidence for a rich foreground population centered on NGC 1980/1981, to the south of the ONC. The overlap of these clusters can make up for more than 10–20% of the ONC population. Luhman summarized the studies carried out in the last 20 years that discovered the population of brown dwarfs. *Webb* will eventually allow for a secure characterization of these systems down to one Jupiter mass.

Also important is defining the youngest sources in the field, which are still embedded in their parental cloud. Reviewing the most recent census of embedded young stellar objects from the *Spitzer* and *Herschel* satellites, Megeath showed that the entire Orion Molecular Cloud, extended across 80 pc, is dotted by small clusters. They provide a unique opportunity to study how the typical products of star formation, like the density and number of young stellar objects or multiplicity, depend on the column density of their natal gas, and on the environment in general. Tobin presented new results from the *Herschel* Orion Protostar Survey, which included a new class of bright red sources that can be interpreted as the most young, deeply embedded protostars with compact outflows and strong shocks. X-ray surveys provide a complementary view of the region, unbiased by extinction. Wolk presented results from a *XMM-Newton* survey of a large part of the Orion A cloud, unveiling more than 1000 X-ray sources. In this case, it is the more evolved class III candidates that appear concentrated in foreground clusters.

The formation of the most massive stars in the ONC, each one a hierarchical multiple system, was reviewed by Tan. Their kinematic status is particularly intriguing, with the well-known IR source Becklin-Neugebauer (BN) being either a runaway star from the Trapezium (as suggested by Tan) or ejected by the much closer source I (as suggested by Bally). Again, ALMA can greatly contribute to clarifying the physical and dynamical status of these sources, as shown by Hirota for source I.

Due to their limited spatial resolution, sub-millimeter observations with SOFIA and *Herschel* in the core of the ONC are hampered by source confusion and high background; however, Salgado illustrated how these facilities can still provide key information on the physical properties of dust, in terms of spatial distribution, temperature and mass. At centimeter wavelengths, the Jansky Very Large Array (JVLA) has the capability to disentangle coronal-type non-thermal radio emission from the thermal emission from outflows. Forbrich reported the results from a simultaneous 24-hr monitoring of the ONC with JVLA and *Chandra*, showing the strong correlation between time variability of non-thermal radio emission and X-ray flaring.

Henney discussed the dynamical status of the Orion Nebula, based on the most recent numerical simulations and observations of the ionized gas. Hartmann provided an overall picture for the formation

and evolution of the ONC. He pointed out that gravitational forces still drive the medium on which all other effects (e.g., thermal pressure gradients, stellar winds, radiation pressure, and turbulence) take place.

The last day of the conference was intended to place Orion in the context of star formation in general. Rahman provided an overview of the main characteristics of massive young clusters in the Galaxy, focusing on the different types of feedback on their natal environment they may provide. Feigelson reported on the Massive Young Star-Forming Complex Study in Infrared and X-ray (MYStiX), an infrared and X-ray survey of 19 other main regions within 4 kpc, aimed to produce the largest catalog of pre-main-sequence objects. Willis discussed star formation in other regions like NGC 6334, as probed by *Herschel* and the Submillimeter Array. Lu discussed star formation in extreme environments, such as the Galactic Center, providing evidence for a top-heavy IMF in the Galactic Center Clusters. At larger distances, Sabbi, Panagia, and De Marchi focused on the Large Magellanic Cloud, showing how *Hubble* still provides the only possibility to study the interplay between different generations of star in the context of star-cluster formation. The same is true for the effect of varying metallicity on disk lifetime. The local group dwarf galaxy NGC 6882, at a distance 1000 times larger than the Orion region, offered Carlson an opportunity to showcase a possible template for the next evolutionary phase of the Orion Nebula.

The conference hosted a number of talks focusing on theoretical studies. Offner presented new results from full 3-D numerical simulations, including radiative post-processing that can be directly compared with observations in Orion (core structure, stellar kinematics and luminosity) to further constrain the model assumptions. Parmentier presented a semi-analytical model capable of explaining the observed relation between the gas surface density and the stellar density, and the stellar age spreads in clusters with different densities. Other contributions focused on physical processes like two-fluid turbulence (Balsara) and super-thermal electrons (Dopita). All webcast presentations and original slides are available at **https://webcast.stsci.edu/webcast/searchresults.xhtml?searchtype=20&eventid=198&sortmode=1.**

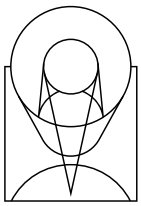

Contact STScI:

The Institute's website is: **http://www.stsci.edu**
Assistance is available at *help@stsci.edu* or 800-544-8125.
International callers can use 1-410-338-1082.
For current *Hubble* users, program information is available at:
http://www.stsci.edu/hst/scheduling/program_information.

The Space Telescope Science Institute Newsletter is edited by Robert Brown, *rbrown@stsci.edu*, who invites comments and suggestions.
Contents Manager: Sharon Toolan, *toolan@stsci.edu*
Design: Pam Jeffries, *jeffries@stsci.edu*
To record a change of address or to request receipt of the Newsletter, please send a message to *address-change@stsci.edu*.

Contents:

Calendar

Visit by Chief Scientist Ellen Stofan . . . . . 9 July 2014

HST SEQ #2 (GSFC) . . . . . 16 July 2014

JWST SWG (GSFC) . . . . . 17–18 July 2014

YAE Family Night . . . . . 18 July 2014
http://www.stsci.edu/institute/conference/youthae/documents/Family_Night_2014_Registration_Form.pdf

IAU Symposium 311 (Oxford) . . . . . 21–25 July 2014

YAE Family Night . . . . . 25 July 2014
http://www.stsci.edu/institute/conference/youthae/documents/Family_Night_2014_Registration_Form.pdf

WFIRST SDT Meeting . . . . . 31 July–1 August 2014

JWST GTO . . . . . 7–8 August 2014

Calibration Workshop . . . . . 11–13 August 2014

AURA BOD (Hawaii) . . . . . 18–19 September 2014

HST SEQ #3 (STScI) . . . . . 23 September 2014

STIC . . . . . 21–22 October 2014

HST SEQ #4 (GSFC) . . . . . 10 December 2014

"*Hubble* 2020: Building on 25 Years of Discovery" (STScI) . . . . . 20–23 April 2015
http://www.stsci.edu/institute/comference/hubble25/

SPACE TELESCOPE SCIENCE INSTITUTE
3700 San Martin Drive
Baltimore, Maryland 21218

www.nasa.gov

NP-2014-6-159-GSFC